

**AN INVESTIGATION ON THE CONTROL OF GOLD
MINERALIZATION IN THE BEARDMORE-GERALDTON
GREENSTONE BELT AND SURROUNDING QUETICO-
WABIGOON SUBPROVINCE BOUNDARY AREA**

Victoria R. Stinson

**Department of Geology
Lakehead University
Thunder Bay, Ontario**

**A thesis submitted to the Faculty of Graduate Studies in partial
fulfillment of the requirements for the degree of
Master of Science**

© Victoria Stinson, 2013

ABSTRACT

The Beardmore-Geraldton greenstone belt is located along the boundary between the Wabigoon and Quetico subprovinces in the Superior province of the Canadian Shield. Historical gold mines and current gold exploration camps are located throughout the Beardmore-Geraldton greenstone belt and adjacent Wabigoon subprovince in moderately to steeply dipping ductile to brittle-ductile shear zones in many types of lithologies, with various metamorphic grades, and alteration styles. The shear zones typically strike east-west along the boundary of the Beardmore-Geraldton greenstone belt with the Wabigoon subprovince to the north as well as along the boundary with the Quetico subprovince to the south.

Field mapping and petrography, including microstructural analysis, were used to characterize the gold mineralization and investigate the control on gold mineralization in the Elmhirst, Castlewood, Pagwachuan, and Milestone properties in Greenstone, Ontario. Two property-scale and seven trench-scale maps were produced from field mapping and one hundred twenty-three transmitted and reflected light thin sections were prepared from samples collected from these properties. Lithology, structure, microstructure, metamorphic grade, alteration, and subprovince were considered as possible controlling factors on gold mineralization.

In the study area gold mineralization is hosted in relatively competent lithologies including schistose to mylonitic metamorphosed granodiorite, syenite, and pegmatite; chlorite-albite schist, schistose amphibolite, and garnet-hornblende-biotite schist. The regional-scale structures that host gold mineralization are ductile to brittle-ductile shear

zones that have a penetrative, schistose foliation and rarely a mylonitic fabric. The property-scale structures that host gold mineralization are folded, mylonitized, and boudinaged quartz veins; shear-related early, late, and complex folds; folded fault breccia, and pressure shadows of rigid minerals within schistose to mylonitic fabric. Gold mineralization is located in areas of micro-folds, micro-boudins, micro-fault breccia, undulatory extinction, and grain size reduction along irregular grain boundaries, subgrain boundaries, folded healed fractures, and in pressure shadows within areas of strain heterogeneity. Gold mineralization is located in both areas of greenschist facies and amphibolite facies metamorphism in the study area. The styles of alteration also vary within the study area with sericite, hematite, ankerite, calcite, and unaltered samples all hosting gold mineralization. Both the Wabigoon and Quetico subprovinces host gold mineralization in similar structures and microstructures as the Beardmore-Geraldton greenstone belt although it is within different lithologies, metamorphic grades, and alteration styles.

Similar structure and microstructure are always present in areas of gold mineralization in the study area while lithology, alteration, metamorphic grade, and subprovince vary. Gold mineralization within stable prograde and retrograde metamorphic minerals indicates that gold mineralization was synchronous with ductile to brittle-ductile deformation and metamorphism. Further gold exploration in the study area should focus on structure and microstructure as indicators for gold mineralization.

ACKNOWLEDGEMENTS

Dr. Mary Louise Hill has been an integral part of this thesis. Her time, patience, and intellectual support have been limitless, and definitely needed! Thank you for your ongoing support, Mary Louise.

I would like to acknowledge and thank Kodiak Exploration Ltd. and Prodigy Gold Inc. for the financial support of this thesis. I sincerely appreciate the intellectual, logistical, and computer support I received from Erik Haroldson, Paul Dunbar, Jerry Solomon, Alex Pleson, Esther Moore, Cheyenne Sica, Marc Patenude, Tanya Couture, Art and Theresa J., and Patty!

Anne Hammond, Al Mackenzie, and Colleen Kurcinka of Lakehead University have all aided this thesis immensely by preparing thin sections and teaching me how to use the scanning electron microscope.

Lastly, I would like to thank my loved ones for their compassion, comfort, and kind support. An extra special thank you for always believing in me Kerrilyn, Kathryn, Marilyn, Terrance, and Gramma Verg!

TABLE OF CONTENTS	
AN INVESTIGATION ON THE CONTROL OF GOLD MINERALIZATION IN THE BEARDMORE-GERALDTON GREENSTONE BELT AND SURROUNDING QUETICO-WABIGOON SUBPROVINCE BOUNDARY AREA	i
ABSTRACT	ii
ACKNOWLEDGEMENTS	ii
TABLE OF CONTENTS	v
LIST OF FIGURES	vii
LIST OF APPENDICES	ix
1-INTRODUCTION	1
1.1 Objective of thesis	1
1.2 Property locations and access	2
1.2.1 Geologic Setting	5
1.2.2 Geologic setting in the Wabigoon subprovince	5
1.2.3 Geologic setting in the Quetico subprovince	10
1.2.4 Geologic setting in the Beardmore-Geraldton greenstone belt	12
1.2.5 Gold mineralization in the Wabigoon subprovince and Beardmore-Geraldton greenstone belt	16
2-DATA COLLECTION	29
2.1 Regional and trench mapping	29
2.2 Petrography and Scanning Electron Microscope (SEM)	29
3-OBSERVATIONS	31
3.1 The Wabigoon subprovince	31
3.2 The Beardmore-Geraldton greenstone belt	53
3.2 The Quetico subprovince	76
3.2 Observations of historical outcrops in the Beardmore-Geraldton greenstone belt ..	85
3.9 Summary of the Wabigoon subprovince	87
3.8 Summary of the Beardmore-Geraldton greenstone belt	90
3.9 Summary of the Quetico subprovince	92
4-DISCUSSION AND INTERPRETATIONS	95
4.1 Overview	95
4.2 Structure	100
4.3 Rheology	104
4.4 Suprovinces and greenstone belt	112

4.4.1	Wabigoon subprovince	112
4.4.2	Beardmore-Geraldton greenstone belt.....	113
4.4.3	Quetico subprovince	115
4.5	Gold mineralization models.....	115
5	SUMMARY AND CONCLUSIONS	120
4.5.1	Recommendations	125
7	REFERENCES	127
Appendix A:	Table of sample locations and descriptions	134

LIST OF FIGURES

Fig. 1.1: The location of Greenstone, Ontario	2
Fig. 1.2: The municipality of Greenstone, highways, and roads	3
Fig. 1.4: The Beardmore-Geraldton greenstone belt between the Wabigoon and Quetico subprovinces.	9
Fig. 1.5: The Humbolt Bay High Strain Zone (HHSZ), Paint Lake Shear Zone (PLSZ), Barton Bay Deformation Zone (BBDZ), Burrows River Deformation Zone (BRDZ), and the Klob and Klotz Lake Shear Zones (KKSZ).....	11
Fig. 1.6: Regional map of historical mines	22
Fig. 3.1: The Elmhirst Lake pluton in the Wabigoon subprovince.....	33
Fig. 3.2: The Wabigoon subprovince study area.	38
Fig. 3.3: Photomicrograph in plane polarized light of the gold mineralized chlorite schist from the Golden Mile trench in the Elmhirst property	39
Fig. 3.4: Photomicrographs in cross-polarized light and reflected light of the gold mineralized quartz vein from the Golden Mile trench in the Elmhirst property.	42
Fig. 3.5: Photomicrographs in cross-polarized light and reflected light of the gold mineralized quartz vein from the Golden Mile trench in the Elmhirst property	43
Fig. 3.6: Photomicrographs of cross-polarized light and reflected light of the gold mineralized quartz vein from the Golden Mile trench in the Elmhirst property	44
Fig. 3.7: Photomicrographs of cross-polarized light and reflected light of the gold mineralized quartz vein from the Golden Mile trench in the Elmhirst property	45
Fig. 3.8: Photomicrographs of cross-polarized light and reflected light the gold mineralized quartz vein from the Golden Mile trench in the Elmhirst property.	46
Fig. 3.9: Findian 3 Trench map.....	47
Fig. 3.9: Photomicrographs in cross-polarized light from the Brenbar trench in the Elmhirst.....	52
Fig. 3.11: Photomicrographs in cross-polarized light from the Castlewood trench in the Castlewood property	53
Fig. 3.12: The Pagwachuan property map	58
Fig. 3.13: Photomicrograph in cross-polarized light from the Pagwachuan trench #1 in the Pagwachuan property.....	61
Fig. 3.14: Pagwachuan Trench 1.....	65
Fig. 3.15: Pagwachuan trench 1	66
Fig. 3.16: Pagwachuan trench 1	67
Fig. 3.17: Pagwachuan trench 1	68
Fig. 3.18: Pagwachuan trench 2.....	71
Fig. 3.19: Photomicrograph in cross-polarized light and reflected light from the Pagwachuan trench #2 in the Pagwachuan property.....	72
Fig. 3.20: Photomicrograph in cross-polarized light and reflected light from the Pagwachuan trench #2 in the Pagwachuan property.....	73
Fig. 3.21: Photomicrograph in cross-polarized light and reflected light from the Milestone property	74
Fig. 3.22: Photomicrographs in reflected light from the Milestone property	75
Fig. 3.23: McKay trench	79
Fig. 3.24: Samples and outcrop from McKay trench.....	80

Fig. 3.25: Photomicrographs in cross-polarized light and reflected light from the McKay trench in the Pagwachuan property	81
Fig. 3.26: Photomicrographs in cross-polarized light and reflected light from the McKay trench in the Pagwachuan property	82
Fig. 3.27: Photomicrographs in cross-polarized light and reflected light from the McKay trench in the Pagwachuan property	83
Fig. 3.28: Photomicrographs in plane-polarized light and reflected light from the McKay trench in the Pagwachuan property	84
Fig. 3.29: Photomicrographs in reflected light from the McKay trench in the Pagwachuan property	85
Fig. 3.30: Outcrop from the Highway 584 and Highway 11 outcrops	88
Figure 3.31: Occurrence and distribution of gold grains in thin section	94
Fig. 4.1: Regional shear zones along the Wabigoon and Quetico subprovince boundary	107

LIST OF APPENDICES

APPENDIX A: Table of sample locations and descriptions.....134

1-INTRODUCTION

1.1 Objective of thesis

The purpose of this study is to investigate the control on gold mineralization in the Beardmore-Geraldton greenstone belt and the surrounding Wabigoon and Quetico subprovinces. The hypothesis is that both structure and microstructure in the study area are more important factors in gold mineralization than any other variable considered, including: lithology, metamorphic grade, alteration, and subprovince.

To test this hypothesis field mapping and petrography were used to characterize the lithology, structure, microstructure, metamorphic grade, alteration, and subprovince and their relationship to gold mineralization in the Elmhirst, Castlewood, Pagwachuan, and Milestone properties. Representative samples were collected from all properties and studied both in hand sample and in thin section. For each property and each sample characteristics associated with gold mineralization were noted in order to identify which, if any, characteristic is common to all gold occurrences. Gold mineralization is observed to occur in a variety of different lithologies, at different grades of metamorphism, and with different styles of alteration within the Beardmore-Geraldton greenstone belt as well as within the adjacent Wabigoon and Quetico subprovinces. However gold mineralization always occurs in deformed rock with evidence for strain heterogeneity during ductile or brittle-ductile deformation. This indicates that structure and microstructure are the most important controls on gold mineralization in the study area.

1.2 Property locations and access

This study is based on an examination of two classic localities in the Beardmore-Geraldton greenstone belt and five properties held by Kodiak Exploration Ltd. and Prodigy Gold Inc. within the Wabigoon and Quetico subprovinces (Fig. 1.1, 1.2, 1.3). The properties in this study are located within the municipality of Greenstone, Ontario. Greenstone is located 255km northeast of Thunder Bay, Ontario (Fig. 1.1). The municipality of Greenstone is located within the study area and includes the communities of Beardmore, Jellicoe, Geraldton, Caramat, and Longlac (Fig. 1.2).



Fig. 1.1: Location map of Greenstone, Ontario

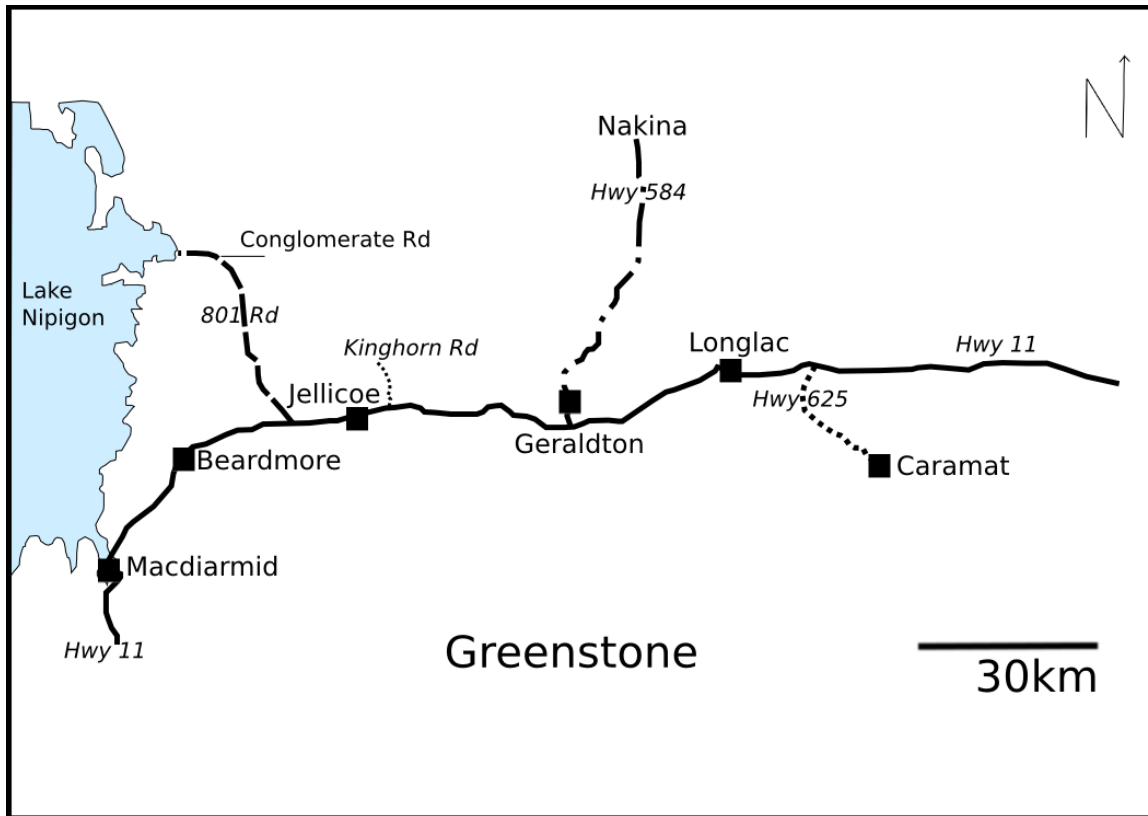


Fig. 1.2: Location map of the municipality of Greenstone, highways, and roads

The classic localities of the Leitch Mine, Highway 11 outcrop, and Highway 584 outcrop are all accessible by the TransCanada Highway 11 (Figs. 1.2, 1.4). The Leitch Mine is accessible by road from the TransCanada Highway 11 and north along Highway 580 (Poplar Point Road) (Fig. 1.2, 1.4). The Highway 584 outcrop is accessible along Highway 584 north of Geraldton, at the junction of Highway 584 and Tower Road (Figs. 1.2, 1.4). The Highway 11 outcrop, that includes the historical MacLeod-Cockshutt Mine site and Porphyry Hill, is located south of Geraldton at the junction of 584 Highway and the TransCanada Highway 11 (Figs. 1.2, 1.4). The outcrops had been recently cleared at the time of study. The Leitch Mine, Highway 584 outcrop, and Highway 11 outcrop are located within the Beardmore-Geraldton greenstone belt (Fig. 1.2-1.4).

The Kodiak Exploration Ltd. and Prodigy Gold Inc. properties include the Elmhirst (including the Golden Mile, Lucky Strike, the Straights, Findian 3, and Brenbar trenches and Missing Link outcrop), Castlewood, Pagwachuan property (including Pagwachuan trench #1, Pagwachuan trench #2, and McKay trench), and Milestone properties (Fig. 1.4). The Elmhirst, Castlewood, and Pagwachuan trenches and outcrops mapped within this study were recently completely cleared at the time of study. The outcrop was freshly uncovered in the property-scale mapping in the Elmhirst and Pagwachuan properties. Only drillcore was studied at Milestone property as no trenches or outcrops were present due to overburden. The Elmhirst, Castlewood, and properties are all located within the Wabigoon subprovince while the Milestone property is located within the Beardmore-Geraldton greenstone belt (Fig. 1.3). (Fig. 1.3). The northern extent of the Pagwachuan property is located within the Beardmore-Geraldton greenstone belt and southern portion is located in the Quetico subprovince (Fig. 1.3).

The Elmhirst property, including the Golden Mile, Lucky Strike, the Straights, and Findian 3 trenches, is accessible via the TransCanada Highway 11, turning north onto the gravel Kinghorn Road (Figs. 1.2, 1.4). Access to the Brenbar trench in the Elmhirst property is accessible from the TransCanada Highway, turning onto the gravel 801 Road and is located at the historic Brenbar mine area (Fig. 1.2). The Castlewood property is accessible north from the TransCanada Highway, via the gravel 801 Road, and east onto Conglomerate Road (Fig. 1.2, 1.4). The Milestone property is accessible via the TransCanada Highway 11 and south onto East Road (Figs. 1.2, 1.4). The Pagwachuan property is accessible via Highway 11, south onto the gravel East Road or Catlinite Road

adjacent to Highway 625, and onto the gravel Seagram Lake Road (Figs. 1.2, 1.4). The Pagwachuan and McKay trenches are located off the Seagram Lake Road. The coordinates for the samples collected from the properties and trenches are listed in Appendix A and are given in the Universal Transverse Mercator (UTM) coordinate system with the North American Datum of 1983 reference system.

1.2.1 Geologic Setting

The study area is located along the boundary of the Wabigoon and Quetico subprovinces in the Superior province of the Canadian Shield (Fig. 1.4). The Wabigoon subprovince is primarily composed of metamorphosed intrusive and extrusive igneous rocks that have been dated to 3000 Ma (Kresz, 1991; Stott *et al.*, 2007). The boundary between the Wabigoon and Quetico subprovince is the host to numerous historic and current gold occurrences (Davis and Smith, 1991). The Quetico subprovince is predominantly metamorphosed sedimentary and metamorphosed intrusive igneous lithologies. No historic gold deposits or occurrences are present in the Quetico subprovince. The study area encompasses the southeastern portion of the Wabigoon subprovince and northeastern portion of the Quetico subprovince (Kresz, 1991; Stott *et al.*, 2007). The western extent of the Wabigoon subprovince in the study area is further categorized as the Onaman-Toshota greenstone belt.

1.2.2 Geologic setting in the Wabigoon subprovince

The study area within the southeastern Wabigoon subprovince extends from the eastern shore of Lake Nipigon to Longlac (Fig. 1.3). The Onaman-Tashota greenstone belt begins at the eastern shore of Lake Nipigon and continues to the north of Jellicoe.

The belt is located along the southern boundary of the Wabigoon subprovince and the northern boundary of the Beardmore-Geraldton greenstone belt. The Onaman-Tashota greenstone belt is composed of primarily felsic to mafic metavolcanic and metaplutonic lithologies and has yielded U-Pb dates of 2700-3050 Ma (Blackburn and Johns, 1988; Stott *et al.*, 1998).

The three largest plutons in the area are the Coyle Lake, Elmhirst Lake, and Kaby Lake plutons (Fig. 1.4) (Mackasey and Wallace, 1978; Kresz, 1991). The plutons are felsic to intermediate and grade from meta-granodiorite to trondhjemite with minor occurrences of granite, quartz monzonite, and quartz diorite (Mackasey and Wallace, 1978). The felsic plutons intrude intermediate to mafic metavolcanic lithologies of the Elmhirst-Rickaby assemblage (Mackasey and Wallace, 1978; Stott *et al.*, 2002).

The Missing Link outcrop and a portion of the Elmhirst property are located within the felsic to mafic Elmhirst-Rickaby metavolcanic assemblage (Fig. 1.4). The Golden Mile, Lucky Strike, the Straights, and Findian 3, and Brenbar trenches are located within the Coyle Lake, Elmhirst Lake, and Kaby Lake plutons.

The Elmhirst pluton and adjacent Kaby Lake pluton yielded U-Pb dates of 2736 ± 1.5 Ma and 2734 ± 1 Ma respectively (Stott *et al.*, 2002). The felsic to mafic metavolcanic lithologies of the Elmhirst-Rickaby assemblage yielded an U-Pb date of 2740 ± 1.1 Ma (Stott *et al.*, 2002).

The Coyle Lake, Elmhirst Lake, and Kaby Lake plutons typically exhibit intercrystalline igneous textures but Mackasey and Wallace (1978) observed that the quartz and microcline along the margins of the Coyle and Elmhirst Lake plutons are strained, anhedral, and when located together exhibit myrmekitic textures (Mackasey and Wallace, 1978).

North of the Coyle Lake, Elmhirst Lake, and Kaby Lake plutons are the Castlewood, Crooked Green Lake, South Onaman, and Boundary gabbro to diorite intrusions (Amukun, 1980) (Fig. 1.4). The Conglomerate Lake metaconglomerate to metasandstone is located within basaltic to andesitic mafic metavolcanic and andesitic to rhyolitic felsic metavolcanic lithologies (Amukun, 1980). The Castlewood property is located within the Conglomerate Lake metaconglomerate to metasandstone and mafic metavolcanic lithologies (Fig. 1.4).

The Onaman-Toshota greenstone belt exhibits an increase in metamorphic grade from lower greenschist facies in the southwest, near Beardmore, and increases to upper greenschist facies in the north, in the Castlewood property north of Jellicoe (Amukun, 1980).

The regional shear zones within the Onaman-Toshota greenstone belt are the Paint Lake shear zone (PLSZ) and the Humbolt Bay High Strain Zone (HHSZ) (Reilly, 1987; Culshaw *et al.*, 2006) (Fig. 1.5). The Paint Lake Shear Zone is within the Elmhirst-Rickaby assemblage and separates the Onaman-Tashota and Beardmore-

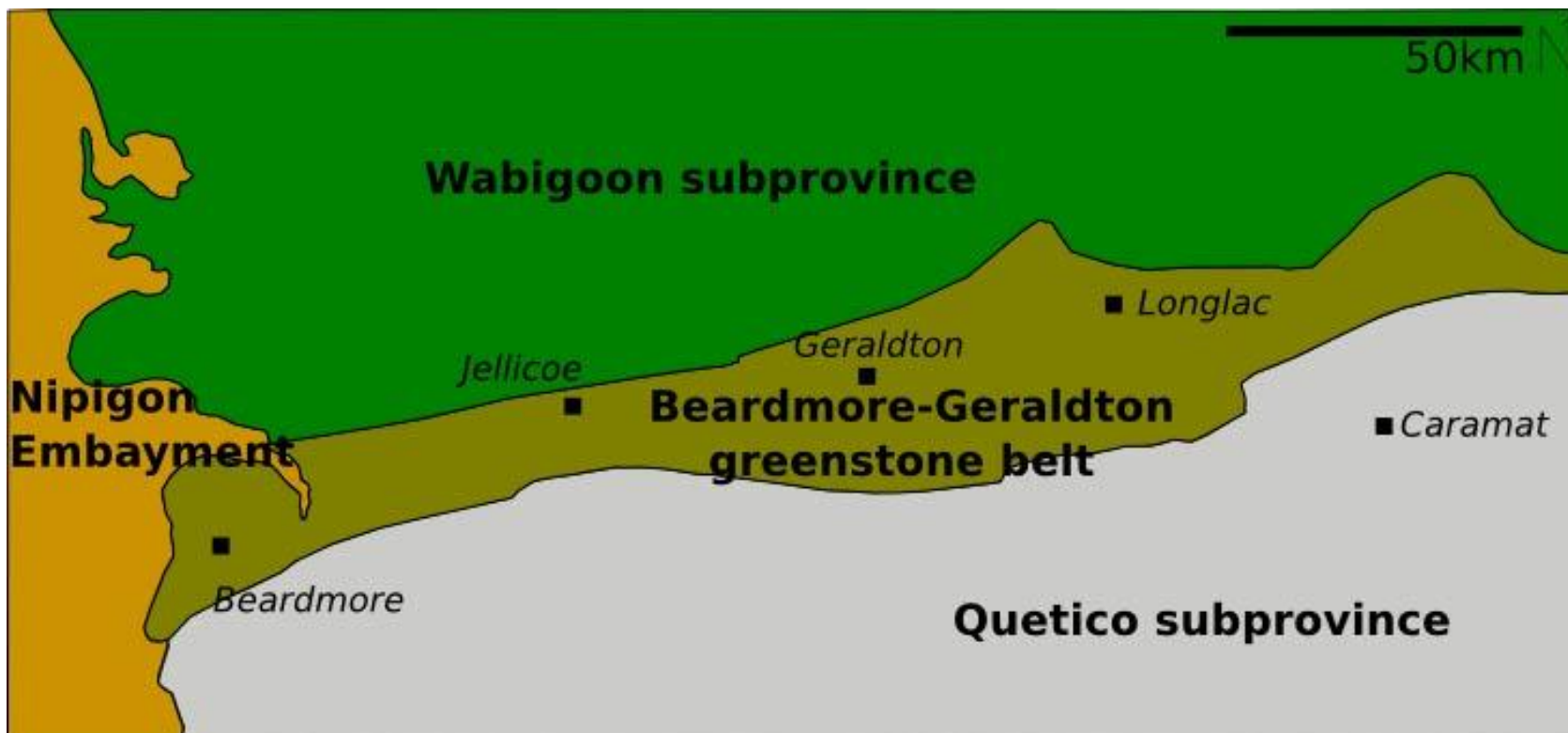


Fig. 1.3: Location map of the Wabigoon and Quetico subprovinces and Beardmore-Geraldton greenstone belt in the Superior Province of Canada (After Johns *et al.*, 2003).

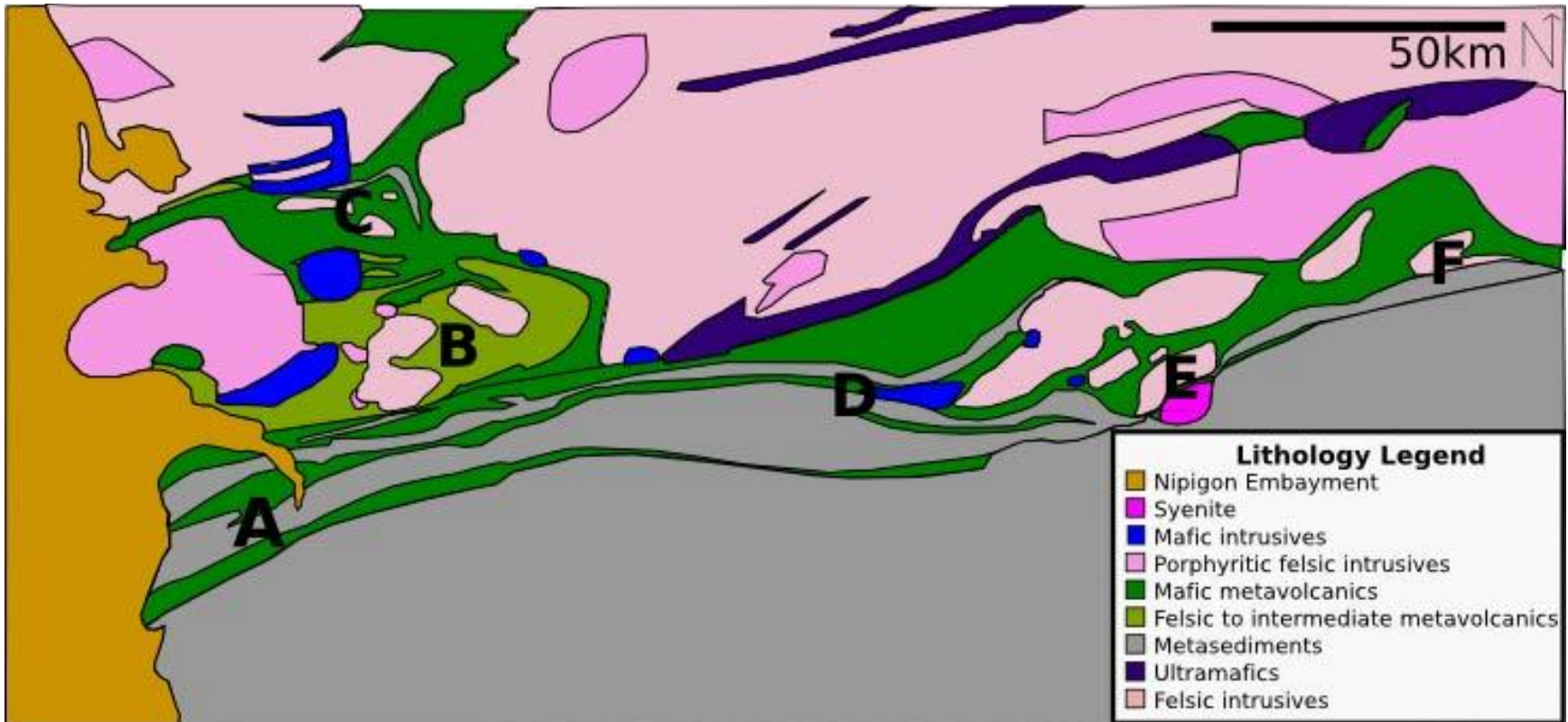


Fig. 1.4: Location and geological map of the Beardmore-Geraldton greenstone belt between the Wabigoon and Quetico subprovinces: A. Leitch Mine, B. Elmhirst property, C. Castlewood property, D. Highway 11 and Highway 584 outcrops, E. Pagwachuan property, F. Milestone property (After Johns *et al.*, 2003).

Geraldton greenstone belts, strikes east-west, and has a vertical dip (Reilly, 1987). The PLSZ is approximately 50 km long and approximately 1 km wide.

The mylonites within the PLSZ exhibit microstructures, such as grain size reduction and recrystallization, that provide evidence for dislocation creep to diffusion creep (Reilly, 1987; Culshaw *et al.*, 2006). The HHSZ is located at the northern edge of the Onaman-Tashota greenstone belt within metavolcanics and metaconglomerate lithologies and is approximately 20 km wide and approximately 800km long (Culshaw *et al.*, 2006).

1.2.3 Geologic setting in the Quetico subprovince

The southernmost portion of the study area is located in the Quetico subprovince near Caramat. The lithologies located in the area include metasandstone, metasilstone, metaconglomerate, metamorphosed banded iron formation, and to a lesser degree various types of granitic plutons, gneisses, and migmatites (Kresz and Zayachivsky, 1993). The Pagwachuan property is located in the Quetico subprovince near Caramat (Fig. 1.4). The Seagram Lake pluton is located within the study area and is an equigranular syenite that crosscuts the metasedimentary lithologies (Fig. 1.4; Kresz and Zayachivsky, 1993). The metavolcanic and metasedimentary lithologies in the Wabigoon subprovince may also continue into the Quetico subprovince study area (Pye *et al.*, 1966; Stott, 1984a, 1984b; Kresz, 1991).

Metamorphic grade within the Quetico subprovince increases from the margins of the subprovince to the centre of the subprovince, from greenschist to amphibolite facies,

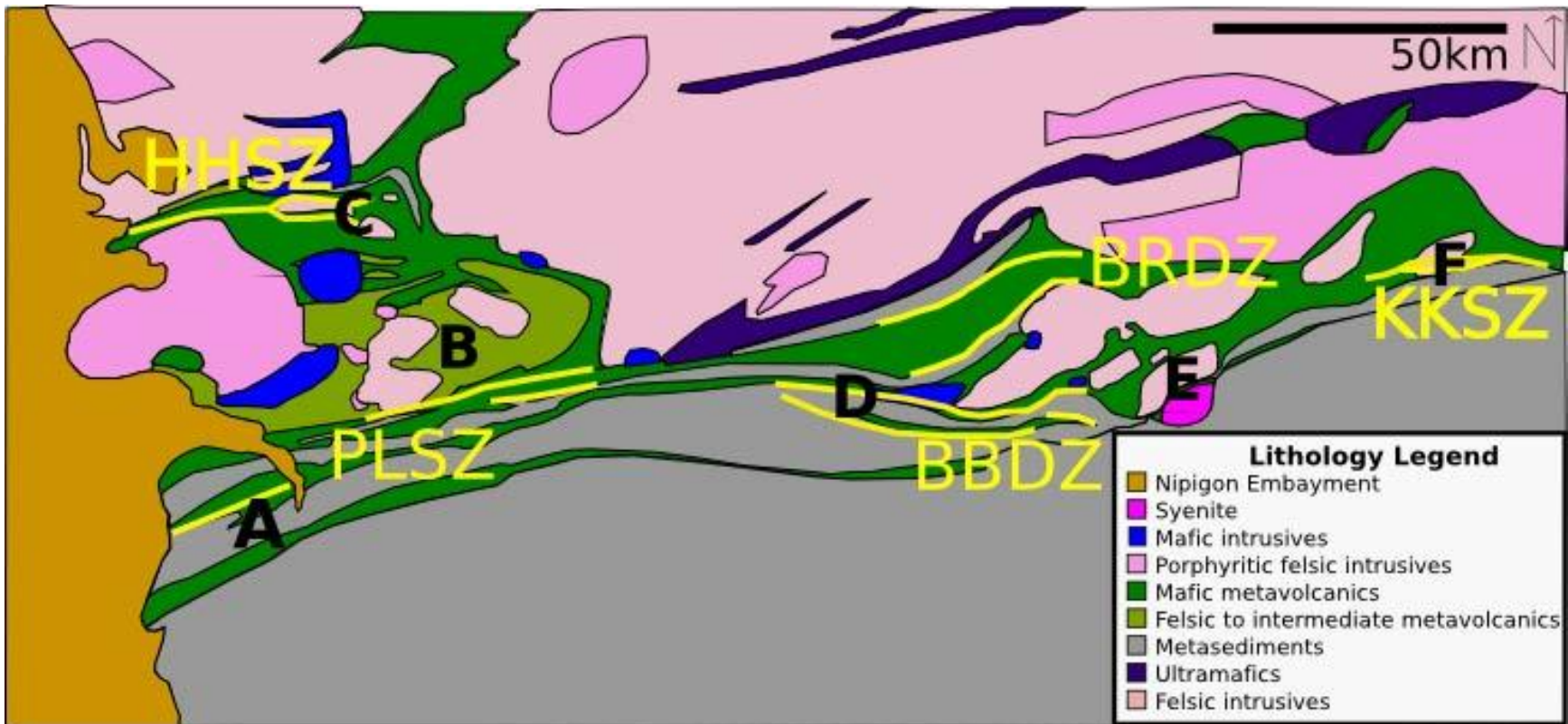


Fig. 1.5: Location and geology map of the Humbolt Bay High Strain Zone (HHSZ), Paint Lake Shear Zone (PLSZ), Barton Bay Deformation Zone (BBDZ), Burrows River Deformation Zone (BRDZ), and the Klob and Klotz Lake Shear Zones (KKSZ) denoted by solid yellow lines (After Johns *et al.*, 2003).

with minor areas of granulite facies in the south-central region of the subprovince (Pan and Fleet, 1994). The northern boundary of the Quetico subprovince has yielded U-Pb dates from detrital zircon of 2698 ± 3 to 3009 ± 4 Ma (Davis *et al.*, 1990). A cross-cutting pluton provides an upper age limit from an U-Pb zircon date of 2688 ± 4 Ma (Davis *et al.*, 1990).

1.2.4 Geologic setting in the Beardmore-Geraldton greenstone belt

The Beardmore-Geraldton greenstone belt is located between the Wabigoon subprovince to the north and the Quetico subprovince to the south (Figs. 1.3, 1.4). The northern boundary of the Beardmore-Geraldton greenstone belt is located along the southern boundary of the Onaman-Tashota greenstone belt within the Paint Lake shear zone. The Beardmore-Geraldton greenstone belt is composed of repeating lithologies of metasedimentary and metavolcanics (Barrett and Fralick, 1986; Devaney and Williams, 1989; Smyk *et al.*, 2005). The northern metasedimentary sub-belt (NMB), northern volcanic sub-belt (NVB), central metasedimentary sub-belt (CMB), central volcanic sub-belt (CVB), southern metasedimentary sub-belt (SMB), and southern volcanic sub-belt (SVB) comprise the six sections of alternating lithologies (Devaney and Williams, 1989; Smyk *et al.*, 2005). Many of these sub-belts have been mapped into the Wabigoon and Quetico subprovinces by other authors (Pye *et al.*, 1966; Stott, 1984a; Stott, 1984b; Kresz, 1991).

The southern metavolcanic sub-belt (SVB) is composed of metamorphosed chlorite schist, mafic tuffs, lapilli tuffs, tuff breccias, felsic to mafic intrusives, and chemical metasedimentary lithologies (Mason *et al.*, 1985; Smyk *et al.*, 2005). The

chemical metasedimentary lithologies, primarily banded iron formation, are commonly discontinuous lenses with an east-west strike and a near vertical dip (Peach, 1951). The chemical metasedimentary lithologies are composed of alternating layers of iron-rich carbonate, recrystallized chert, magnetite, and grunerite (Mason *et al.*, 1985). Mafic metavolcanic rocks host the gold-bearing chemical metasedimentary lithologies and quartz-carbonate veins within the southern mafic-dominated volcanic belt. The Northern Empire gold mine is located within the southern mafic-dominated volcanic belt (Mason *et al.*, 1985).

The central metavolcanic sub-belt (CVB) is predominantly composed of intermediate massive and pillowed flows, tuffs and breccias. The northern volcanic sub-belt (NVB) is also dominated by intermediate lithologies, especially andesite (Smyk *et al.*, 2005). The NVB has been further subdivided into the Bish Bay assemblage to the north and the Poplar Point assemblage to the south (Hart *et al.*, 2002).

The southern metaedimentary sub-belt (SMB) is composed of metasedimentary lithologies such as conglomerate, sandstones (wacke and argillite), and banded iron formation (magnetite, hematite, and jasper) (Mason *et al.*, 1985). Felsic to mafic intrusions and mafic volcanic lithologies are also present throughout the belt. The gold mineralization in the southern metasedimentary-dominated belt is located within shear zones and areas of brecciation in clastic metasedimentary lithologies, felsic to mafic intrusions, sulphides in banded iron formation, and metavolcanic lithologies. Gold

mineralization only occurs in the sub-belt within areas of shear zones, isoclinal folds, and drag folds (Mason *et al.*, 1985).

The central and northern metasedimentary sub-belts (CMB and NMB, respectively) are also dominated by metaconglomerate and metasandstone lithofacies (Smyk *et al.*, 2005). The lithofacies associations within the NMB provide evidence for a fluvial fan and/or a braid plain environment (Devaney and Fralick, 1985). The CMB reflects this depositional environment as well for the top-third of the assemblage. The bottom-third of the CMB is similar to the SMB described above. The SMB lithofacies associations provide evidence for a marine environment, except for the rare metaconglomerate assemblage (Devaney and Fralick, 1985; Smyk *et al.*, 2005).

The regional shear zones within the Beardmore-Geraldton greenstone belt include the Tombill-Bankfield Fault, Portage Shear, Little Long Lac Fault, or collectively known as the Barton Bay Deformation Zone (BBDZ) (Fig. 1.5; Pye, 1951; Buck, 1986). The Burrow River Deformation Zone (BRDZ) is located north of Geraldton (Fig. 1.5). The shear zones typically strike east-west with a near-vertical dip. The shear zones anastomose and show evidence for ductile and brittle-ductile deformation (Lavigne, 1983; Buck and Williams, 1984). Protomylonites to ultramylonites exhibit evidence for deformation mechanisms in thin section, including grain size reduction from 100 μm to 5 μm (Buck, 1986).

The Pagwachuan property is located along the boundary between the Beardmore-Geraldton greenstone belt and the Wabigoon subprovince, adjacent to the Hollowrock Lake stock (Figs. 1.3, 1.4). The Pagwachuan trench #2 is located completely within the Hollowrock Lake stock (Fig. 1.4). The Milestone property is located within the Paglamin Lake stock within amphibolite and meta-granodiorite (Fig. 1.4).

The regional shear zones in the Beardmore-Geraldton greenstone belt in and around Longlac include the eastern continuation of the Barton Bay deformation zone (BBDZ) and Burrows River deformation zone (BRDZ), as well as the Klob Lake and Klotz Lake shear zones (KKSZ) (Kresz and Zayachivsky, 1993; Fig. 1.5). The shear zones are kilometers to metres wide, kilometers to tens of kilometers long, and anastomose around competent lithologies in the study area (Kresz and Zayachivsky, 1993).

The Beardmore-Geraldton greenstone belt in and around Longlac is characterized by the Croll Lake, Theresa, Hollowrock Lake, O'Meara Lake, Wee David Lake, and Paglamin Lake felsic to intermediate plutons within mafic to intermediate metavolcanic lithologies (Fig. 1.4; Amukun, 1983; Kresz, 1991). The felsic Croll Lake, Theresa, and Hollowrock Lake plutons and metavolcanic host rock have been proposed to be a set of lithologies that extend from the eastern shore of Lake Nipigon to Longlac, a distance of 145 km (Pye *et al.*, 1966; Stott, 1984a, 1984b; Kresz, 1991). The Croll Lake pluton ranges from an equigranular to foliated meta-granodiorite with minor amounts of granite, monzonite, quartz monzonite, and quartz monzodiorite (Kresz, 1991). The Theresa stock

ranges from metadiorite to metatonalite. The historical Theresa gold mine was located within the Theresa pluton (Speed and Craig, 1992). The metatonalite exhibits evidence of recrystallization in thin section (Kresz and Zayachivsky, 1993). The Hollowrock Lake pluton is an equigranular to foliated meta-granodiorite and tonalite (Kresz, 1991). The O'Meara Lake stock is equigranular to foliated meta-granodiorite to porphyritic granodiorite. The Wee David Lake pluton is equigranular to foliated metamorphosed trondhjemite to granodiorite. The Paglamin Lake stock is equigranular to foliated metagranodiorite to trondhjemite. The Paglamin Lake stock exhibits blue quartz "eyes", sericitized plagioclase phenocrysts, and xenoliths of amphibolite (Kresz and Zayachivsky, 1993). In thin section the quartz within the stock exhibits grain size reduction, recrystallization, and undulatory extinction (Amukun, 1983). Minor amounts of amphibolite commonly occur within metavolcanics lithologies and rare lamprophyre dykes crosscut all lithologies (Kresz and Zayachivsky, 1993).

The shear zones within the Wabigoon and Quetico subprovinces and Beardmore-Geraldton greenstone belt exhibit deformation features that suggest both transcurrent and transpressive components (Buck, 1986; Reilly, 1987; Culshaw *et al.*, 2006). Structures that have been documented suggest that transcurrent deformation outweighs the transpressive components (Smyk *et al.*, 2005).

1.2.5 Gold mineralization in the Wabigoon subprovince and Beardmore-Geraldton greenstone belt

The study area has a long history of gold mining, from Beardmore in the west to Longlac in the east (Fig. 1.6). Current gold exploration is present within past mine sites

and newly discovered zones within the Wabigoon and Quetico subprovinces and Beardmore-Geraldton greenstone belt (Speed and Craig, 1992; Smyk *et al.*, 2005).

The Maloney Sturgeon Mine is located approximately 2.4 km northeast of Twin Falls on the Sturgeon River (Namewaminikan River) in the Wabigoon subprovince (Fig. 1.6; Speed and Craig, 1992). Laird (1937) described the ore as a glassy, fractured quartz vein with a strike of 50° and dip of 70°S within fairly massive diorite. Pyrite was the most abundant sulphide in the ore zone. A shear zone was noted striking at 45° adjacent to the ore zone. Stockwork quartz veins hosted within feldspar porphyry only a few feet away from the ore exhibited little to no mineralization (Laird, 1937; Speed and Craig, 1992).

The Brenbar Mine is located in the northeastern portion of Irwin Township, west of the Sturgeon River Mine, and south of the Sturgeon River (Namewaminikan River) in the Wabigoon subprovince (Fig. 1.6; Speed and Craig, 1992). Mackasey (1975) reported that the Brenbar area is underlain by deformed tuff, flows, and pyroclastic breccia of felsic to intermediate composition and quartz feldspar porphyry that strike 80° . Quartz veins strike 75° and dip 80°S and exhibit folding and pinch and swell features. Laird (1937) observed gold in fractures in pyrite and related to slip planes in quartz, sericite, and chlorite (Laird, 1937; Speed and Craig, 1992).

The Sturgeon River Mine is located 20.9 km northeast of Beardmore in the Wabigoon subprovince (Fig. 1.6; Speed and Craig, 1992). Mackasey (1975) stated that

the quartz veins that host gold mineralization strike N13°E and dip 70°E to 70°W. The quartz veins are hosted within schistose intermediate to felsic metavolcanic lithologies and granodiorite. Bruce (1937a) described the quartz as being younger than calcite and exhibiting different grain sizes. Gold mineralization is associated with sericite and occurs with pyrite, chalcopyrite, and sphalerite (Bruce, 1937; Speed and Craig, 1992).

The Greenoaks Mine site is located approximately 27 km northeast of Beardmore in the Wabigoon subprovince (Fig. 1.6; Speed and Craig, 1992). Mason and White (1986) described the Greenoaks Mine area as being hosted along the Elmhirst granodiorite pluton and metavolcanic host rock margin in a shear zone striking 75°-85°. They stated that the gold mineralization is found within quartz veins located in ductile shear zones within metavolcanic lithologies. The smokey-grey quartz veins strike 115°/80°S with gold mineralization occurring as free gold associated with sulphides, like pyrrhotite (Mason and White, 1986; Speed and Craig, 1992).

The Dik-Dik Mine site is located north of Atigogama Lake in the northeastern area of Rickaby Township, adjacent to the western boundary of Lapierre Township in the Wabigoon subprovince (Fig. 1.6; Speed and Craig, 1992). Mason and White (1986) described the area of the Dik-Dik Mine, or Orphan Mine, as being underlain by the Kaby Lake Stock granodiorite that intrudes a felsic to intermediate metavolcanic unit. Bruce (1937a) stated that a competency contrast between the stock and the metavolcanic lithologies might have created the gold mineralized quartz veins and lenses. Shear zones strike at 40° with a near vertical dip along the contact of the two lithologies. Bruce

(1937a) also stated that the shear zones postdate the Kaby Lake Stock as “gneissoid” fabric is located in the pluton and the contact is offset. He found that the quartz in the vein is so fine-grained that it appears “chalcedonic”. His petrographic work recognized that gold was a late mineral and occurred in pyrite or associated with galena (Bruce, 1937a; Speed and Craig, 1992).

Mackasey (1976) described the gold mineralization around Jellicoe as being hosted in quartz veins and granodiorite while in Beardmore and Geraldton the gold mineralization is hosted in banded iron formation. The banded iron formation around Jellicoe does not host gold although it is similar to the iron formation in Beardmore and Geraldton (Mackasey, 1976).

Tyson (1945) stated that there is a profound spatial relationship between the Paint Lake Fault (PLSZ) and gold mineralization. He suggested that channelways could provide a path for gold-bearing solutions to flow and concentrate (Tyson, 1945). Although further research by Smyk *et al.* (2005) and Magi (2010) suggests that gold mineralization is erratic directly within the Paint Lake shear zone.

The Sand River Mine is located approximately 10 km northwest of Beardmore in the Beardmore-Geraldton greenstone belt (Fig. 1.6; Speed and Craig, 1992). Ferguson *et al.* (1971) described the Sand River quartz vein as striking 60-70° within a shear zone in greywacke that strikes and dips 85°/80°N. Mason and White (1986) continue this description by stating that the mine site is continuous with the Leitch Mine in the western

portion of the site and as such should exhibit similar features. The gold mineralization within the quartz vein is located within greywacke and is associated with chlorite, sericite, ankerite, pyrite, arsenopyrite, and tetrahedrite. Laird (1937) described the quartz veins in detail and described how the veins follow the shear zones at 60-70° and pinch and swell along strike and dip. The quartz veins that strike perpendicular are a later generation and do not host gold. The sinuous quartz veins are also cut off and displaced by later, eastern dipping thrust faults. Laird also noted that the quartz veins are sometimes folded (Laird, 1937; Speed and Craig, 1992).

The Leitch Mine is located approximately 4 km west-northwest of Beardmore in the Beardmore-Geraldton greenstone belt (Fig. 1.6; Speed and Craig, 1992). Mason and White in Patterson *et al.* (1985) described the lithologies and gold mineralization in the Leitch Mine area in the southern metasedimentary sub-belt and southern metavolcanic sub-belt. The southern metasedimentary sub-belt is composed of greywacke, conglomerate, argillite, iron formation, and mafic intrusions while the southern metavolcanic sub-belt is composed of intermediate to mafic metavolcanic lithologies (Patterson *et al.*, 1985; Speed and Craig, 1992).

The southern metasedimentary sub-belt has hosted up to 94% of the gold mined in the Leitch Mine (Patterson *et al.*, 1985; Speed and Craig, 1992). The gold mineralization is hosted in two sets of quartz veins within fractures in greywacke. The quartz veins are parallel to the regional shear zones and contain folds and healed tension gashes. The quartz veins are white to grey with chlorite and sericite occurring in fractures within the

veins. Sulphides present in the veins are arsenopyrite, pyrite, tetrahedrite, and sphalerite (Patterson *et al.*, 1985; Speed and Craig, 1992).

The historic Northern Empire Mine is located 1.6 km northeast of Beardmore within the Beardmore-Geraldton greenstone belt (Speed and Craig, 1992; Fig. 1.6). Mason and White (1986) described the mine site as being located at the boundary between the southern metavolcanic and southern metasedimentary belts at the edge of the Wabigoon subprovince. The boundary is a 2 m wide shear zone with fault gouge present within. The host rock is at the contact between metamorphosed turbidities and stretched, metamorphosed pillow basalts. The boudinaged quartz vein that hosts the ore intrudes schistose intermediate to mafic metavolcanic lithologies and strikes $72^{\circ}/80^{\circ}\text{S}$ (Mason *et al.*, 1985).

Pyrite, arsenopyrite, pyrrhotite, native gold, carbonate, galena, and tourmaline mineralize the quartz vein. Gold mineralization is located within the quartz vein and the sheared host rock (Mason and White, 1986). Langford (1929) stated that the quartz vein is milky-white to blueish-white in colour and structurally pinches and swells both vertically and horizontally as well as diverges in some areas (Speed and Craig, 1992).

The Jellicoe Mine site is located west of the Tombill and Bankfield properties within the eastern portion of Lindsley Township in the Beardmore-Geraldton greenstone belt (Fig. 1.6; Speed and Craig, 1992). The ore from the Jellicoe Mine is hosted in

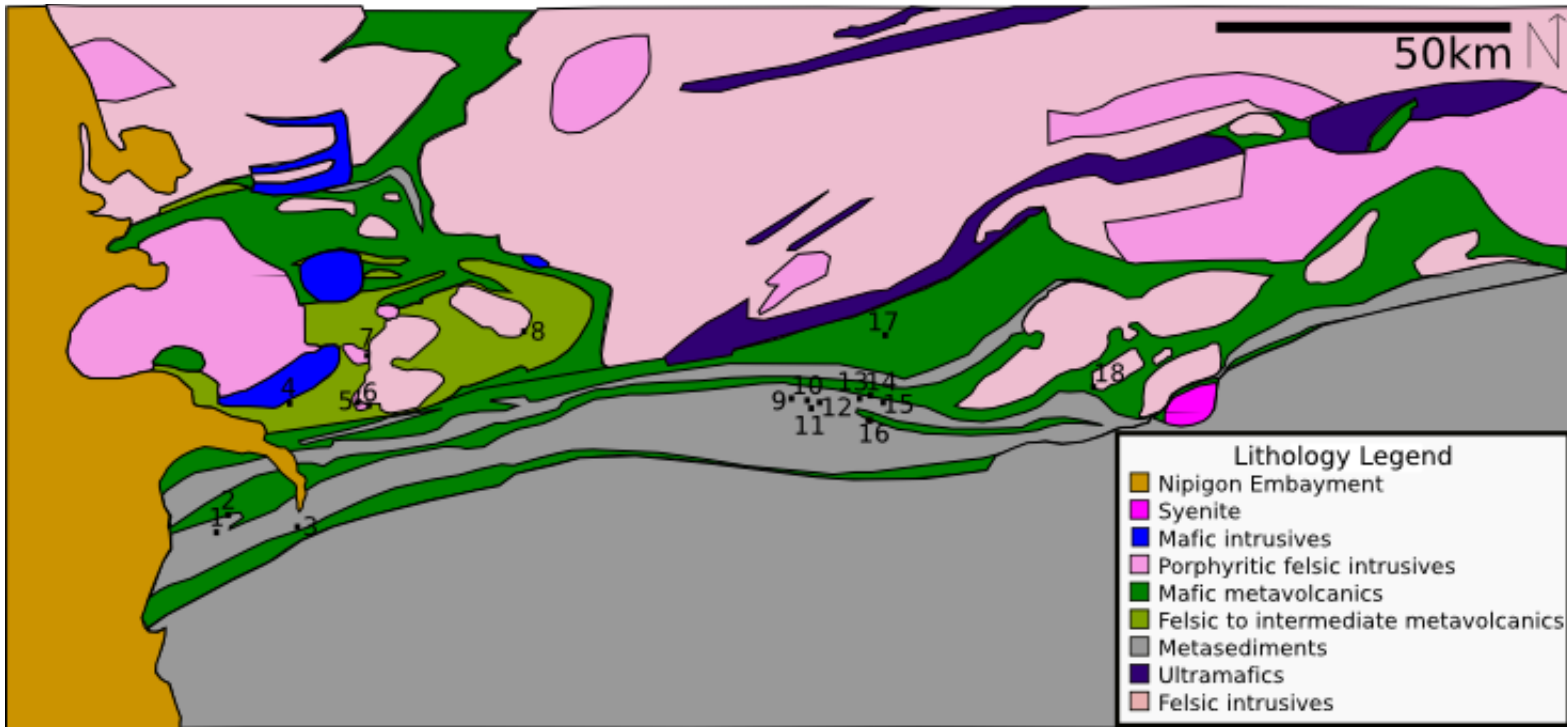


Fig. 1.6: Location and geological map of historical mines: 1. Sand River Mine, 2. Leitch Mine, 3. Northern Empire Mine, 4. Maloney Sturgeon Mine, 5. Brenbar Mine, 6. Sturgeon River Mine, 7. Greenoaks Mine, 8. Dik-Dik Mine, 9. Jellicoe Mine, 10. Bankfield Mine, 11. Tombill Mine, 12. Magnet Consolidated Mine, 13. Little Long Lac Mine, 14. Talmora Long Lac Gold Mine, 15. Hardrock Mine, 16. MacLeod-Cockshutt and Mosher Long Lac Mines, 17. Hutchinson Mine, 18. Theresa Gold Mine (After Speed and Craig, 1992; Johns *et al.*, 2003).

metamorphosed arkose beds with interbedded greywacke and shale units with intrusions of quartz-feldspar porphyry dykes (Matheson, 1948; Mason and White, 1986). Mason and White (1986) described the gold mineralization as being associated with sulphides as well as found in its native state within sheared and brecciated arkose in smokey-grey quartz veins and stringers. The ore from the mine was located in one S-shaped quartz vein in a shear zone within an arkose lithology. The vein had a strike of 60° with a dip to the south, although offshoots of the vein had steep, northward dips (Matheson, 1948; Speed and Craig, 1992).

The Bankfield Mine is located 8.25 km west of the town of Geraldton, along the southwestern part of Magnet Lake in the Beardmore-Geraldton greenstone belt (Fig. 1.6; Speed and Craig, 1992). Ferguson *et al.* (1971) stated that greywacke, with minor conglomerate, slate, and iron formation, is intruded by diorite and quartz porphyry. The contact between the host rock and intrusions is the main ore zone and is highly sheared, brecciated, and silicified. The ore zone strikes 72° - 85° , and dips 70° - 78° S with an average width of 2 m (Speed and Craig, 1992).

The Tombill Mine is located 0.4 km to the southeast of the Bankfield Mine along the eastern boundary of Lindsley Township, north of the TransCanada Highway 11 in the Beardmore-Geraldton greenstone belt (Fig. 1.6; Speed and Craig, 1992). Ferguson *et al.* (1971) and Bruce (1937b) described the ore as being hosted in greywackes and felsic intrusive lithologies within a shear zone. Pyrite, arsenopyrite, pyrrhotite, and gold are hosted within quartz veins in the property (Ferguson *et al.*, 1971; Speed and Craig, 1992).

The Magnet Consolidated Mine is located approximately 8 km southwest of Geraldton in the Beardmore-Geraldton greenstone belt (Fig. 1.6; Speed and Craig, 1992). Pye (1951) described the lithologies present at the Magnet Mine as being mainly metasedimentary, including conglomerate, wacke, slate, iron formation, diorite, diorite porphyry, and albite porphyry. The ore zone is hosted in a shear zone and crosscuts minor folds. Quartz veins as fracture fillings and replacements in greywacke and iron formation host the gold mineralization. The near vertical quartz veins exhibit roll structures. Sulphides rarely comprise more than 5% of the ore and include arsenopyrite, pyrite, and pyrrhotite. Gold mineralization occurs as blebs and as fracture fillings within pyrite and arsenopyrite and also along quartz and calcite vein cleavage planes as irregular grains (Pye, 1951).

The property of Little Long Lac Mine is located near the southern shore of Barton Bay on Lake Kenogamisis Lake, approximately 3.2 km south of Geraldton in the Beardmore-Geraldton greenstone belt (Fig. 1.6; Speed and Craig, 1992). The Little Long Lac Mine is composed of complexly folded metasedimentary lithologies such as conglomerate, arkose, greywacke, slate, and iron formation that have been deformed by an east-west shear zone (Bruce, 1936b). Mason and White (1986) describe the Little Long Lac Mine ore body as being a Z-shaped fold on the north limb of the Barton syncline, which plunges 45° - 55° to the west and in other areas 50° east (Bruce, 1936b).

Pye (1951) described the ore bodies as parallel quartz veins and stringers hosted in fractured, massive arkose beds. The sulphide mineralization in the ore, like

arsenopyrite, pyrrhotite, and sphalerite, rarely comprise more than 3% of the ore (Pye, 1952; Speed and Craig, 1992).

The Talmora Long Lac Gold Mine is located on the south end of Barton Bay on Kenogamisis Lake, approximately 4 km southwest of Geraldton in the Beardmore-Geraldton greenstone belt (Fig. 1.6; Speed and Craig, 1992). Ferguson *et al.* (1971) described the general geology of the mine as being composed of greywackes interbedded with iron formation and intruded by diorite forming westerly-plunging anticlines. Shear zones near the diorite-greywacke contact strike 60° - 80° with 45° - 90° dip north. Quartz lenses and veins are located at the greywacke-diorite contact and are typically less than one foot thick. Pyrite and arsenopyrite are associated with the gold mineralization (Ferguson *et al.*, 1971; Speed and Craig, 1992).

The Hardrock Mine is located 5.6 km southeast of Geraldton in the Beardmore-Geraldton greenstone belt (Fig. 1.6; Speed and Craig, 1992). Horwood and Pye (1955) have described the gold mineralization as being hosted within and between the contact of metasedimentary lithologies and quartz-albite porphyry. The metasedimentary lithologies that host gold mineralization are typically greywacke and iron formation, and to a lesser extent, slate and conglomerate. Shear zones are noted in the slates, typically in chlorite schist, when present adjacent to massive iron formation. Not only are the quartz-albite porphyry and metasediments complexly folded, but also all of the lithologies in the mine site are folded. The fold hinges typically strike east-west and generally plunge 20° - 25° (Horwood and Pye, 1955; Speed and Craig, 1992).

Mason and White (1986) characterized the gold mineralization in Hardrock Mine into three distinct categories. The first category includes the quartz veins and mineralized zones within and adjacent to the contacts of the quartz-albite porphyry. Stringers of sulphides, like pyrite, pyrrhotite, and arsenopyrite, occur along fractures in the quartz veins. The gold is associated with the sulphides and is located in the veins and wallrock.

The second category includes massive lenses of sulphides and quartz that crosscut the folded greywacke and iron formation they are hosted within. Gold mineralization is only present in this category in the wall rocks where sulphides like pyrite, arsenopyrite, and pyrrhotite are present.

The third category is described as gold-bearing quartz stringers within shear zones along the metasedimentary and quartz-albite porphyry contact. Lenses up to 1 m long occur where stringer zones have merged. Carbonates, sulphides, and tourmaline are present within the quartz stringers in this category (Mason and White, 1986; Speed and Craig, 1992).

The MacLeod-Cockshutt Mine is located approximately 5.5 km southeast of Geraldton in the Beardmore-Geraldton greenstone belt (Fig. 1.6; Speed and Craig, 1992). The MacLeod-Cockshutt Mine area is composed of metavolcanic tuffs, gabbro, and metasedimentary lithologies (Horwood and Pye, 1955). The ore bodies are intensely folded and strike east-west and plunge west at 20°. The ore bodies are adjacent to the

Bankfield-Tombill fault zone along the southern edge of the property. A transverse fault with a north-south strike and a 45°E dip that exhibits fault gouge and breccia cuts the sulphide ore in the eastern area of the property. In areas of the Hard Rock mine detailed mapping has shown evidence of thrust fault movement (Horwood and Pye, 1955).

The Mosher Long Lac Mine is the western extension of the MacLeod-Cockshutt Mine in the Beardmore-Geraldton greenstone belt (Fig. 1.6; Speed and Craig, 1992). Ferguson *et al.* (1971) described the host rock as being composed of metasediments and metavolcanics with felsic to mafic intrusions. The gold mineralization in the ore is adjacent to the feldspar porphyry that plunges gently towards the west (Speed and Craig, 1992).

The Hutchinson Mine, or Maylac/Gulch Mine, is located 6.4 km north of Geraldton in the Beardmore-Geraldton greenstone belt (Fig. 1.6; Speed and Craig, 1992). The host rock at the Hutchison Mine is intermediate to mafic metavolcanic lithologies ranging from flows to tuffs that strike 80° along the regional foliation with steep or near vertical foliation (MacDonald, 1943). Complex folds are common in the area with foliation changes ranging from 35° to 80° and dips from south to north. The complexly folded quartz veins host the gold mineralization as well as pyrrhotite, sphalerite, chalcopyrite, and galena. The gold forms as blebs and MacDonald (1943) has categorized the styles in which he observed the gold as being in quartz veins; in pyrite, sphalerite, and galena as blebs and veinlets; and along contacts between sphalerite and quartz as well as penetrating the sphalerite (Speed and Craig, 1992).

The Theresa Gold Mine is located 9.5 km south of Longlac in the Beardmore-Geraldton greenstone belt (Fig. 1.6; Speed and Craig, 1992). Fairbairn (1938) stated that the host rocks are altered mafic rocks, agglomerate, and metasedimentary lithologies that have been intruded by quartz diorite-granodiorite plutons. A steeply dipping shear zone with a strike of 40° is located along the contact of the agglomerate and quartz diorite. The contact between the two lithologies hosts the gold-mineralized-quartz veins that strike $085^\circ/55^\circ\text{N}$ at the contact but exhibit folding. Gold mineralization is accompanied by pyrite, chalcopyrite, and pyrrhotite (Fairbairn, 1938; Speed and Craig, 1992).

2-DATA COLLECTION

2.1 Property and trench mapping

Property and trench mapping for this thesis was conducted as a summer student employee of Kodiak Exploration Ltd. in 2010 and Prodigy Gold Inc. in 2011. The property-scale mapping conducted in the summer of 2010 was focused north of Jellicoe within the Elmhirst and Castlewood properties, in and around the Onaman-Toshota greenstone belt of the Wabigoon subprovince. The property and trench mapping in the summer of 2011 was conducted between Caramat and Longlac, in and around the Hollowrock Lake pluton within the Beardmore-Geraldton greenstone belt and Quetico subprovince. Structural measurements were taken throughout the properties and lithology and alteration were documented. Gold mineralization was tested using assay results provided by Kodiak Exploration Ltd. and Prodigy Gold Inc.

One hundred fifty-four oriented hand samples were collected from the field and drill core during the 2010 and 2011 summers for the purpose of examining the lithology, structure, alteration, metamorphic grade, and their relationship to gold mineralization. The sample numbers, description, drill hole, and location are listed in Appendix A. The language used to describe the structural features in the mapping area is based on current knowledge (Brodie *et al.*, 2007; Twiss and Moores, 2007).

2.2 Petrography and Scanning Electron Microscope (SEM)

The samples for microscopic study were collected to characterize structure, microstructure, lithology, protolith, alteration, metamorphic grade, and gold

mineralization. Microstructures were described using current language and our present understanding of them (Tullis, 2002; Passchier and Trouw, 2005; and Trouw *et al.*, 2009). The most common microstructures observed within the study were straight fractures, folded healed fractures, undulatory extinction, irregular grain boundaries, subgrains, grain boundary area reduction, and grain size reduction. Grain size reduction was assessed based on strain gradients within the same sample as well as compared to the host rock. The fractures and folded fractures are typical of brittle and brittle-ductile deformation respectively, while the others are typical of ductile deformation (Tullis, 2002; Passchier and Trouw, 2005; and Trouw *et al.*, 2009). Evidence of strain heterogeneity is frequently observed in thin section as competent minerals (i.e. garnet) act as rigid bodies and exhibit fractures while the surrounding matrix (i.e. quartz) deforms ductilely. Fluid inclusions were observed and described however no fluid inclusion study was conducted. Samples were classified according to the International Union of Geological Sciences (IUGS) rock classification scheme (Appendix A) (Le Maitre *et al.*, 1989; Mitchell, 1994; Árkai *et al.*, 2007; Brodie *et al.*, 2007; Schmid *et al.*, 2007; Coutinho *et al.*, 2007).

Anne Hammond at Lakehead University prepared one hundred covered and polished thin sections for reflected and transmitted light microscopy. Anne also prepared twenty-three discs to be used with the scanning electron microscope (SEM).

3-OBSERVATIONS

3.1 The Wabigoon subprovince

The property mapping, trench mapping, and petrography completed within the Wabigoon subprovince include the Elmhirst and Castlewood properties north of Jellicoe (Fig. 1.4). One hundred eight oriented samples and samples from drill core were collected from this area.

Mapping was conducted along the eastern Elmhirst Lake pluton margin in the Elmhirst property. The trench mapped for this study within the Elmhirst Lake pluton is the Findian 3 trench. Structural measurements and oriented samples were collected for petrography from the Golden Mile, Lucky Strike, and Brenbar trenches in the Elmhirst property and the trench in the Castlewood property.

The mapping area north of Jellicoe in the Wabigoon subprovince is composed primarily of felsic to mafic metavolcanic lithologies of the Elmhirst-Rickaby assemblage around the Elmhirst Lake granodiorite pluton (Fig. 3.1). The metavolcanic lithologies are typically intermediate to mafic, medium grey-blue, fine-grained ash tuff to crystal tuff with subangular, plagioclase crystals up to 3mm in length along the c-axis. Lapilli tuff occurs rarely in the area and rarely grades into green-grey pyroclastic bombs that are typically less than 10cm³ and subangular to subrounded. Fine-grained, disseminated, euhedral pyrite composes less than 5% modal percentage of the metavolcanic lithologies. Shear zones are rare within the metavolcanic lithologies and are oriented 242°/64°. The shear zones increase in abundance and width towards the Elmhirst Lake pluton margins.

In thin section the metavolcanic lithologies typically display equigranular, hypidiomorphic textures. Evidence for dislocation creep, like undulatory extinction in quartz, or metamorphic reactions, like chlorite replacing pyroxene and amphibole, occurs only in the metavolcanic lithologies samples collected from within shear zones.

No gold mineralization was found in assay within the felsic to mafic metavolcanic lithologies around the Elmhirst pluton. Stringers to massive galena, chalcopyrite, and sphalerite were noted in the metavolcanics in and around the Sturgeon River area.

Adjacent to the Elmhirst Lake meta-granodiorite pluton the typically intermediate, fine-grained tuff exhibits extensive silicification and erratic hematite alteration. At the contact and transition from intermediate tuff to granodiorite a ductile to brittle-ductile shear zone with strong, penetrative foliation strikes northeast approximately $160^{\circ}/63^{\circ}$. Another ductile shear zone with penetrative foliation is also noted trending $220^{\circ}/80^{\circ}$. The two foliations anastomose around the Elmhirst pluton and occur within the two sets of black lines denoted in Figure 3.1. Boudinage is rare and boudins of quartz veins strike at $229^{\circ}/71^{\circ}$. The meta-granodiorite at or near the margin is silicified with epidote and chlorite replacing plagioclase and hornblende, respectively. In rare examples the meta-granodiorite in the study area transitions into quartz diorite and pegmatite. The pegmatite typically strikes 220° - 230° with a vertical dip. In less deformed areas of the pluton the meta-granodiorite is coarse-grained, euhedral, and equigranular.

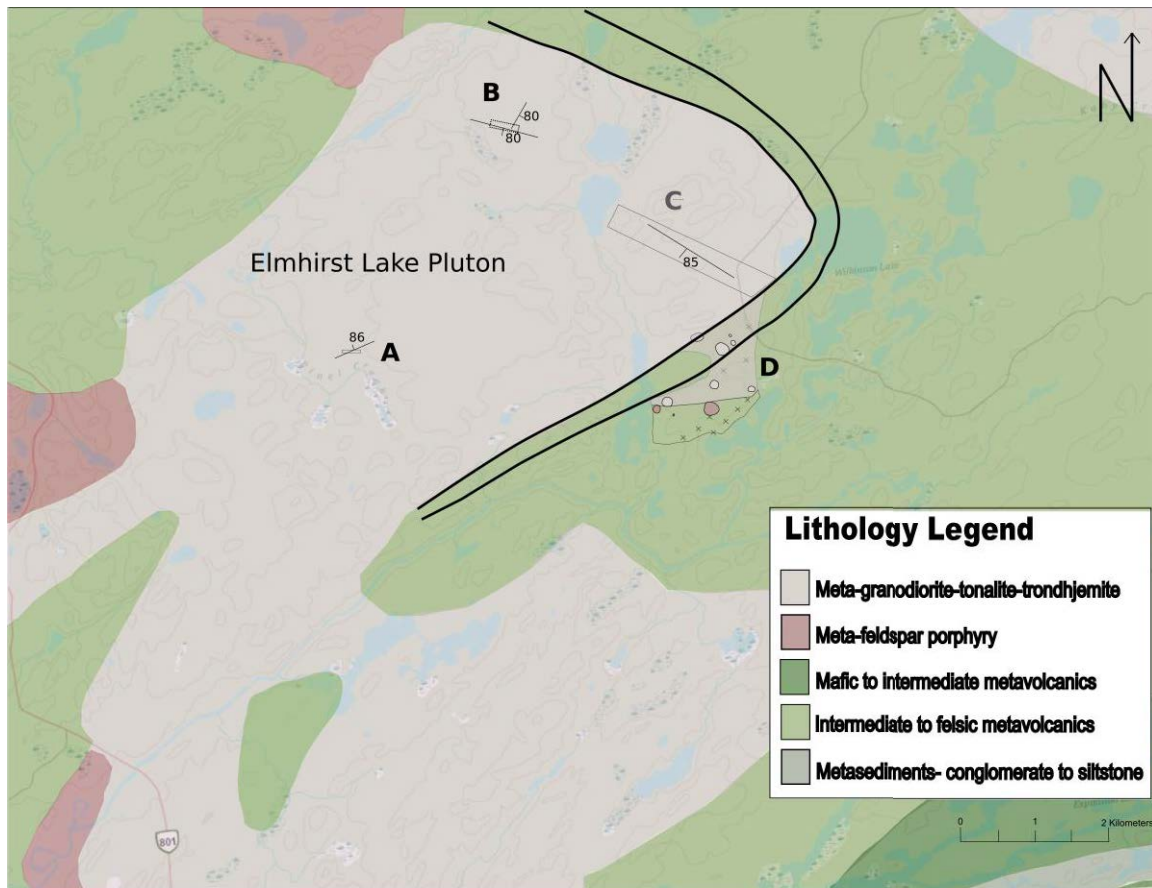


Fig. 3.1: Geological map of the Elmhirst Lake pluton in the Wabigoon subprovince. Trenches are indicated with solid boxes: A) Findian 3; B) the Straights; C) Golden Mile and Lucky Strike. Mapping is denoted with dashed lines: D) Elmhirst property map. A solid, curved black line denotes a mapped portion of the Paint Lake Shear zone.

Feldspar porphyry and diabase exhibit primary hypidiomorphic, crystalline textures and do not display a penetrative foliation nor quartz veins. The feldspar porphyry and diabase are minor and are too small to plot on the maps. Through cross-cutting relationships the diabase is the youngest lithology in the area and the porphyry is second youngest. The porphyritic granite is light pink, medium-grained with coarse-grained plagioclase phenocrysts. The porphyritic phase is magnetic and appears as geophysical magnetic highs throughout the region. The diabase ranges from aphanitic to coarse grained near its centre. Within the coarse-grained centre the diabase exhibits subophitic texture. A well-defined, straight dyke contact strikes 28°/82°. The geophysical magnetic lows in the area are typically diabase dykes.

No gold mineralization was found within metavolcanic lithologies in the study area although very fine grained to coarse-grained, disseminated euhedral to stringers of pyrite are present and comprise up to 2% of the hand samples. Gold assay results provided by Kodiak Exploration Ltd. suggest that no gold mineralization is present within the feldspar porphyry or diabase.

Assay results by Kodiak Exploration Ltd. provide evidence for gold mineralization being located within the Elmhirst Lake pluton from the margins of the pluton to the centre of the pluton, although with decreasing abundance towards the centre. The pluton margins between the Elmhirst Lake pluton and surrounding metavolcanic lithologies, like the Brenbar trench, host gold mineralization both within folded, boudinaged quartz veins and in schistose meta-granodiorite. The gold

mineralization occurs within strong, tightly spaced, penetrative, and moderately rough, anastomosing foliation in the meta-granodiorite and chlorite schist where ductilely deformed quartz veins are present (Fig. 3.2). The quartz veins within the Elmhirst Lake pluton displays undulatory extinction, grain size reduction, irregular grain boundaries, subgrains, and boudinage. At the margins of the Elmhirst Lake pluton the gold mineralization is located in areas where ductile shear zones intercept the pluton. At these interceptions, fractures and in filled fractures in the form of quartz and quartz-carbonate veins, deviate from the east-west trend of the shear zones and typically strike northeast (Fig. 3.2).

The Golden Mile trench is located within the Elmhirst Lake pluton and is 3 km long and up to nine metres wide (Fig. 3.1). Meta-granodiorite, chlorite schist, and quartz veins are the lithologies present within the trench. The quartz vein is white to smokey-grey and is generally straight. Meta-granodiorite and chlorite schist wall rock are observed throughout the vein, commonly folded. The quartz vein follows the regional shear zone at an average strike of $125^{\circ}/75^{\circ}$. S-C fabric occurs rarely within the schistose meta-granodiorite and chlorite schist and suggests dextral, ductile deformation during deformation. Rare instances of mullion structures are present along the quartz vein and chlorite schist contacts, suggesting that at least some quartz veins were more competent than chlorite schist during deformation. The veins exhibit vertical and subvertical mineral fiber lineations along the host rock and vein boundaries.

The quartz vein hosts the majority of the gold mineralization within the trench area. Adjacent to the quartz vein the schistose meta-granodiorite and chlorite schist also host gold mineralization but to a lesser degree. Gold mineralization is typically lower within the meta-granodiorite and chlorite schist than the quartz vein, except in areas where it is complexly folded, typically as a shear-related late folds, and hosts gold mineralization similar to the quartz vein (Carreras *et al.*, 2005). Fault breccia and fault gouge are present along the hanging wall of the quartz vein and have not been overprinted by ductile deformation. No gold mineralization is present within fault breccia or gouge.

Hematite alteration is patchy, up to 5% of the lithology, and is located throughout the Golden Mile trench and occurs rarely as veins. Calcite is common within the quartz vein and cross-cut the quartz vein. Sericite alteration commonly occurs within the meta-granodiorite adjacent to the Golden Mile trench within the meta-granodiorite. Very fine-grained to coarse-grained, anhedral to euhedral, disseminated to rare stringers of pyrite are located throughout the quartz vein. Anhedral, disseminated, fine-grained chalcopyrite is also rarely found throughout the quartz vein. Rare, fine-grained, anhedral azurite, malachite, and visible gold are observed within the trench.

Nine oriented samples collected at the Golden Mile trench for petrography include folded, boudinaged, and mylonitized quartz veins, chlorite schist, and meta-granodiorite. The samples were collected within and adjacent to the quartz vein as

well as at a distance of 80 cm to 2 m away from the vein. The quartz veins exhibit microstructures, including intense grain size reduction, undulatory extinction, grain bulging, irregular grain boundaries, recrystallization, and subgrains.

The samples collected adjacent to the quartz vein displayed evidence of dislocation creep with grain size reduction, undulatory extinction, and subgrains present within quartz (Tullis, 2002). Undulatory extinction is present in the larger quartz grains that host the subgrains. Within the meta-granodiorite the quartz displays evidence of irregular grain boundaries. The chlorite and pyrite defines the foliation and anastomoses around fractured albite (Fig. 3.3). The samples collected at a distance of 80 cm to 2 m from the quartz vein contain quartz grains that show evidence of recrystallization, less irregular grain boundaries and undulatory, and no subgrain formation compared to the samples adjacent to the quartz vein. Adjacent to the quartz vein the sericite alteration comprises up to 30% of the meta-granodiorite and decreases to trace amounts away from the quartz vein. The hematite alteration is greatest within the quartz vein, often comprising up to 5% of the lithology.

Gold mineralization in the Golden Mile trench is located in the quartz vein. In thin section the quartz vein is composed of many smaller quartz veins and microboudins. Gold mineralization is located in areas in the quartz vein that display evidence for grain size reduction in 15-30% of the quartz in the sample (Fig. 3.4). Within areas of grain size reduction the gold mineralization is located along quartz-quartz irregular grain boundaries and subgrain boundaries. Fluid inclusions are

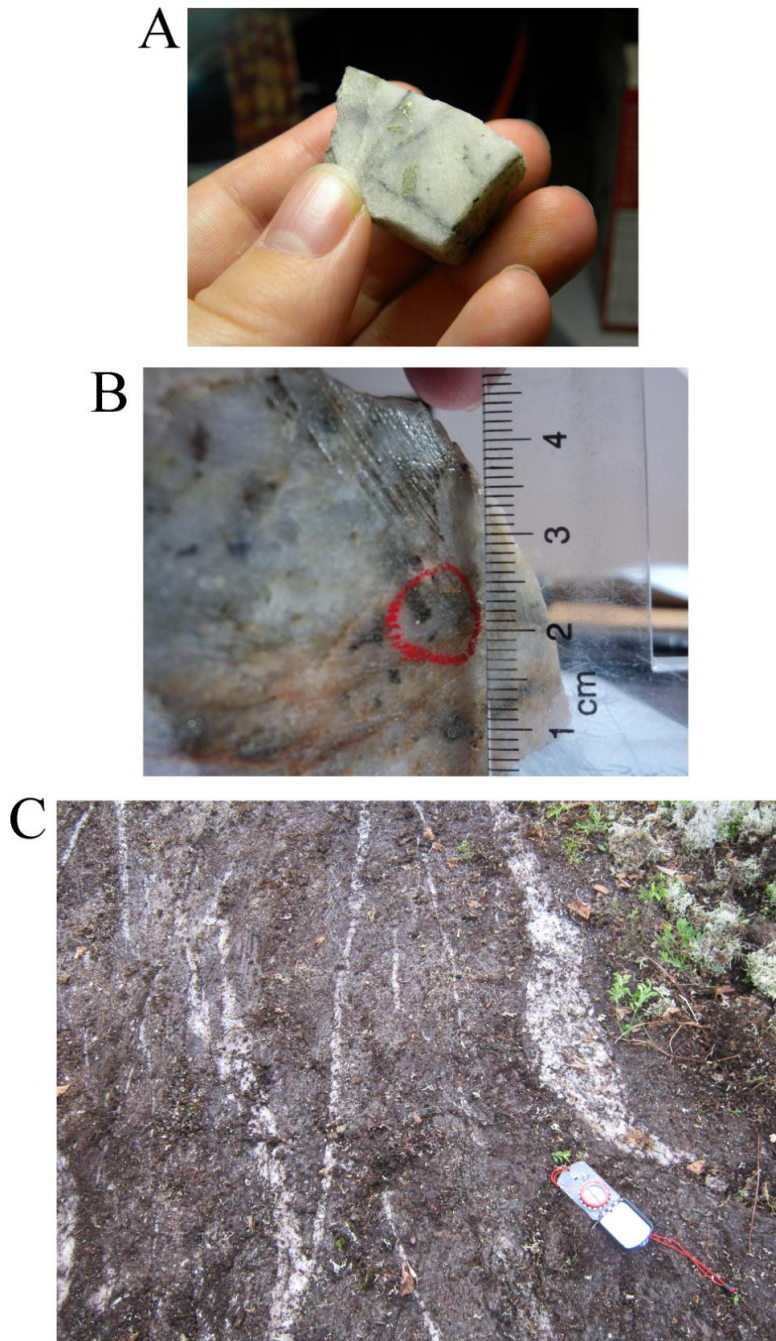


Fig. 3.2: The Wabigoon subprovince study area. A) Sample of quartz vein from the Elmhirst property with gold along quartz-pyrite grain boundaries and within a folded fracture. B) Sample of quartz vein from the Brenbar trench with gold along the quartz-pyrite grain boundary. C) Folded and boudinaged quartz veins within schistose metagranodiorite along the Elmhirst Lake pluton boundary.

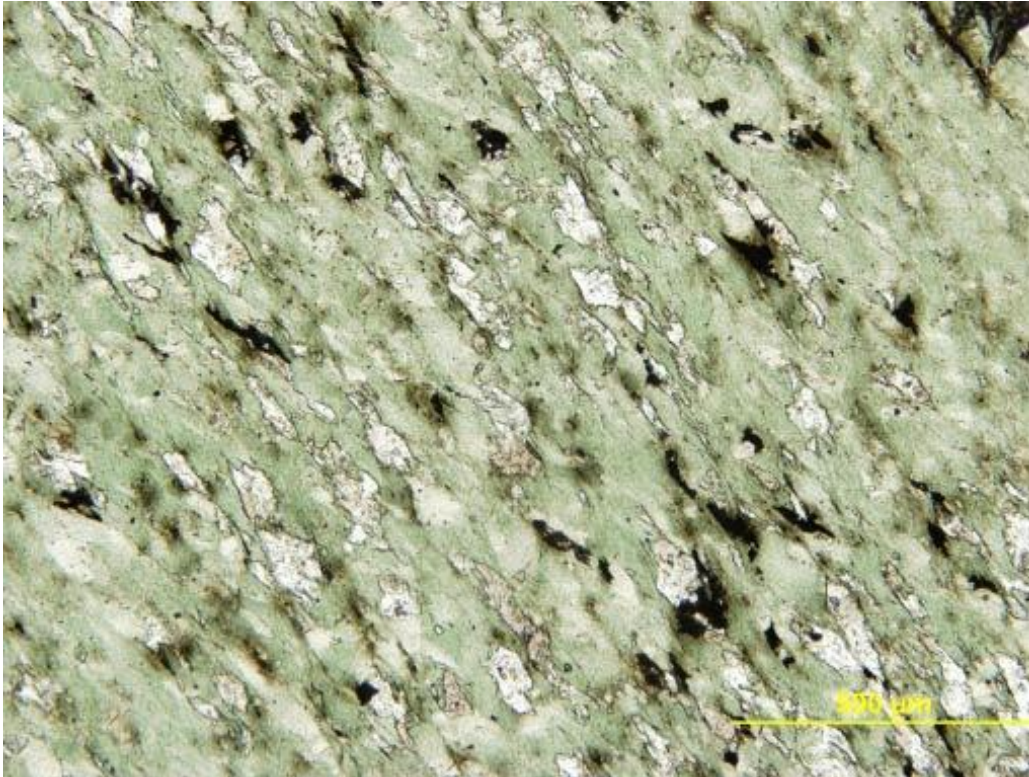


Fig. 3.3: Photomicrograph in plane polarized light of the gold mineralized chlorite schist from the Golden Mile trench in the Elmhirst property near Jellicoe (Sample MVS097). The chlorite and quartz matrix anastomoses around fractured albite. The scale bar is 500 μ across.

commonly associated with gold mineralization in quartz veins and in sample MVS091 the fluid inclusion appeared to host the gold mineralization. The gold mineralization in the fluid inclusion was too fine-grained for a clear photograph to be displayed. In addition to quartz-quartz grain and subgrain boundaries, pyrite-quartz, muscovite-quartz, and muscovite-muscovite grain boundaries also host gold mineralization. Gold mineralization is common along the pyrite-quartz grain boundary and defines the foliation in sample MVS091 (Figs. 3.5, 3.6). Gold mineralization is also commonly located within the pressure shadows of the euhedral pyrite and as inclusions in pyrite (Fig. 3.7). Healed fractures in quartz veins host gold

mineralization along quartz-muscovite grain boundaries. Gold mineralization is also common along muscovite-muscovite grain boundaries.

Five oriented samples were collected from the Lucky Strike trench, located 200 m west of the Golden Mile. The Lucky Strike is a quartz vein similar to the Golden Mile with a strike and dip of $134^{\circ}/59^{\circ}$. The lithologies present in the Lucky Strike trench are also meta-granodiorite, chlorite schist, and quartz vein. The lithologies in the Lucky Strike trench exhibit fewer folds than the Golden Mile and assay results by Kodiak Exploration Ltd. suggest that it hosts less gold mineralization. The smaller quartz veins within the trench vary but are typically 1 m wide and trend $142^{\circ}/57^{\circ}$ to $135^{\circ}/21^{\circ}$. Wallrock of meta-granodiorite and chlorite schist are present throughout the quartz vein and exhibit schistose texture. The widest part of the quartz vein also hosts the greatest gold mineralization in the trench. The fault breccia in the Lucky Strike also does not host gold mineralization, based on assay results by Kodiak Exploration Ltd. and petrography. Fine-grained to coarse-grained, anhedral to euhedral, disseminated pyrite is located within the quartz veins. Fine-grained, anhedral and disseminated chalcopyrite is also rarely present in the quartz vein.

The oriented samples collected from the trenches of quartz vein and meta-granodiorite from within the Lucky Strike trench (MVS007, MVS012A, MVS012B, MVS013, MVS019) exhibit nearly identical microstructures within the Golden Mile trench (MVS002-005, MVS008, MVS010, MVS014, MVS017-018). Seventy-three samples collected from drill core from the Golden Mile and Lucky Strike area of the

Elmhirst pluton were also analyzed for microstructures. Similarly to the oriented samples, the microstructures from within the area closest to the quartz vein show the greatest evidence of intense grain size reduction (e.g., quartz grains ranging from 600 μm to 20 μm within sample MVS091) and subgrains while irregular grain boundaries, recrystallization, and bulging are most common further away from the quartz vein (e.g., sample MVS014 located 2 m north of the Golden Mile quartz vein).

Folded quartz veins and microboudins are noted in thin section as they commonly are coarser grained than the surrounding matrix (Fig. 3.8). Muscovite, pyrite, chlorite, and calcite are common throughout the quartz veins. Muscovite and chlorite are typically located at grain boundaries of quartz and rarely exhibit undulatory extinction. Pyrite is euhedral and strain fringe of quartz is commonly present around it. Calcite exhibits deformation twins and is present along grain boundaries within quartz veins or as calcite veins perpendicular to quartz veins.

The meta-granodiorite is composed mainly of albite feldspar, biotite, and quartz. The albite feldspar exhibits deformation twins and extensive sericite alteration along cleavage planes. Titanite needles are present throughout the chlorite and oriented randomly. Carbonate is also found throughout the metagranodiorite and is subhedral.

The lithologies present within the Findian 3 trench are schistose meta-granodiorite, chlorite schist, diabase, and quartz veins (Fig. 3.9). The greatest amount

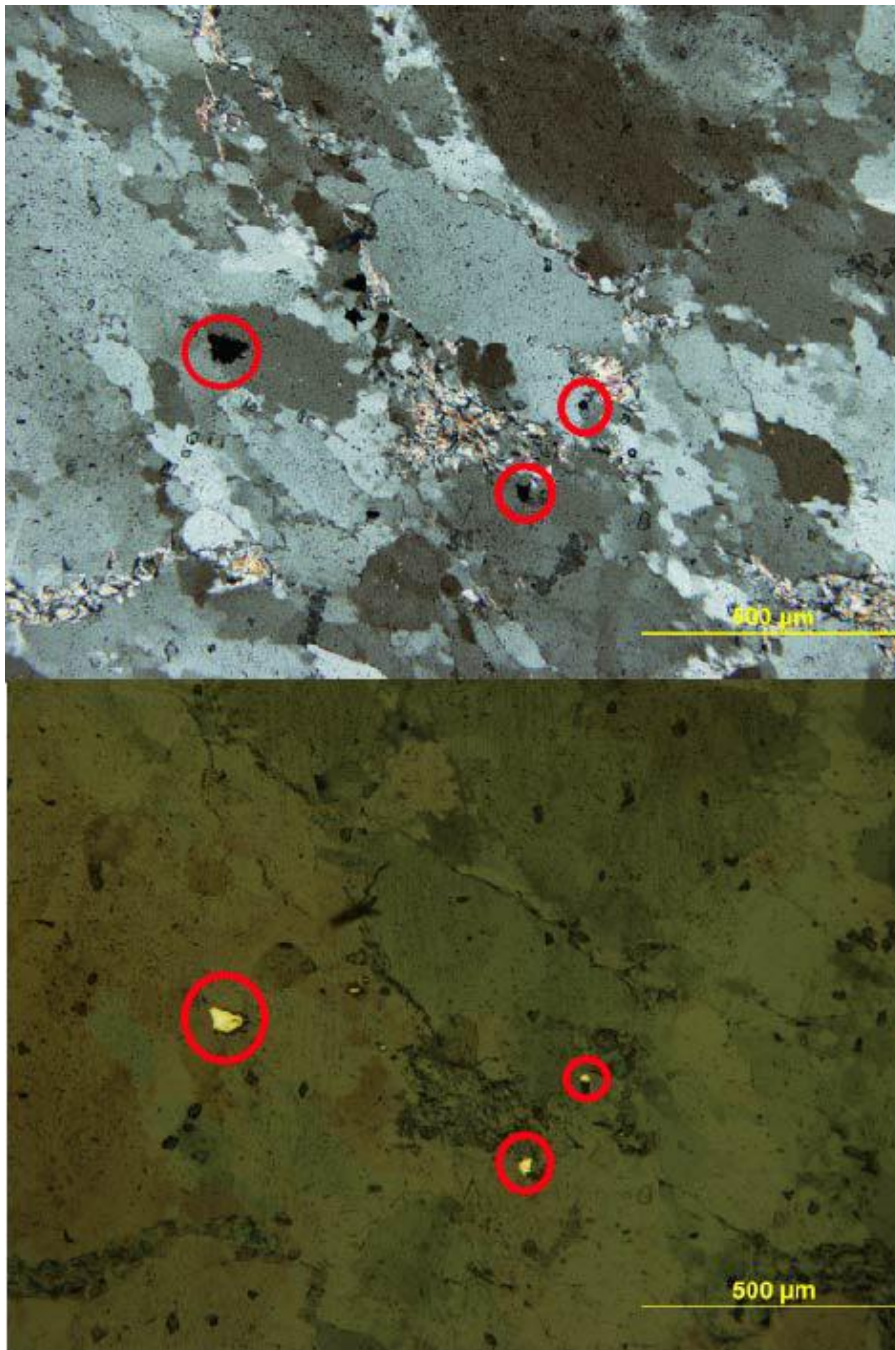


Fig. 3.4: Photomicrographs in cross-polarized light (above) and reflected light (below) of the gold mineralized quartz vein from the Golden Mile trench in the Elmhirst property near Jellicoe (Sample MVS091). Undulatory extinction, irregular grain boundaries, and subgrains are present within the larger quartz grains in the quartz vein. Gold mineralization is located along irregular grain boundaries of larger grains of quartz (left).



Fig. 3.5: Photomicrographs in cross-polarized light (above) and reflected light (below) of the gold mineralized quartz vein from the Golden Mile trench in the Elmhirst property near Jellicoe (Sample MVS091). Undulatory extinction, irregular grain boundaries, and subgrains are exhibited in quartz in the quartz vein. Euhedral pyrite has a quartz fringe (left). Gold mineralization is located along irregular grain boundaries of quartz, in the pressure shadow of pyrite, and along the pyrite-quartz grain boundary where it defines the foliation.

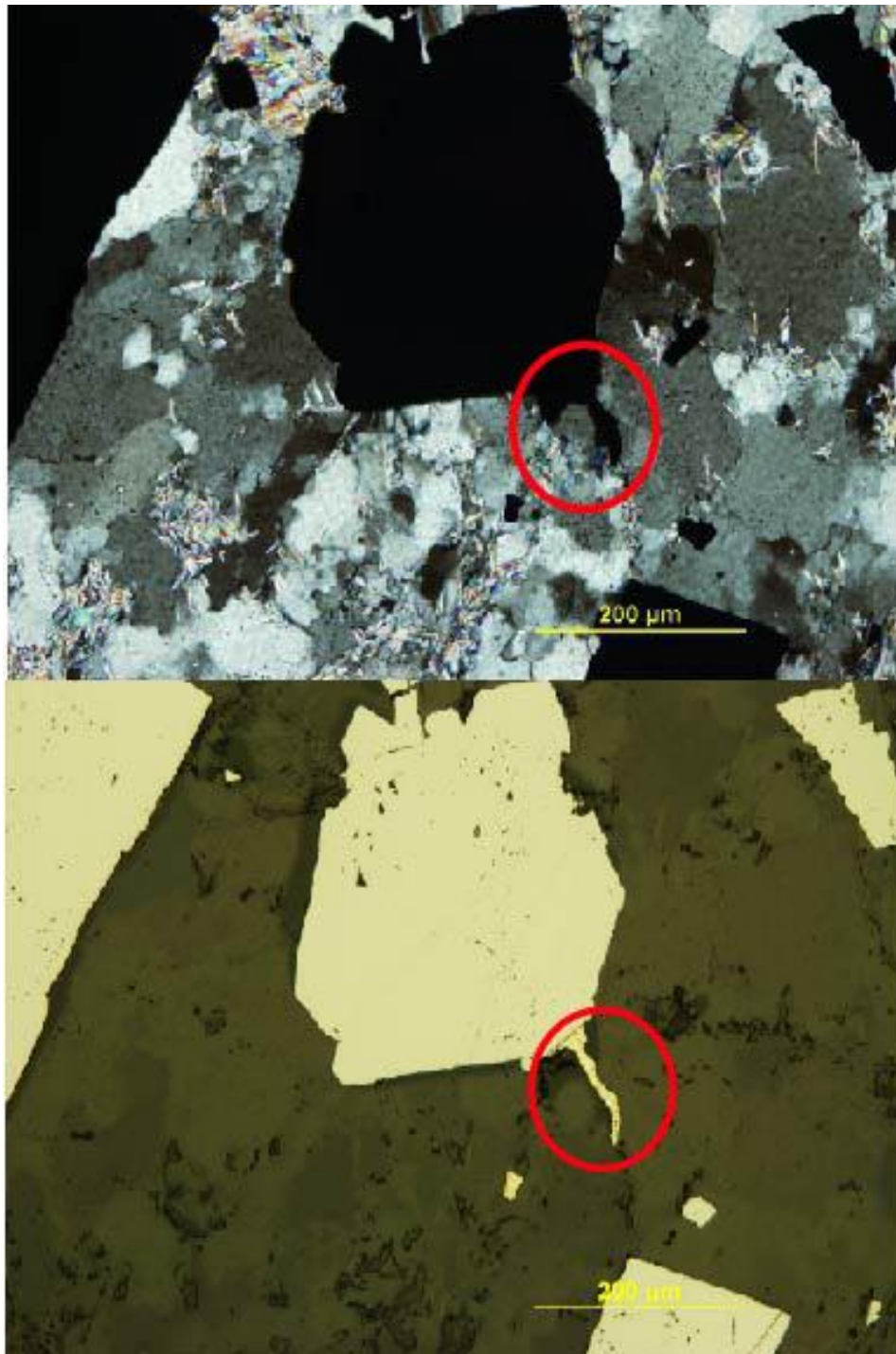


Fig. 3.6: Photomicrographs of cross-polarized light (above) and reflected light (below) of the gold mineralized quartz vein from the Golden Mile trench in the Elmhirst property near Jellicoe (Sample MVS091). The quartz in the quartz vein displays undulatory extinction and subgrains (lower, centre). Gold mineralization is located along a pyrite-quartz grain boundary and defines the foliation.



Fig. 3.7: Photomicrographs of cross-polarized light (above) and reflected light (below) of the gold mineralized quartz vein from the Golden Mile trench in the Elmhirst property near Jellicoe (Sample MVS091). The quartz vein displays undulatory extinction and subgrains in quartz. The gold mineralization is located in pressure shadows around pyrite and as inclusions in pyrite.

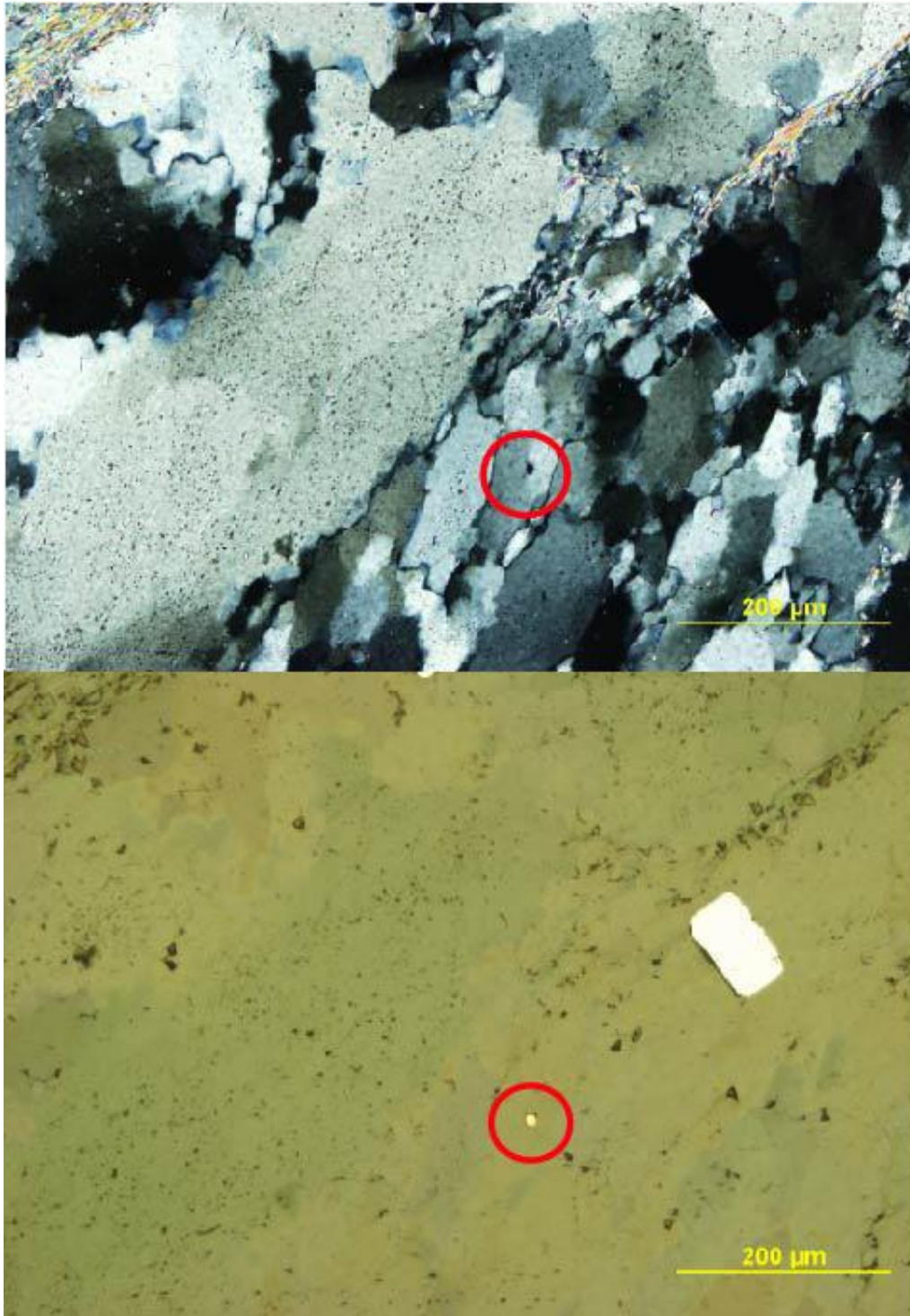


Fig. 3.8: Photomicrographs of cross-polarized light (above) and reflected light (below) the gold mineralized quartz vein from the Golden Mile trench in the Elmhirst property near Jellicoe (Sample MVS091). A quartz microboudin (lower left to top right) is coarser grained than the surrounding quartz vein. The quartz of the microboudin displays undulatory extinction while the smaller grains display evidence of grain size reduction and subgrains. Gold is located along a subgrain boundary in quartz.



Fig. 3.9: Geological map of the Findian 3 Trench map imposed on an aerial photo from within the Elmhirst Lake pluton in the Wabigoon subprovince. The blue outline denotes the chlorite schist, red the quartz veins, and the pink outline meta-granodiorite. The greatest gold mineralization is hosted within folded quartz veins.

of gold mineralization is located within folded quartz veins (Fig. 3.9). Gold mineralization also occurs within schistose meta-granodiorite and chlorite schist. The quartz veins are commonly folded and have wall rock, of meta-granodiorite and chlorite schist, hosted within the vein. Chlorite schist and meta-granodiorite host lesser amounts of gold mineralization than quartz veins. The foliation in the chlorite schist and meta-granodiorite and quartz veins all strike at 065-090°/80°-90°. Fine-grained to medium-grained, anhedral to euhedral, disseminated pyrite is located within the quartz veins and metagranodiorite. Sericite alteration is prevalent within schistose meta-granodiorite and calcite is common within quartz veins. The unmetamorphosed diabase dykes strike 0°/90° do not host gold mineralization.

The Straights trench hosts straight quartz veins within meta-granodiorite host rock and minor amounts of chlorite schist. Wallrock of chlorite schist and meta-granodiorite are located throughout the quartz veins. The two quartz veins are straight and roughly perpendicular to one another. One quartz vein strikes north-south with a near vertical dip while the other is onstrike with the Lucky Strike and Golden Mile quartz veins. No gold mineralization is present in the Straights. Calcite and ankerite alteration are commonly located within the quartz veins. Fine-grained to medium-grained, anhedral to subhedral, disseminated pyrite is located within the quartz veins and meta-granodiorite in the trench.

The Brenbar trench located within the historic Brenbar gold mine property hosts a 0.5 m wide quartz vein within chlorite schist, muscovite schist, and pegmatite (Fig. 1.6).

The quartz vein, and foliated chlorite schist, muscovite schist strike 86° - 93° / 85 - 89.5° . A crenulated foliation in the chlorite schist and muscovite schist has a strike and dip of 056° / 39° . Ankerite alteration is common throughout the pegmatite and is rarely present within the chlorite schist. The pegmatite is rarely parallel to the regional foliation and is typically brecciated and overprinted by ductile deformation. The breccia is deformed parallel to foliation with rare angular clasts noted. The breccia has a very fine-grained schorl tourmaline matrix. Gold mineralization is located within the quartz vein and is also present in the deformed pegmatite. Pyrite is common throughout the quartz vein and pegmatite breccia and is typically fine- to coarse-grained, disseminated, and euhedral. Visible gold is present along pyrite-quartz boundaries in quartz veins (Fig. 3.2).

Six oriented samples and six samples collected from drill core of quartz vein and chlorite-muscovite schist were from the Brenbar property. The schist exhibits tightly spaced, penetrative, smooth foliation and is defined by chlorite and muscovite. The chlorite-muscovite schist is adjacent to the pegmatite and brecciated pegmatite, with and without tourmaline mineralization. The pegmatite is composed of twinned albite feldspar, sericite, pyrite, and quartz. The feldspar exhibits deformation twins and sericite alteration. The quartz exhibits evidence for ductile deformation through dislocation creep. Microscopic folds and boudins of quartz veins host gold mineralization collected from the quartz vein and pegmatite in the Brenbar trench. The quartz exhibits microstructures of undulatory extinction, irregular grain boundaries, and subgrain boundaries of quartz. Folded healed fractures in quartz veins occur at oblique angles to euhedral pyrite and also host gold mineralization (Fig. 3.9, 3.10). The pegmatite exhibits

healed, folded fractures on the microscopic scale that also host gold mineralization. Gold is not observed within folded quartz fringe around euhedral pyrite (Fig. 3.9).

Four oriented samples were collected from the Castlewood trench. The Castlewood trench hosts meta-granite dykes and quartz veins within chlorite schist and metaconglomerate. The foliation follows the regional strike and dip of $261\text{-}298^\circ/85^\circ\text{-}89^\circ$. The strike and dip of a crenulation foliation of $062^\circ/84^\circ$ is also apparent in the chlorite schist. Intense ankerite alteration is present throughout the Castlewood property within both the quartz veins and chlorite schist. Gold mineralization is located within mylonitized and folded quartz veins and along lithological contacts. Gold mineralization is not present within or adjacent to open synclines or anticlines in the trench area but is located within complexly folded shear-related early and late folds (Carreras *et al.*, 2005). Euhedral pyrite is located throughout the chlorite schist, meta-granite, and quartz veins as fine to coarse-grained, disseminations to rare stringers.

Chlorite schist and metasedimentary lithologies exhibit undulatory extinction in quartz and chlorite defines the foliation. Quartz and biotite fringe is common around competent pyrite (Fig. 3.9-11). Microstructures within samples are similar to previous samples described in the Golden Mile, Lucky Strike, Findian 3, and Brenbar properties. Undulatory extinction, irregular grain boundaries, and subgrain boundaries occur in quartz. The euhedral pyrite is typically fractured and commonly has inclusions of magnetite, sphalerite, and pyrrhotite. Gold mineralization is also present within albite in areas of sericite alteration or deformation twins.

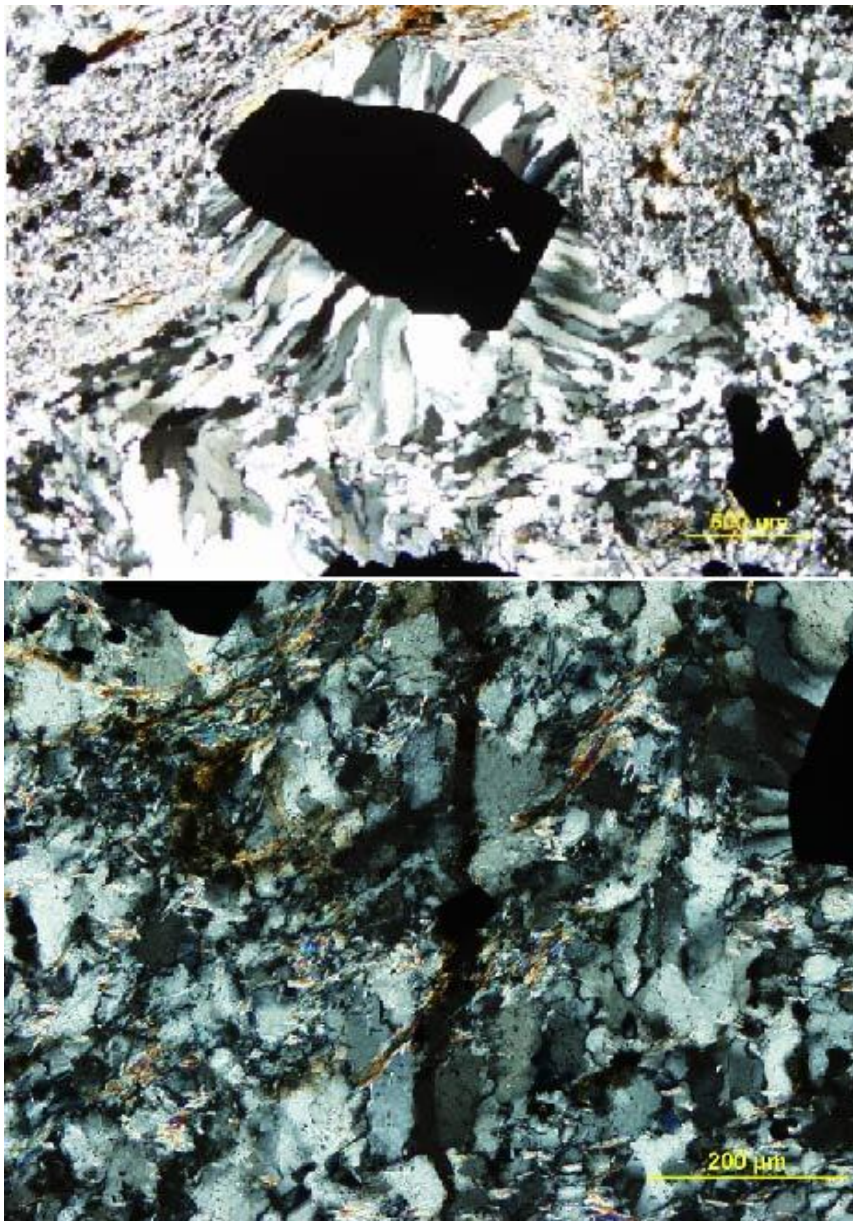


Fig. 3.9: Photomicrographs in cross-polarized light from the Brenbar trench in the Elmhirst property near Jellicoe (Sample MVS025). (Top) Folded quartz fringe around pyrite hosts no gold mineralization. (Bottom) A folded healed fracture (centre) adjacent to quartz fringe around pyrite (right) does host gold mineralization.



Fig. 3.10: Photomicrographs in cross-polarized light (top) and reflected light (bottom) from the Brenbar trench in the Elmhirst property near Jellicoe (Sample MVS025). Quartz fringe is present around pyrite (top left) and gold mineralization is located within folded healed fractures (top right).

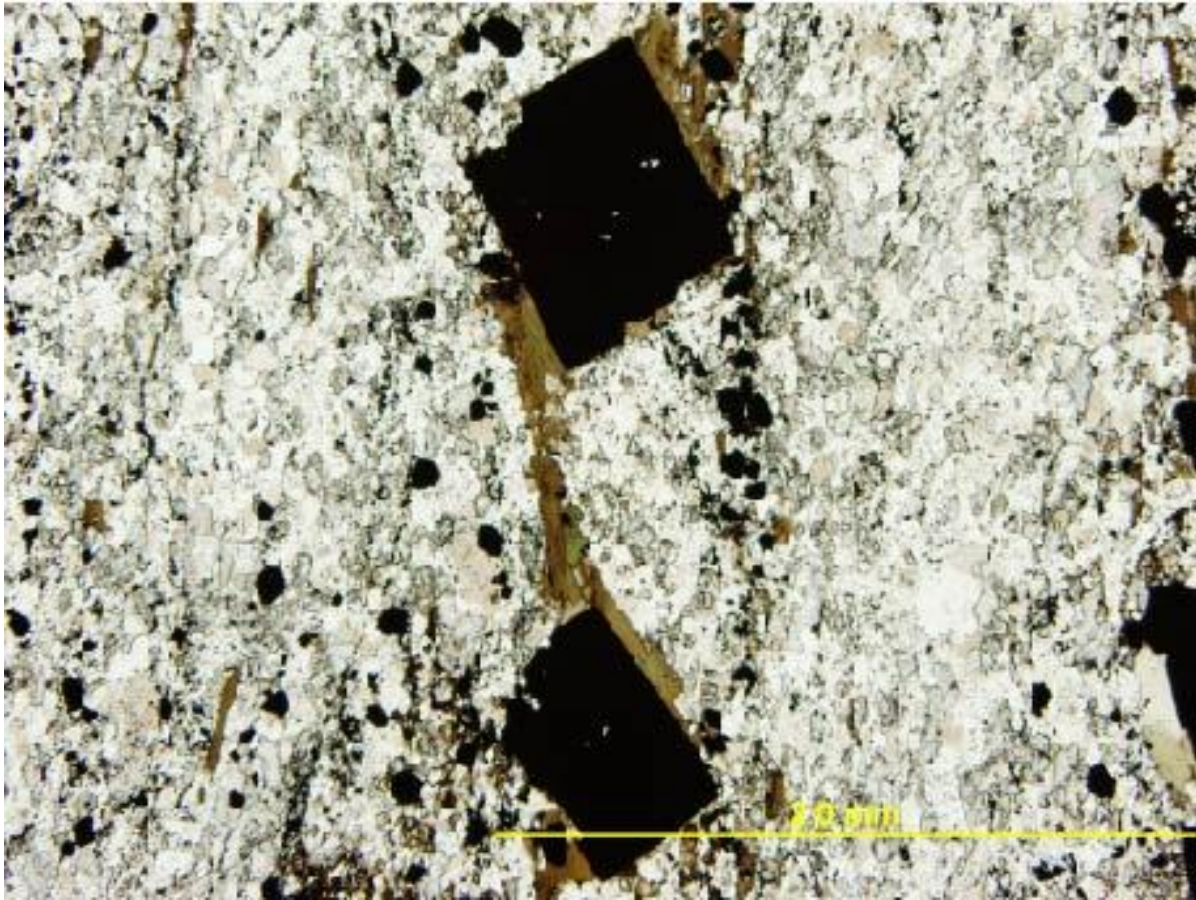


Fig. 3.11: Photomicrographs in cross-polarized light from the Castlewood trench in the Castlewood property near Jellicoe (Sample MVS025). Biotite fringe is present around euhedral pyrite (centre).

3.2 The Beardmore-Geraldton greenstone belt

The property mapping, trench mapping, and petrography completed within the Beardmore-Geraldton greenstone belt include the Pagwachuan property in and around the Seagram Lake pluton, east of Caramat and the Milestone property in and around the Paglamin Lake pluton, east of Longlac (Fig. 1.4). The Pagwachuan and Milestone properties are along strike to the Beardmore-Geraldton greenstone belt, hosted in similar lithologies, located within the eastern extensions of Barton Bay Deformation Zone (BBDZ) and similar shear zones, gold mineralized, and as such have been included in this study as the eastern extent of the Beardmore-Geraldton greenstone belt. Ten oriented

samples were collected from the Pagwachuan property and ten samples from drill core were collected from the Milestone property.

The Pagwachuan property mapping area is located within the area of the Seagram Lake syenite pluton and Hollowrock Lake meta-granodiorite pluton is an eastern extension of the Beardmore-Geraldton greenstone belt (Fig. 3.12). The Beardmore-Geraldton greenstone belt has been previously mapped as far east as the Theresa Lake pluton and historic Theresa gold mine (Fig. 1.6). The mapping conducted in and around the communities of Caramat and Longlac suggests that the Beardmore-Geraldton greenstone belt extends to at least the mapping area and possibly further eastward. The boundaries of the Wabigoon and Beardmore-Geraldton greenstone belt are well defined near Beardmore and Jellicoe, however the eastern boundaries are less well defined.

Two freshly cleared trenches are located within the Pagwachuan property area in the Beardmore-Geraldton greenstone belt and are named Pagwachuan trench #1 and #2. Pagwachuan trench #1 is located north of Seagram Lake and Pagwachuan trench #2 is located east of Hollowrock Lake (Fig. 3.12). No trenches could be cleared in the Milestone property due to the depth of overburden.

In the mapping area the Seagram Lake pluton intrudes mafic metavolcanic lithologies and meta-granodiorite and is a predominantly equigranular, pink syenite with minor areas of quartz syenite and light pink quartz monzonite. Rare, white granite dykes and pegmatites also occur within the syenite. The differentiated quartz syenite and quartz

monzonite lithologies are very rare and insignificant. The syenite is pink to creamy-pink in colour, commonly coarse-grained, equigranular, and is composed of >95% potassium feldspar and minor quartz (<5%).

The Hollowrock Lake pluton is a light pink to light grey meta-granodiorite with textures ranging from equigranular to strongly foliated and deformed. Where the meta-granodiorite is equigranular the rock is light pink with coarse-grained plagioclase and quartz. Quartz and muscovite rarely define a foliation and plagioclase commonly defines a mineral lineation within shear zones in meta-granodiorite. Quartz ribbons in meta-granodiorite are present in areas of greatest ductile deformation.

Meta-gabbro, primarily leucogabbro, is less common and is composed of 50% fine-grained, euhedral, white plagioclase and 50% fine to medium-grained, bladed, euhedral, black hornblende giving it a salt-and-pepper colour. No chlorite is present within the meta-gabbro, as is typical within the high strain areas in the Milestone property. Meta-diorite is rare and is found as very small intrusions near the contact with the Seagram Lake syenite. Both meta-gabbro and meta-diorite are equigranular and display no lineation or foliation.

Mafic volcanics, typically metamorphosed mafic flows and pillows, are weakly foliated, green, and aphanitic. Pillow selvages are darker and well defined. The pillows average 30 cm long and 15 cm wide. No vesicles were observed.

Migmatite is rare and only occurs where xenoliths of metasediment have partially or completely recrystallized within syenite as neosome. Migmatite is only located at syenite-metasediment contacts. The migmatite is medium-grained, and composed solely of 40% white, euhedral feldspar, 40% grey quartz, and 20% black biotite. White migmatite dykes composed of quartz and feldspar range in size from 0.75 to 5 cm wide. The largest dykes commonly show pinch-and-swell structures. The dykes are parallel to the regional foliation at approximately 100°/90°.

Metasedimentary lithologies include polymictic meta-conglomerate, muscovite-biotite schist, biotite schist, garnet-biotite schist, grunerite-biotite schist, metamorphosed iron formation, and albite-muscovite schist. Polymictic conglomerate is present within the regional mapping area north of Seagram Lake adjacent to metamorphosed banded iron formation. The clasts within the meta-conglomerate are rounded, average approximately 10cm³ in volume, and are composed of metamorphosed iron formation, granite, and granodiorite.

The muscovite-biotite schist is the most common metasedimentary lithology and ranges in grain size from very fine-grained to coarse-grained muscovite-biotite schist, with a possible protolith of greywacke. One unique lithology of albite-muscovite schist was observed in the study area east of Pagwachuan trench #2 and has a possible protolith of a single bed of arkose. Biotite schist occurs as small lenses within coarse-grained muscovite-biotite schist and albite-muscovite schist. The biotite schist may have a protolith of silt-rich lenses within sandstone. Garnet-biotite schist and grunerite-biotite

schist only occur in Pagwachuan trench #1. The garnet-biotite schist is located between units of biotite schist and the grunerite-biotite schist occurs adjacent to metamorphosed banded iron formation.

The metasedimentary lithologies are the oldest lithologies based on field relationships within the mapping area. Metamorphosed intermediate to mafic igneous rocks, like chlorite schist and amphibolite, intrudes into the metasediment within Pagwachuan trench #1. Syenite is younger than the metasedimentary sequence as it intrudes into it and also has xenoliths of metasedimentary, mafic volcanics, and amphibolite. Granite dykes within the syenite cross-cut all previously described lithologies. The youngest lithology is the diabase, which crosscuts all lithologies and is unmetamorphosed. Diabase dykes are minor in the mapping area and strike 200-360°/90°. The dykes are aphanitic aside from characteristic fine-grained, white, euhedral plagioclase crystals.

Primary sedimentary structures are rare within the mapping area. Graded bedding within metasandstone at the northern edge of Seagram Lake suggests younging towards 352°, or approximately north, which is supported by evidence of pillow tops along the southwestern boundary of Seagram Lake that also young to the north. One silt lens within metasandstone north of Seagram Lake also shows evidence for primary bedding striking at 80° and foliation striking at 100°. Evidence for brittle deformation within the mapping area is minor. Joints and joint sets are often parallel to foliation in schistose units or strike 174°.

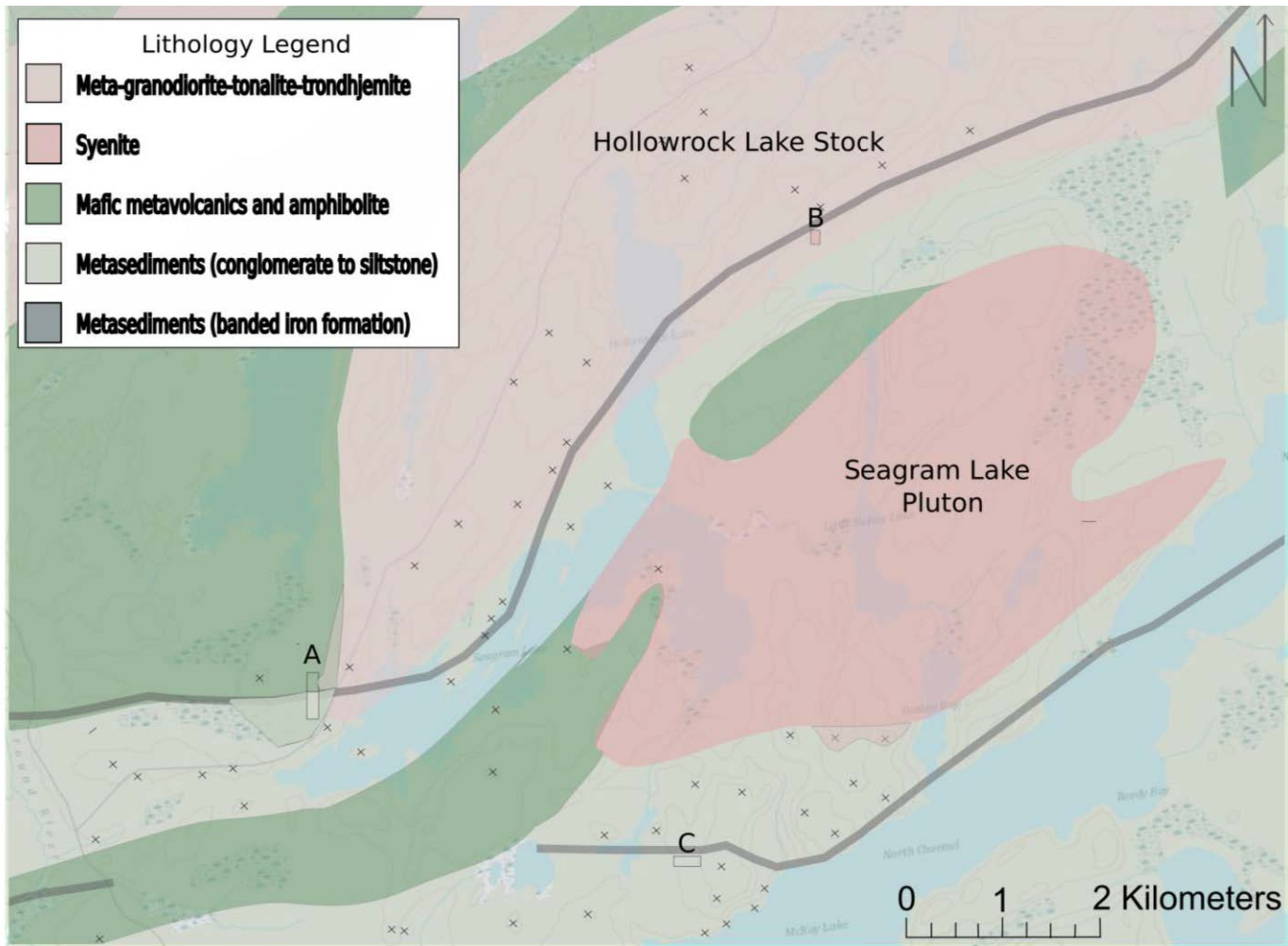


Fig. 3.12: Geological map of the Hollowlake and Seagram Lake plutons along the Wabigoon-Quetico subprovince and Beardmore-Geraldton greenstone belt boundary. The Pagwachuan trench #1 (A), Pagwachuan trench #2 (B), and McKay trench (C). The crosses denote major outcrops.

Minor faults are common within areas of multiple lithologies and strike north-south with dips west and east. Offset in faults are usually minimal, sinistral, and usually less than 20 cm. Ductile to brittle-ductile shear zones in the Pagwachuan property strike 80° to 100° and are a continuation of the Barton Bay deformation zone from the historic Theresa Mine. The shear zones throughout the mapping area have a penetrative, smooth to rough foliation. Foliation within shear zones typically strikes 100° with minor deviation to 80° . The shear zones in the mapping area are located between the black, continuous lines on the map in Figure 3.12. Quartz veins in the Pagwachuan property are common in muscovite-biotite schist and are typically white to smoky grey, with pinch and swell structures, boudinage, and folds. Within areas of banded iron formation, garnet-biotite schist, and garnet-hornblende-biotite schist the ductilely deformed quartz veins are more common and larger. The quartz veins in these lithologies are up to 50 cm wide. Minor folds, with less than 20 cm between hinge planes, and less than 5cm wide sheath folds, trend parallel to foliation.

Patchy, weak to moderate hematite alteration, up to 10% of the lithology, is present within metasandstone adjacent to intermediate to mafic intrusives in the mapping area. Limonite is present on weathered surfaces of garnet-hornblende-biotite schist and banded iron formation. Epidote veins are commonly present near metasediment xenoliths within syenite and are <1cm wide. No carbonate alteration is present within the study area. In most locations within the Pagwachuan property the alteration, if present, is minimal.

The mapping area reached at least amphibolite facies metamorphism as noted by the presence of fine-grained to coarse-grained amphibolite. The presence of garnet-biotite schist is also consistent with evidence for at least the amphibolite facies metamorphism.

Sulphide mineralization occurs along garnet-biotite grain boundaries in garnet-biotite schist, suggesting sulphide mineralization was contemporaneous with metamorphism. Pyrrhotite occurs subhedral to anhedral, fine to medium-grained, and rarely magnetic.

The Pagwachuan trench #1 is composed of muscovite schist and muscovite-biotite schist (fine-grained to coarse-grained metasandstone with minor amounts of granule size lenses), biotite schist (metasiltstone), garnet-biotite schist, grunerite-biotite schist, and metamorphosed banded iron formation (Figs. 3.13-17). The garnet-biotite schist is composed of euhedral, coarse-grained almandine garnet, black biotite and pyrrhotite. In thin section the garnet is brittlely deformed by fractures while the quartz displays evidence of dislocation creep with undulatory extinction, subgrain formation, and ribbons (Fig. 3.13). Banded iron formation is strongly magnetic and gently folded. Amphibolite is located between metasedimentary units and as small cross-cutting stocks. Amphibolite is coarse grained with euhedral plagioclase and chlorite partially replacing hornblende.

The northern portion of the trench is comprised mainly of mafic volcanic lithologies and granodiorite of the Wabigoon subprovince (Fig. 3.17). The mafic

volcanic is aphanitic and partially altered to chlorite. Granodiorite is white and coarse-grained except within the apophysis off the main pluton. An apophysis of meta-granodiorite is fine-grained with very fine-grained plagioclase and fine-grained quartz comprising the rock (Fig. 3.17).

Intense ductile deformation in shear zones can be readily observed in the metasediments as they strike approximately 100° with folded and boudinaged quartz veins throughout (Fig. 3.15). Quartz veins are always present at contacts between coarse-grained metasandstone and fine-grained sandstone contacts. Quartz veins range in width

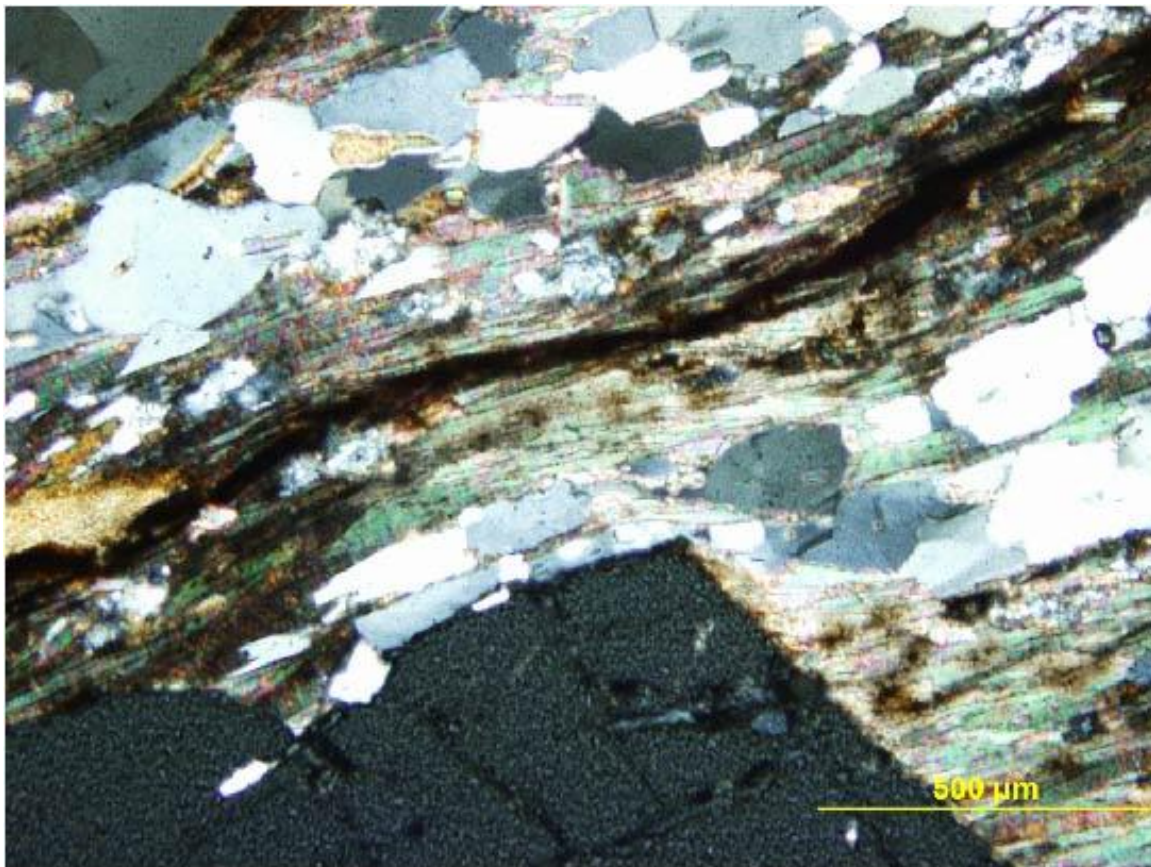


Fig. 3.13: Photomicrograph in cross-polarized light from the Pagwachuan trench #1 in the Pagwachuan property near Caramat (Sample MVS147). Quartz ribbons and biotite define the foliation (centre). Brittle fractures in garnet host pyrrhotite (bottom).

from millimeter to 40 cm wide with folds and pinch-and-swell structures (Fig. 3.15-3.17). Within the biotite schist are sheath folds that are observed to open parallel to foliation and the shear zone (Fig. 3.14).

Trace to 2% euhedral pyrite is located within the meta-granodiorite and quartz veins in the meta-granodiorite. Up to 3% anhedral, fine-grained, blebs of pyrrhotite are located within garnet-biotite rich areas of garnet-biotite and biotite schist (Fig. 3.15). Weak hematite alteration is found throughout many of the lithologies, especially in quartz veins within the metasedimentary lithologies. Assay results by Prodigy Gold Inc. suggest that no gold mineralization is present within this trench.

The meta-granodiorite host rock in the Pagwachuan trench #2 is medium to coarse-grained with euhedral plagioclase, quartz, hornblende and minor biotite (Fig. 3.18). Dykes of syenite 5-40 cm in width have intruded the meta-granodiorite. The syenite ranges in composition from an alkali feldspar syenite to a quartz syenite with fine- to medium-grained alkali feldspar and quartz crystals. The later, simple pegmatite is composed of coarse to very coarse-grained alkali feldspar and quartz. It intrudes into both the meta-granodiorite and syenite with rare, folded syenite breccia within the pegmatite.

The meta-granodiorite, syenite, and pegmatite are cross-cut by a bifurcating shear zone and lamprophyre dyke. In the northernmost portion of the trench the shear zone and lamprophyre dyke splits into two separate zones, one striking 330° and the other at 40°.

A 2 cm wide fault gouge and breccia, which is commonly composed of angular clasts ranging from 0.1-0.5 cm wide of meta-granodiorite. An increase of biotite to 15% is located within these zones. The lamprophyre dyke is weathered with the only discernable minerals being medium-grained, euhedral, cubic pyrite, medium grained phlogopite, and moderate hematite alteration. In thin section Na-rich pyroxene is partially replaced by Na-rich amphibole.

The meta-granodiorite, syenite, and pegmatite are schistose at the boundaries of the shear zones and over-printing faults. The faults have 40 cm sinistral displacement near the middle of the trench. Fractures and healed fractures are noted within meta-granodiorite adjacent to the faults. Euhedral, medium-grained pyrite and purple fluorite are commonly found within healed fractures. 10 cm wide, white to smoky quartz veins are parallel to the fault gouge, breccia, and lamprophyre dykes.

Other quartz veins within the trench are narrower, millimeter to centimeter wide, fractured quartz veins, folded pegmatite quartz veins, and ductile deformed pegmatite quartz veins with deformed syenite breccia clasts. Millimeter wide, folded deformed quartz veins striking north-south and east-west are found within yellow-clay- altered meta-granodiorite.

Ductilely deformed quartz veins, syenite dykes, lamprophyre, and metagranodiorite samples were studied in thin section from the Pagwachuan trench #2. The syenite is so named due to the abundance of alkali feldspar and plagioclase in the syenite

field on a QAPF diagram (Streckeisen, 1974). The lamprophyre is composed of phlogopite, amphibole (partially to completely replacing pyroxene), and euhedral pyrite.

The quartz vein located along the lamprophyre-syenite and meta-granodiorite boundary exhibits undulatory extinction and subgrain boundaries. The syenite has quartz veins that display fractures cross-cutting quartz grains with undulatory extinction and irregular grain boundaries. The alkali feldspar, sometimes perthitic, also displays cross-cutting fractures with undulatory extinction and subgrains (Fig. 3.19). The meta-granodiorite is composed of albite feldspar and quartz, both of which display undulatory extinction, irregular grain boundaries, and subgrains.

Gold mineralization is present within the quartz vein along subgrain boundaries. Gold mineralization is present in the deformed syenite in subgrains and along exsolution lamellae in perthitic alkali feldspar (Fig. 3.19). Sericite also hosts gold mineralization within exsolution lamellae in perthite. One instance of gold mineralization is found within a fractured rutile grain in perthite (Fig. 3.20).

Pyrite ranges from very fine-grained to coarse-grained, disseminated to blebs, but is typically 1-3%, fine-grained and disseminated within areas adjacent to faults, within areas that are fracture sealed, and strongly to intensely altered with hematite or yellow clay. Pyrite is not typically associated with pegmatite or syenite dykes unless it is adjacent to the faults and altered. Pyrite found within fault gouge is medium to coarse-grained, striated, and cubic. One instance of caries texture is observed in a coarse-

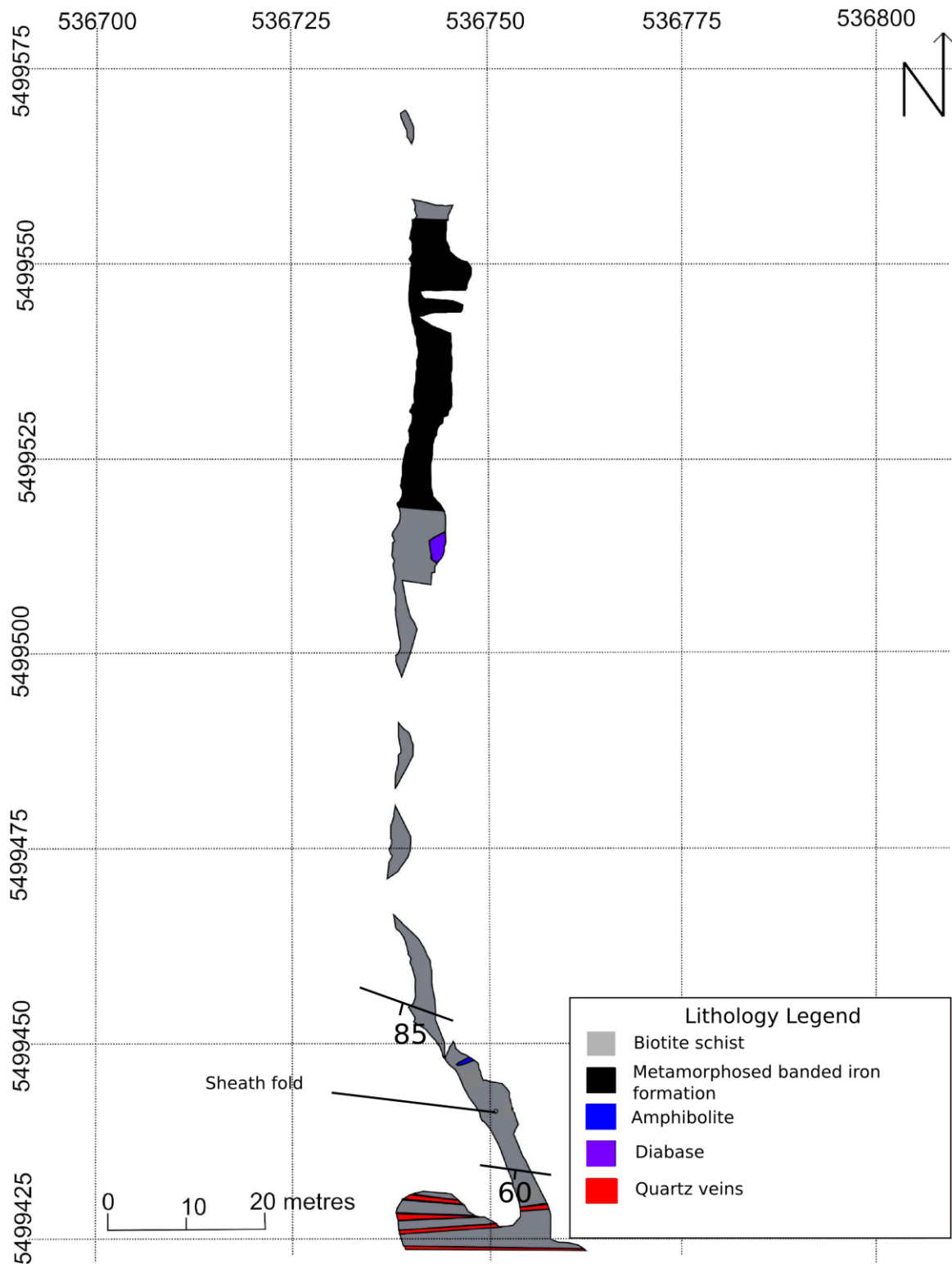


Fig. 3.14: Geological map of the Pagwachuan Trench 1 (A) along the boundary of the Quetico subprovince and Beardmore-Geraldton

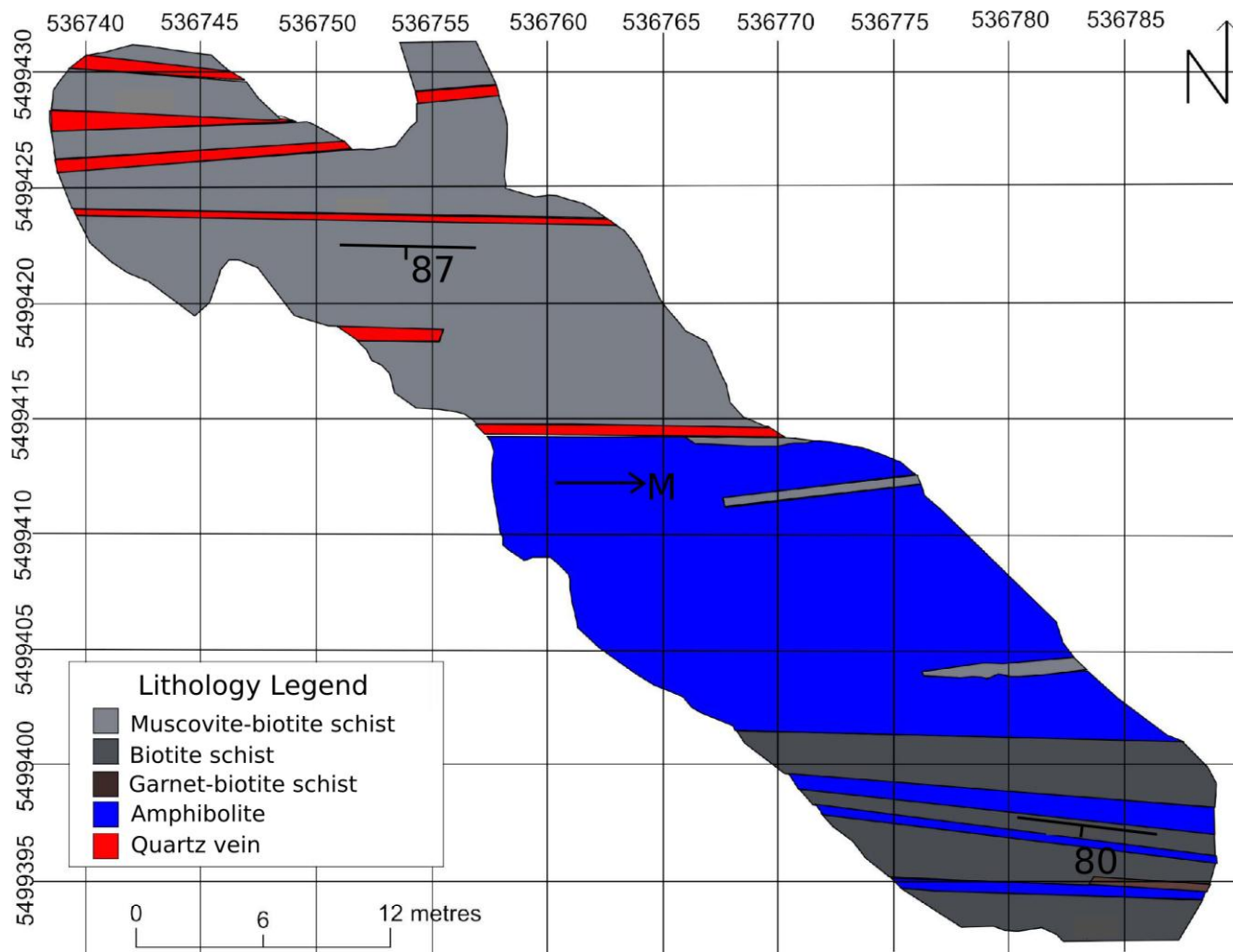


Fig. 3.15: Geological map of the Pagwachuan trench 1 (B) along the boundary of the Quetico and Wabigoon subprovinces and Beardmore-Geraldton greenstone belt

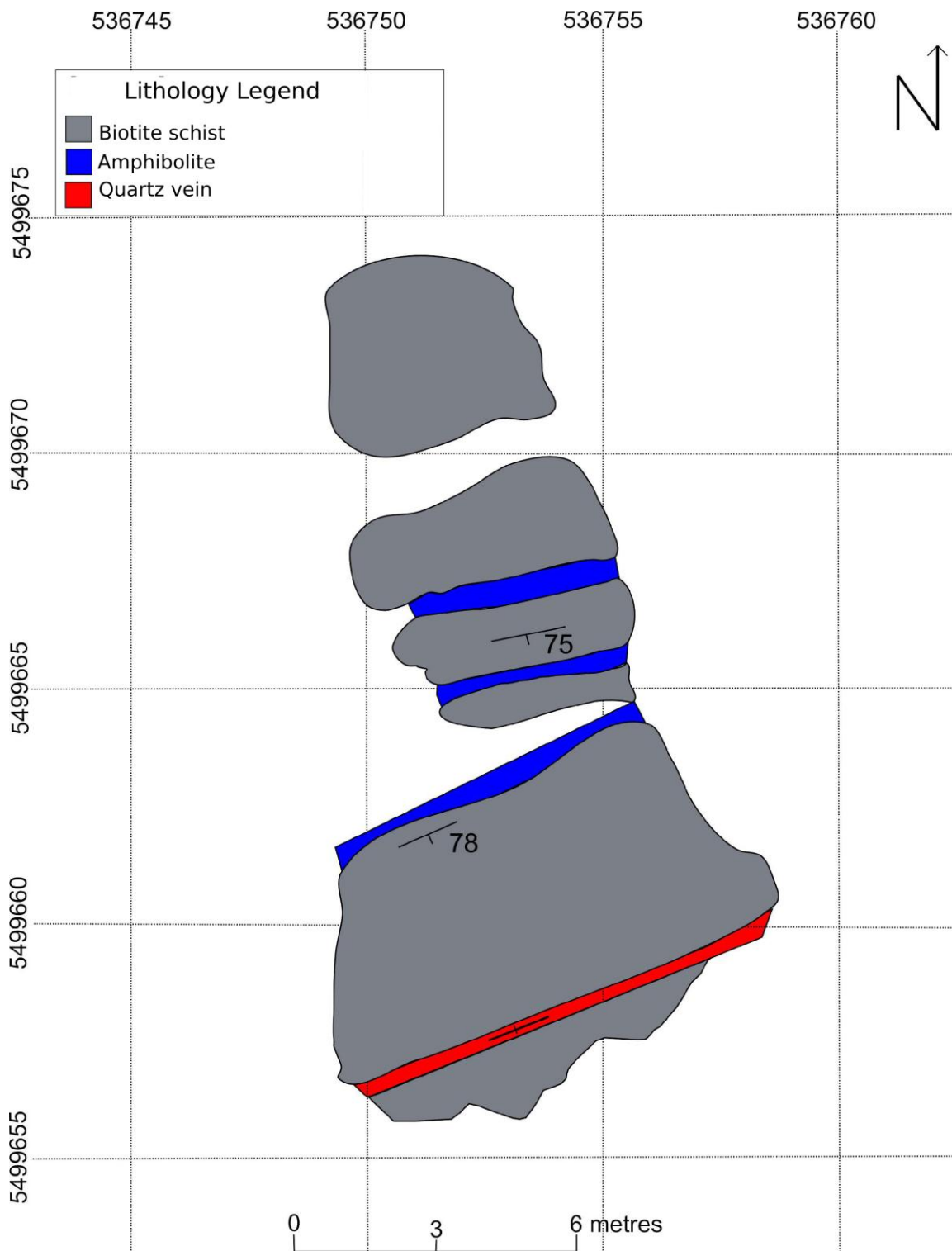


Fig. 3.16: Geological map of the Pagwachuan trench 1 (C) along the boundary of the Quetico and Wabigoon subprovinces and Beardmore-Geraldton greenstone belt

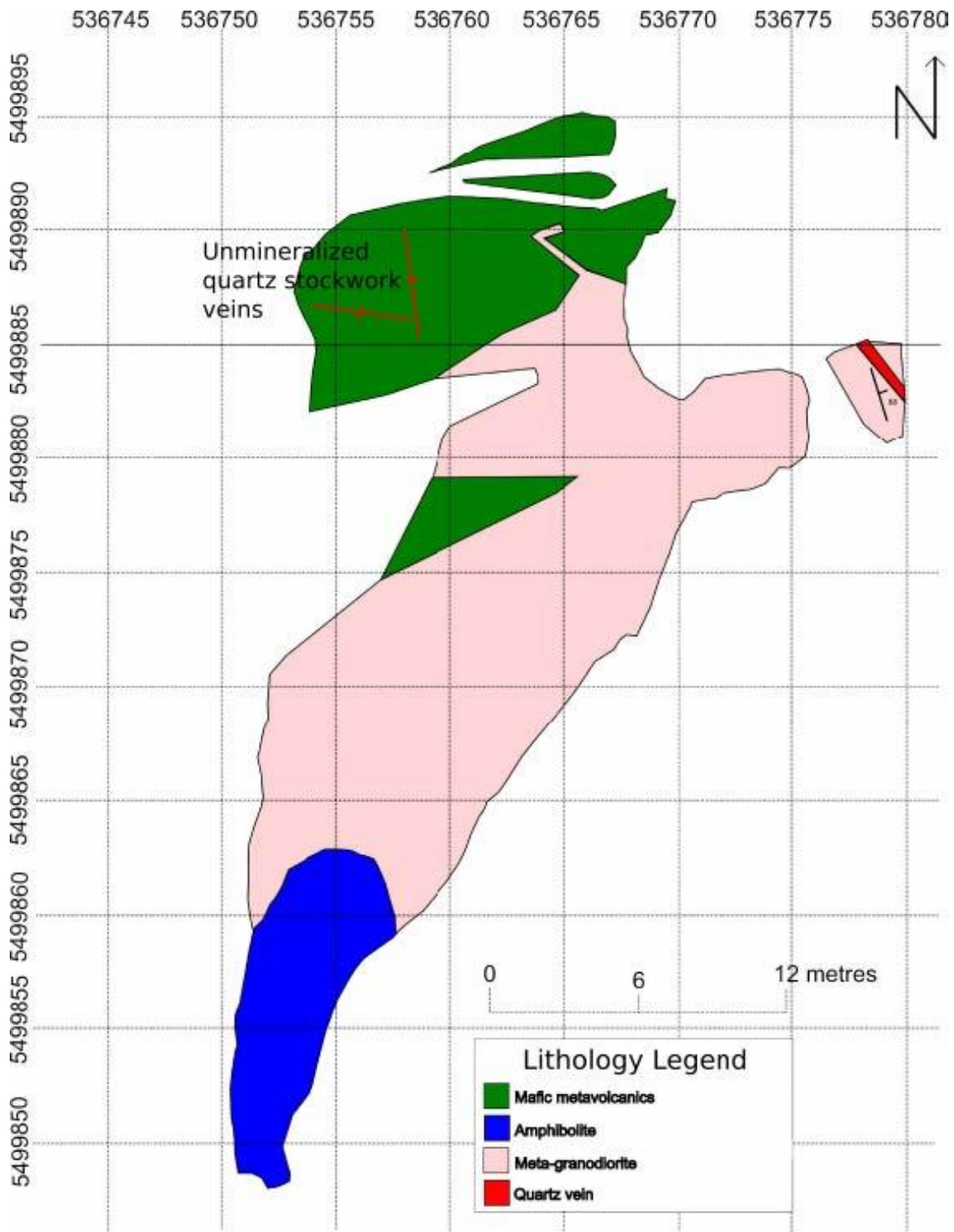


Fig. 3.17: Geological map of the Pagwachuan trench 1 (D) along the boundary of the Wabigoon subprovince and Beardmore-Geraldton greenstone belt

grained pyrite within an area of hematite alteration and filled fractures. The pyrite mineralization does not appear to have any correlation with gold mineralization.

A metasomatized meta-granodiorite is commonly noted within the fault gouge which is comprised of as much as 20% biotite and 20% euhedral, medium-grained pyrite, and intense hematite alteration. Hematite alteration is found where fractured and fracture healed deformation has occurred related to the fault. Yellow clay is another type of alteration found only within the granodiorite that has been ductilely deformed. Neither the hematite nor the clay alterations are present within areas of gold mineralization.

The Milestone property is located east of Longlac in the Paglamin Lake pluton. The host rock to the gold mineralization is amphibolite and meta-granodiorite. The overburden in the area provides no access to gold mineralization in outcrop so samples from drill core were collected. Samples collected from drill core from the Milestone property include amphibolite and quartz veins within amphibolite. Quartz from the quartz veins within amphibolite display undulatory extinction, with and without grain size reduction, subgrains, and irregular grain boundaries. The plagioclase also displays evidence of dislocation creep with evidence of undulatory extinction, grain size reduction, and subgrains present. The quartz veins typically display evidence of boudinage where there has been less grain size reduction. The amphibolite is composed of hornblende, plagioclase, and epidote, chlorite, and quartz. Epidote, chlorite, and quartz are commonly present within areas of greatest ductile deformation. Where

chlorite and epidote are present they partially to completely replace hornblende (Fig. 3.21).

Gold mineralization is present within Milestone samples as inclusions within hornblende and at grain boundaries between chlorite, plagioclase, and hornblende (Fig. 2.22). Gold as inclusions are located within pyrite or albite. When gold is located within quartz veins it is anhedral and forms along irregular grain and subgrain boundaries within areas of quartz boundins. Gold also occurs in pressure shadows, such as next to competent minerals, like hornblende or at high angles to competent minerals in folded, healed fractures. Gold is present within areas of chlorite and biotite that have replaced hornblende during retrograde greenschist facies metamorphism (Fig. 3.21).

Gold, pyrrhotite, chalcopyrite, magnetite, sphalerite, arsenopyrite, and cobaltite mineralization is also located within competent and fractured pyrite as inclusions along fractures or anhedral inclusions (Fig. 3.22). In one sample from Milestone a speck of gold is visibly inside a fluid inclusion at room temperature. No vapour or other crystals were noted in the inclusions at room temperature.

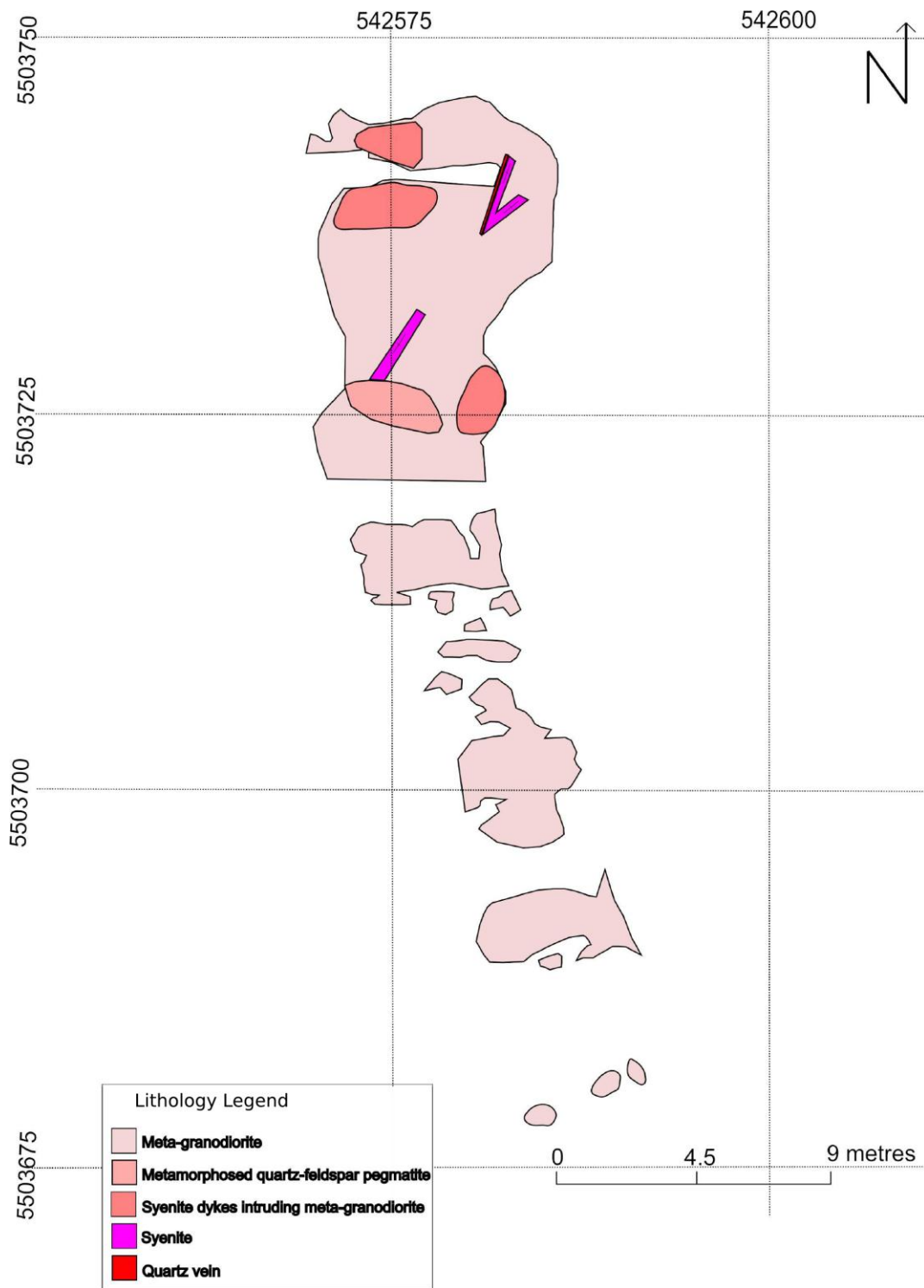


Fig. 3.18: Geological map of the Pagwachuan trench 2 along the boundary of the Wabigoon subprovince and Beardmore-Geraldton greenstone belt

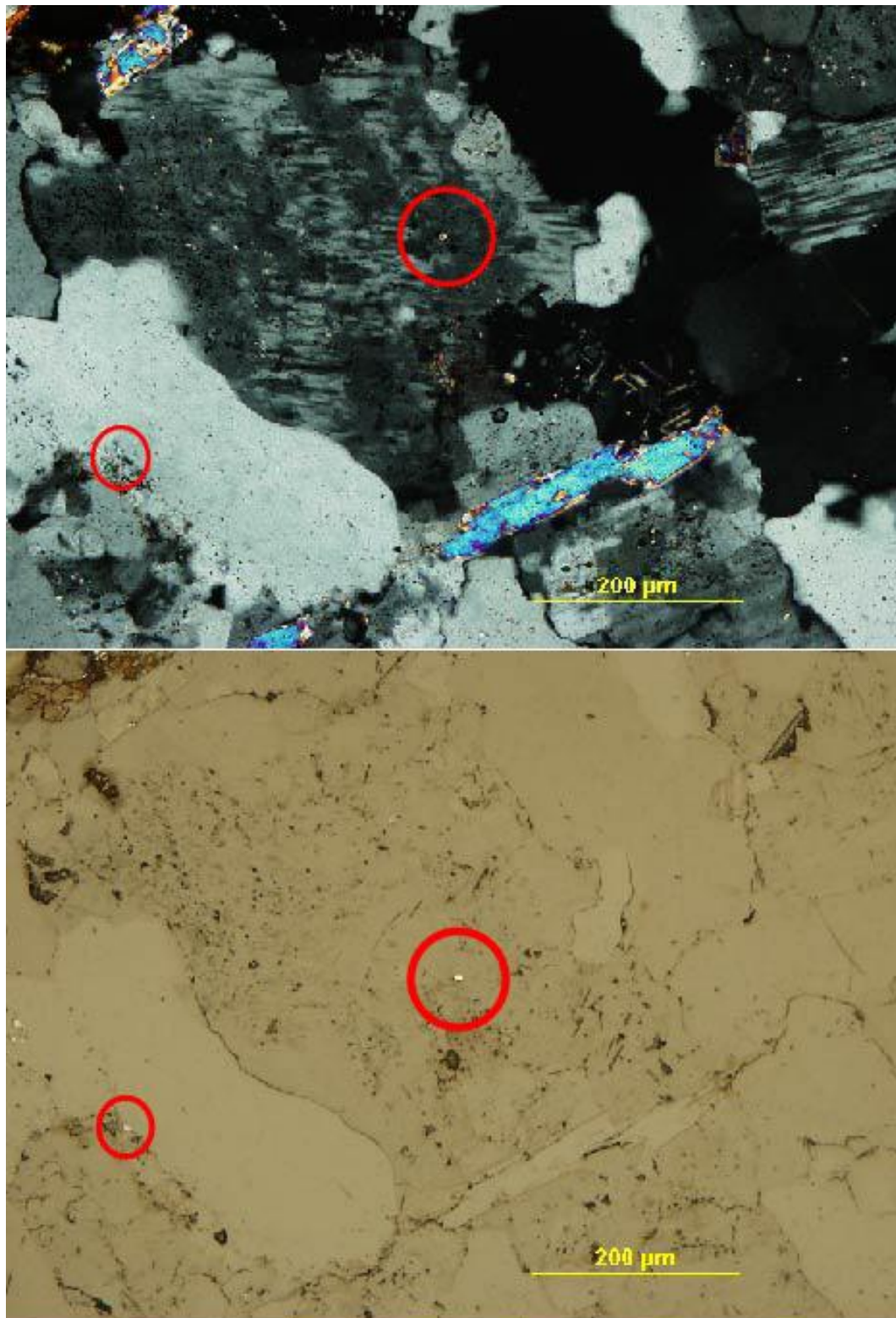


Fig. 3.19: Photomicrograph in cross-polarized light (top) and reflected light (bottom) from the Pagwachuan trench #2 in the Pagwachuan property near Caramat (Sample MVS148). Gold mineralization along boundary of exsolution lamellae in perthite in syenite (centre) and subgrains in feldspar (left).

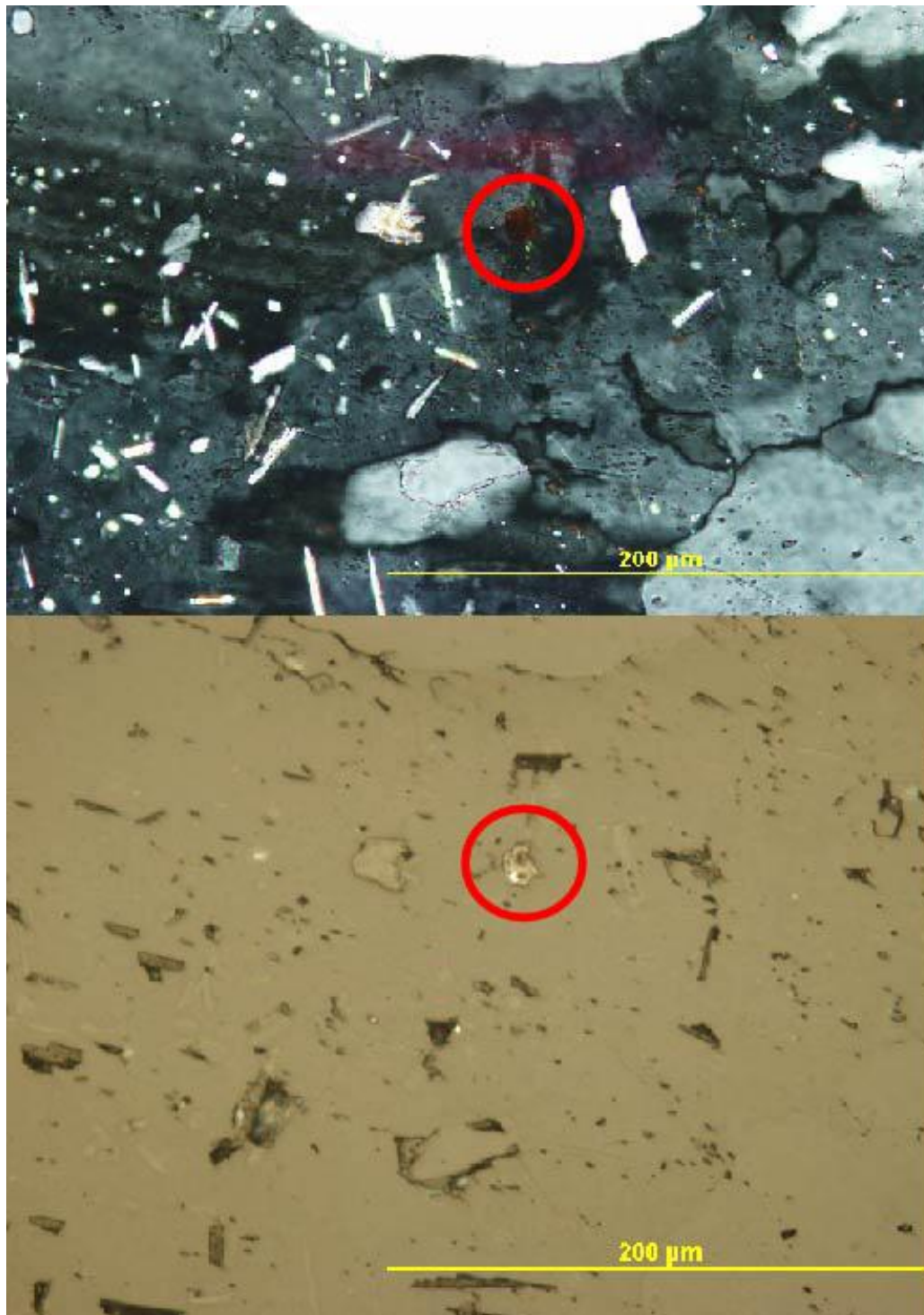


Fig. 3.20: Photomicrograph in cross-polarized light (top) and reflected light (bottom) from the Pagwachuan trench #2 in the Pagwachuan property near Caramat (Sample MVS148). Gold mineralization within subgrains in feldspar within fractured rutile and sericite in syenite.



Fig. 3.21: Photomicrograph in cross-polarized light (top) and reflected light (bottom) from the Milestone property near Longlac (Sample MVS111). Gold mineralization is located along chlorite-chlorite grain boundaries within hornblende in amphibolite.

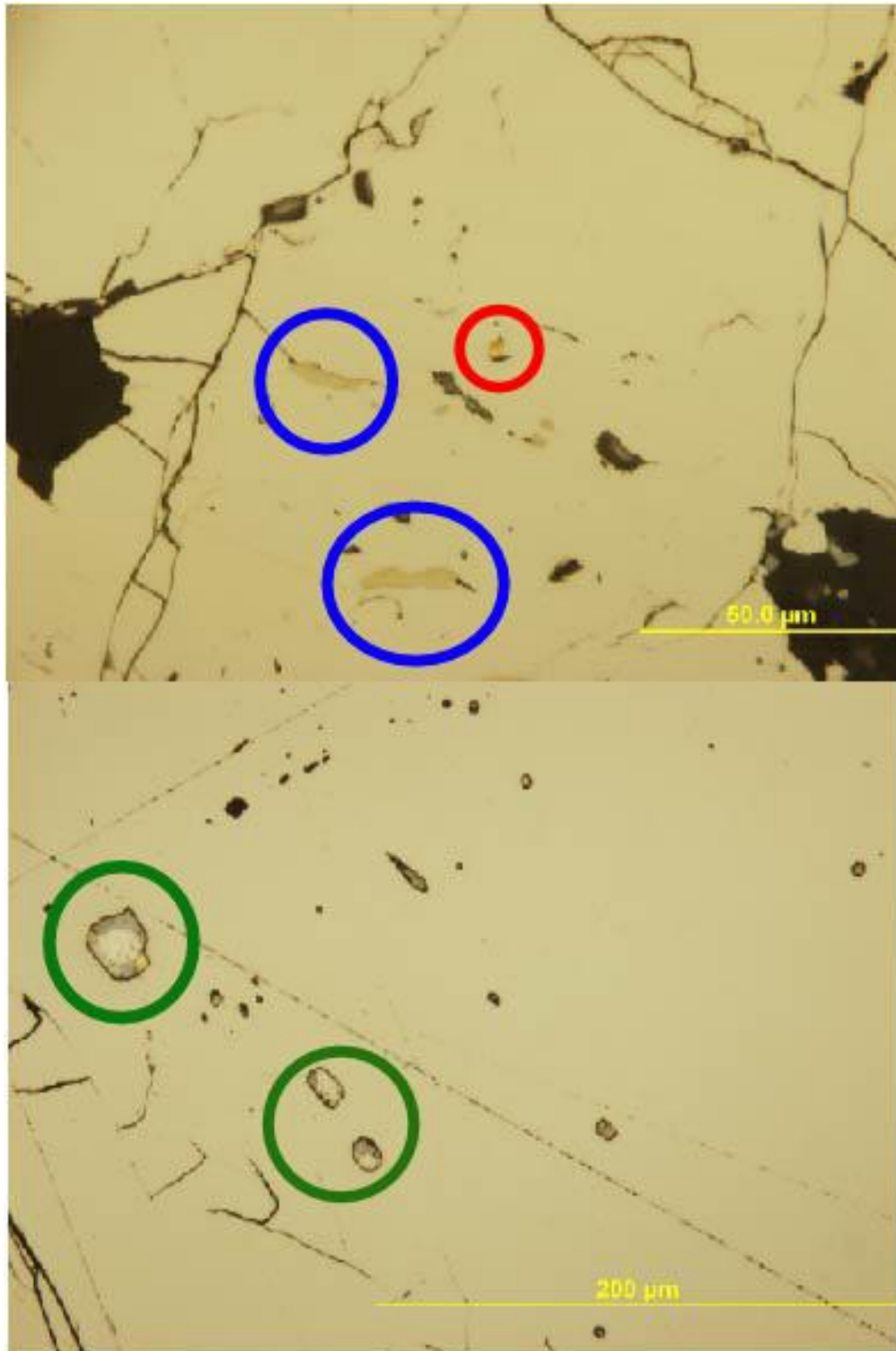


Fig. 3.22: Photomicrographs in reflected light from the Milestone property near Longlac (Top sample, MVS114; bottom sample, MVS113). Gold mineralization is present within amphibolite in fractured pyrite as inclusions (red circle). Pyrrhotite inclusions are also present (blue). Inclusions of gold, pyrrhotite, arsenopyrite, magnetite, and cobaltite are also present together (green).

3.2 The Quetico subprovince

The property mapping, trench mapping, and petrography conducted in the Quetico subprovince includes the southern portion of the Pagwachuan property that extends south of Seagram Lake, near Caramat into the Quetico subprovince. The McKay trench is located north of McKay Lake and Seagram Lake within the Pagwachuan property (Fig. 3.23).

The lithologies present within the Quetico subprovince in the Pagwachuan property include polymictic meta-conglomerate, muscovite-biotite schist, biotite schist, garnet-hornblende schist, kyanite-muscovite schist, metamorphosed iron formation, migmatite, and minor amounts of syenite, diorite, and granite (Fig. 3.23). Polymictic meta-conglomerate is present within the mapping area north of McKay Lake adjacent to metamorphosed banded iron formation. The clasts within the meta-conglomerate are rounded, average approximately 10 cm³ in volume, and are composed of metamorphosed iron formation, granite, and meta-granodiorite.

The metasedimentary lithologies have a 90-120°/80-88° strike and dip and a crenulation foliation of 180°220°/50-60°. The minor lithologies of syenite, diorite, and granite do not have any structural fabric. Quartz veins are common within the metasedimentary lithologies, especially at the boundaries between coarse-grained and fine-grained muscovite-biotite schist. Quartz is present in the QF-domain of the crenulation hinges but does not host gold mineralization. Complex folds in quartz veins,

typically as shear-related late folds, are present within garnet-hornblende schist. Parasitic and ptigmatic quartz veins are common in migmatite.

The lithologies present within the McKay trench in the Pagwachuan property are muscovite-biotite schist, biotite schist, garnet-hornblende-biotite schist, and kyanite-muscovite schist (Fig. 3.24). Biotite schist is rare in the study area and is only present within biotite-muscovite schist, typically within units <10cm thick. Biotite schist is a darker grey than the biotite-muscovite schist as it contains up to 30% black biotite. Within the muscovite-biotite schist at the McKay trench a localized unit of kyanite-muscovite schist is present. The porphyroblastic kyanite has a typical bladed habit and is blue, with occasional purple, zoned cores, and up to 2 cm long (Fig. 3.24). The kyanite has been partially to entirely replaced by medium-grained muscovite. Garnet-hornblende-biotite schist is extremely rare and is only located within the McKay trench area. Porphyroblasts of almandine garnet within the garnet-hornblende schist are euhedral and commonly form a vertical mineral lineation. Porphyroblasts of hornblende are black, euhedral, bladed, and up to 0.5cm long.

Kyanite-muscovite schist is out of equilibrium, with muscovite almost completely replacing the aluminosilicate. Kyanite has been noted in a few instances to be boudinaged parallel to crenulation, suggesting it was more competent than the muscovite-biotite schist during deformation. The kyanite displays undulatory extinction in thin section suggesting it was deformed at high temperature after formation.

The samples collected for petrography from the McKay trench include garnet-hornblende-biotite schist, metamorphosed banded iron formation, muscovite-biotite schist, and kyanite-muscovite schist. The garnet-hornblende-biotite schist is composed of porphyroblastic, euhedral almandine garnet, euhedral hornblende that commonly replaces subhedral blue-green amphibole (crossite), anhedral quartz, muscovite, and brown biotite. The biotite and quartz anastomose around the more competent garnet and amphiboles. The quartz exhibits subgrains and undulatory extinction.

Pyrrhotite and pyrite are both located adjacent to and within stable garnet, biotite, and hornblende suggesting sulphide mineralization was contemporaneous with metamorphism (Fig. 3.24). Gold mineralization is located within shear zones in garnet-hornblende schist, with and without pyrrhotite and pyrite. The gold mineralization is located in fractures in garnet and along quartz-amphibole grain boundaries (Figs. 3.25, 3.26). Gold mineralization is also located along fractured amphibole-biotite grain boundaries and within biotite at oblique angles to foliation (Fig. 3.27). Quartz veins are common within the gold mineralized garnet-hornblende-biotite schist and are even more common on the microscopic scale. Microscopic folds and micro-boudins are typical within quartz veins and host gold mineralization. Gold mineralization is located in quartz veins along smooth quartz subgrain boundaries, with and without inclusions present (Fig. 3.28). In addition to quartz veins, schistose fault breccia and folded healed fractures are also present within areas of gold mineralization (Fig. 3.29). No gold mineralization is present within the oxide facies of metamorphosed banded iron formation.

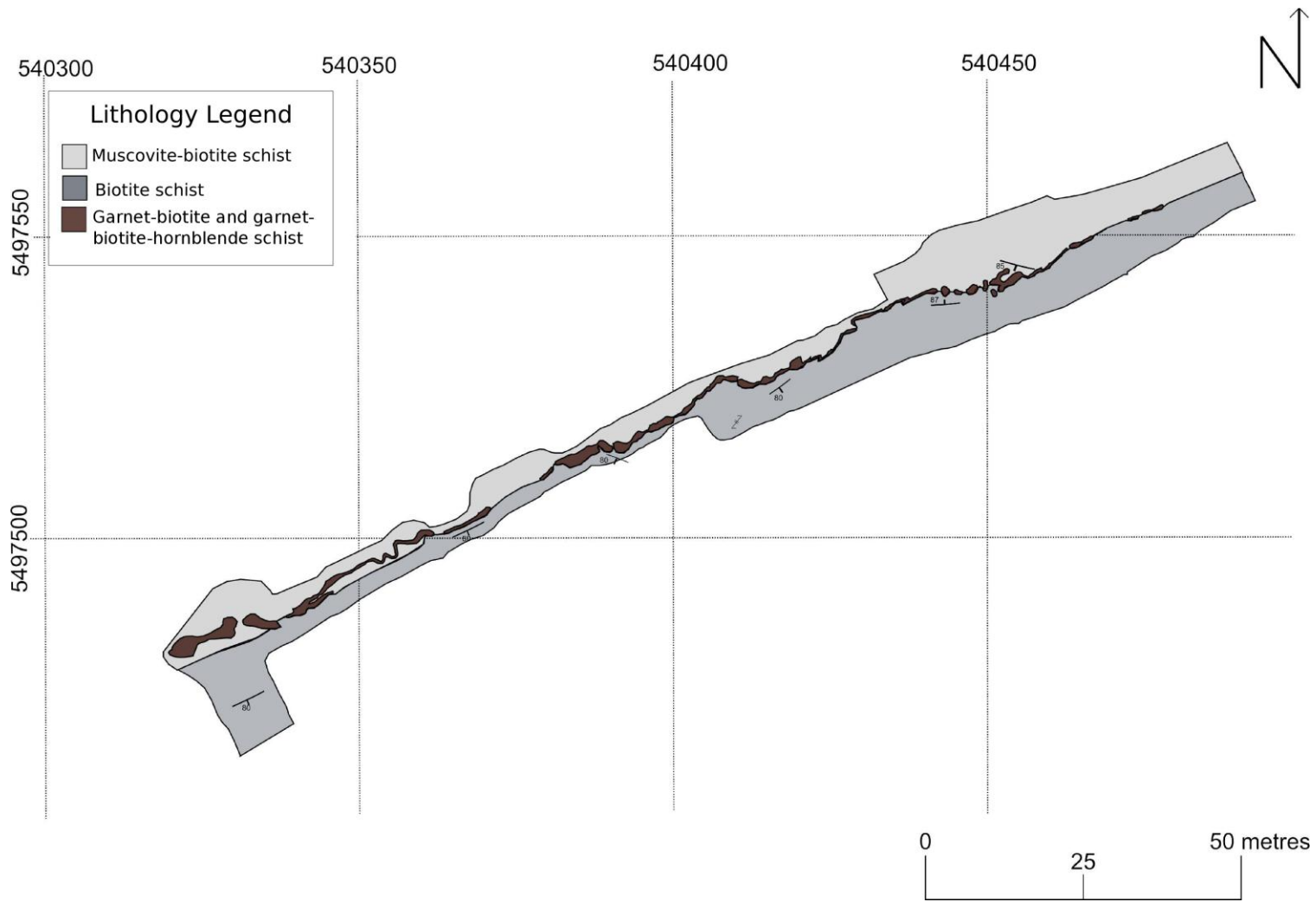


Fig. 3.23: Geological map of the McKay trench within the Qetico subprovince

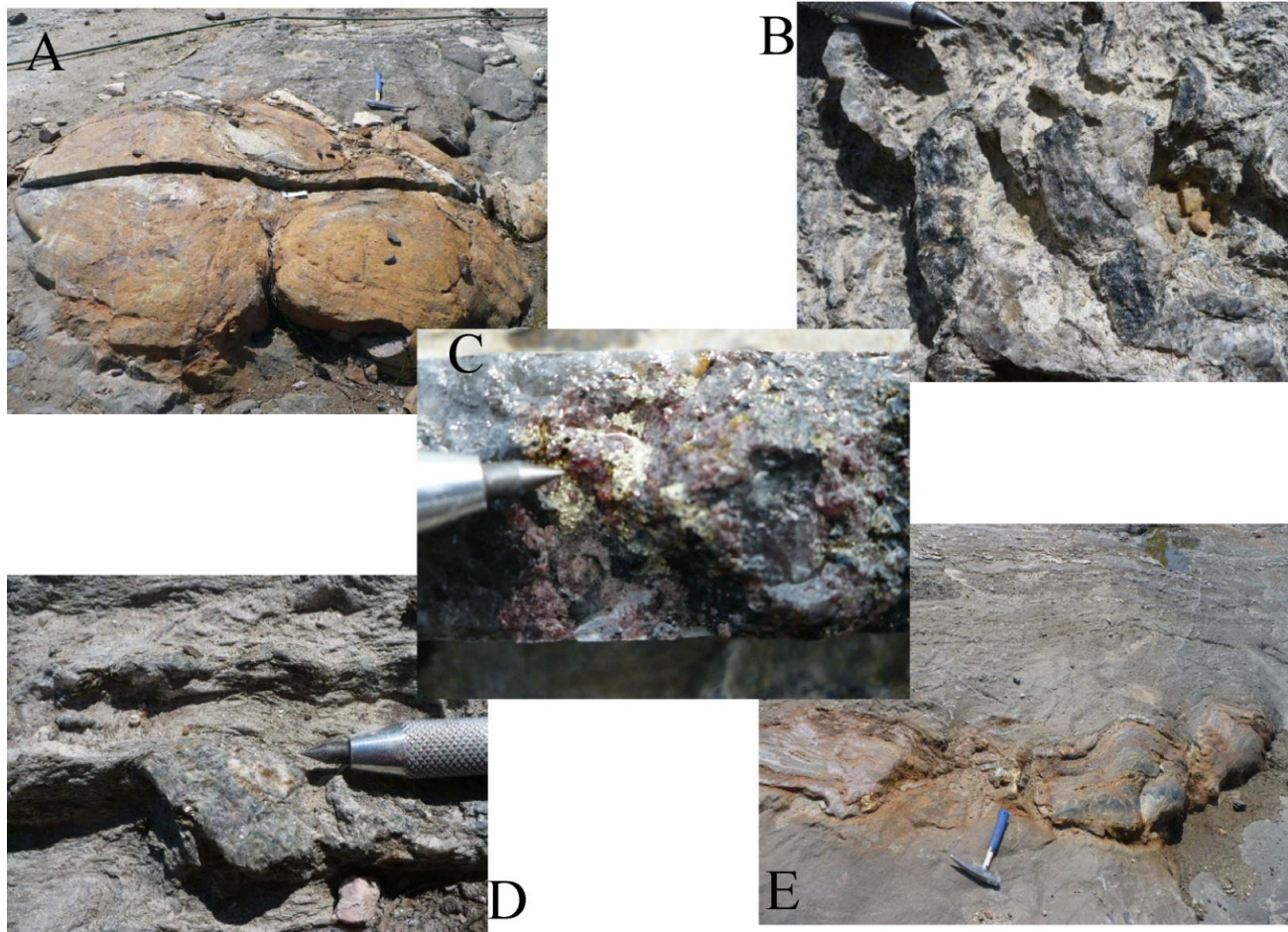


Fig. 3.24: Photos of samples and outcrop from McKay trench in the Quetico subprovince. A) Garnet-biotite schist in metasandstone, B) Boudinaged kyanite, C) Pyrrhotite and gold along biotite-garnet grain boundaries, D) Subhedral kyanite, E) Boudinaged garnet-biotite schist in muscovite-biotite schist.

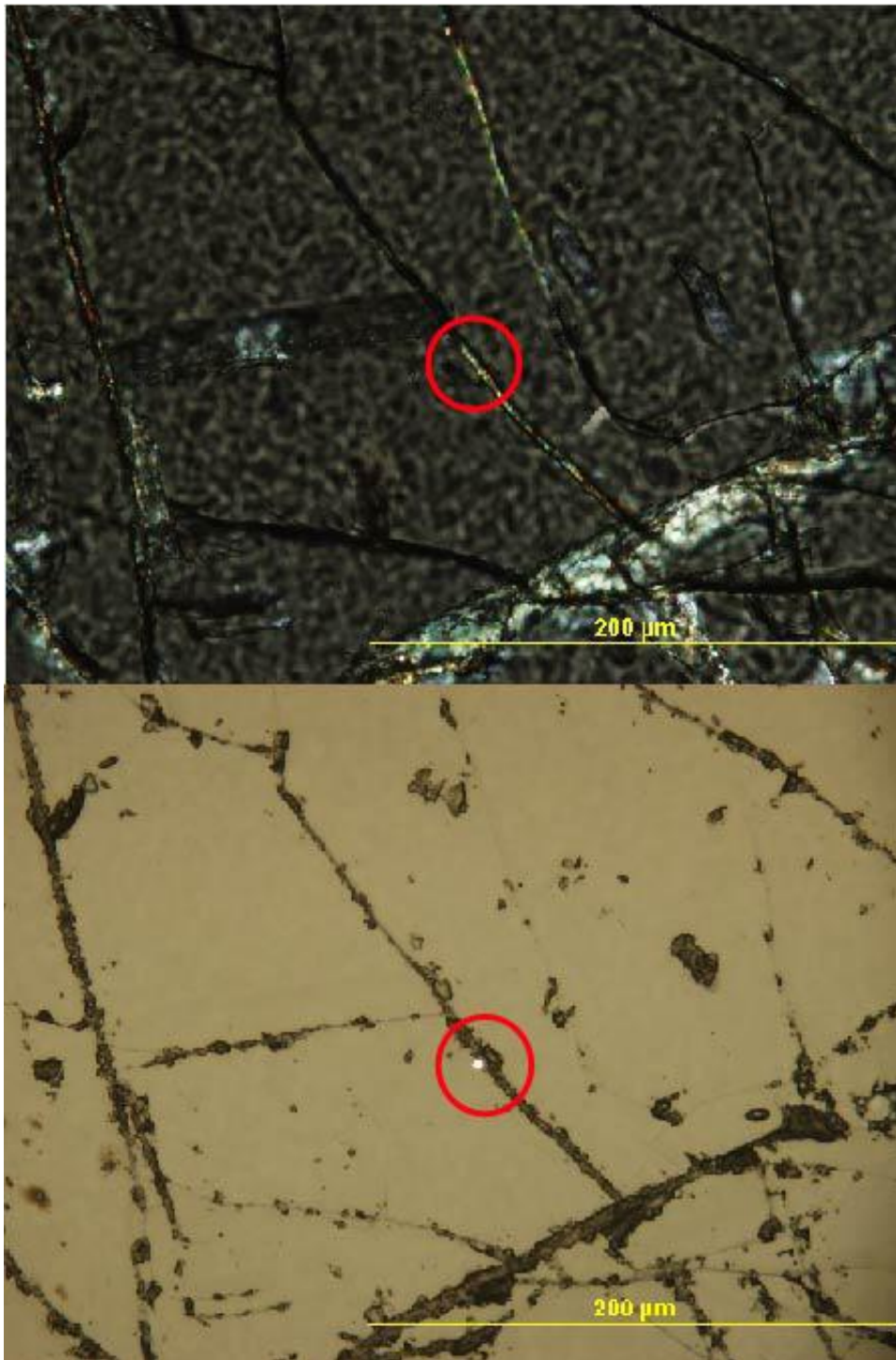


Fig. 3.25: Photomicrographs in cross-polarized light (top) and reflected light (bottom) from the McKay trench in the Pagwachuan property near Caramat (Sample MVS153). Gold mineralization is located in fractured garnet within garnet-hornblende-biotite schist.

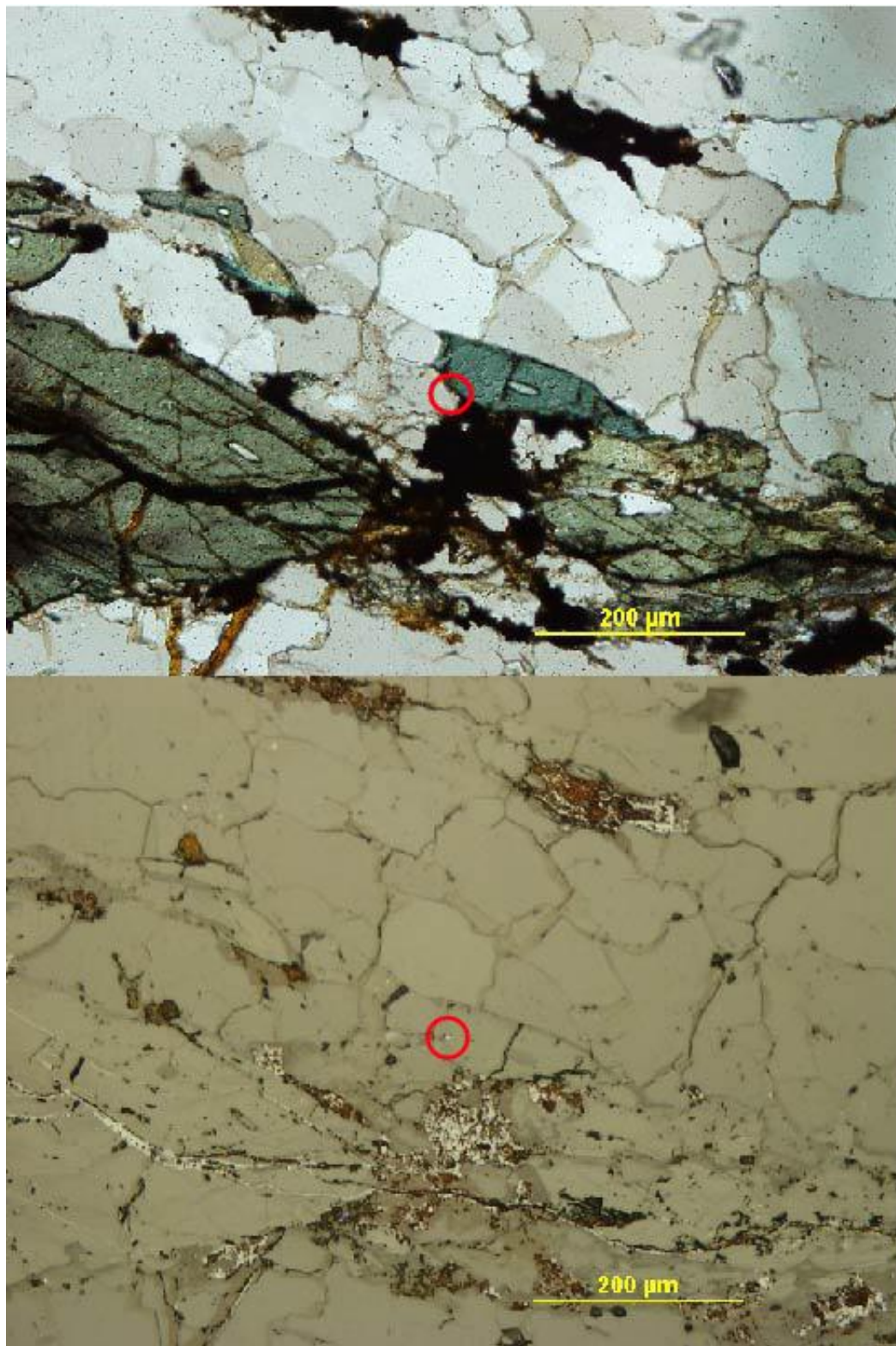


Fig. 3.26: Photomicrographs in cross-polarized light (top) and reflected light (bottom) from the McKay trench in the Pagwachuan property near Caramat (Sample MVS153). Gold mineralization is located along hornblende-quartz vein boundary.



Fig. 3.27: Photomicrographs in cross-polarized light (top) and reflected light (bottom) from the McKay trench in the Pagwachuan property near Caramat (Sample MVS153). Gold mineralization is located in biotite between fractured amphibole in garnet-hornblende-biotite schist.

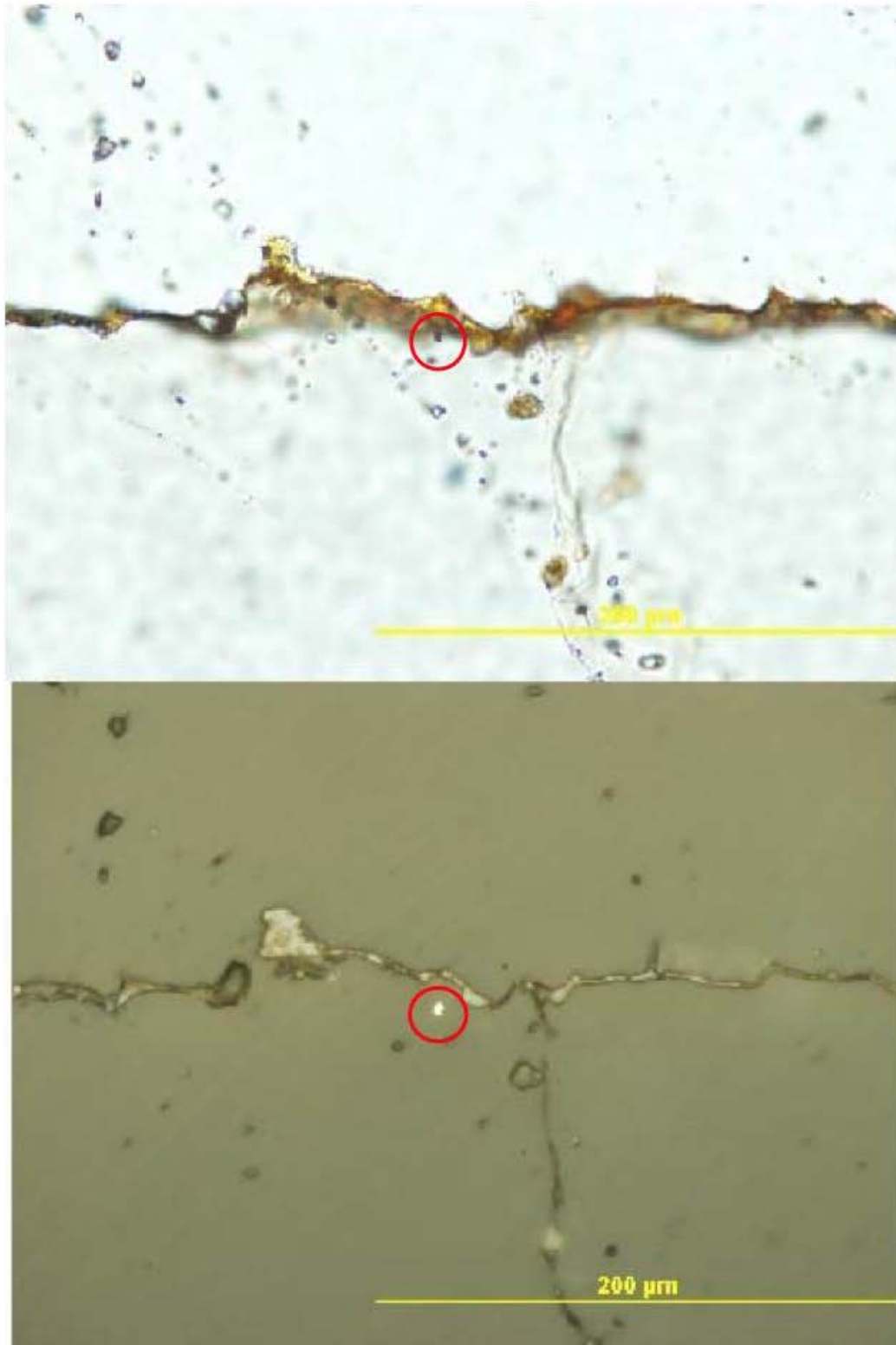


Fig. 3.28: Photomicrographs in plane-polarized light (top) and reflected light (bottom) from the McKay trench in the Pagwachuan property near Caramat (Sample MVS153). Gold mineralization is located adjacent to folded healed fractures and fluid inclusions within a quartz vein in garnet-hornblende-biotite schist.

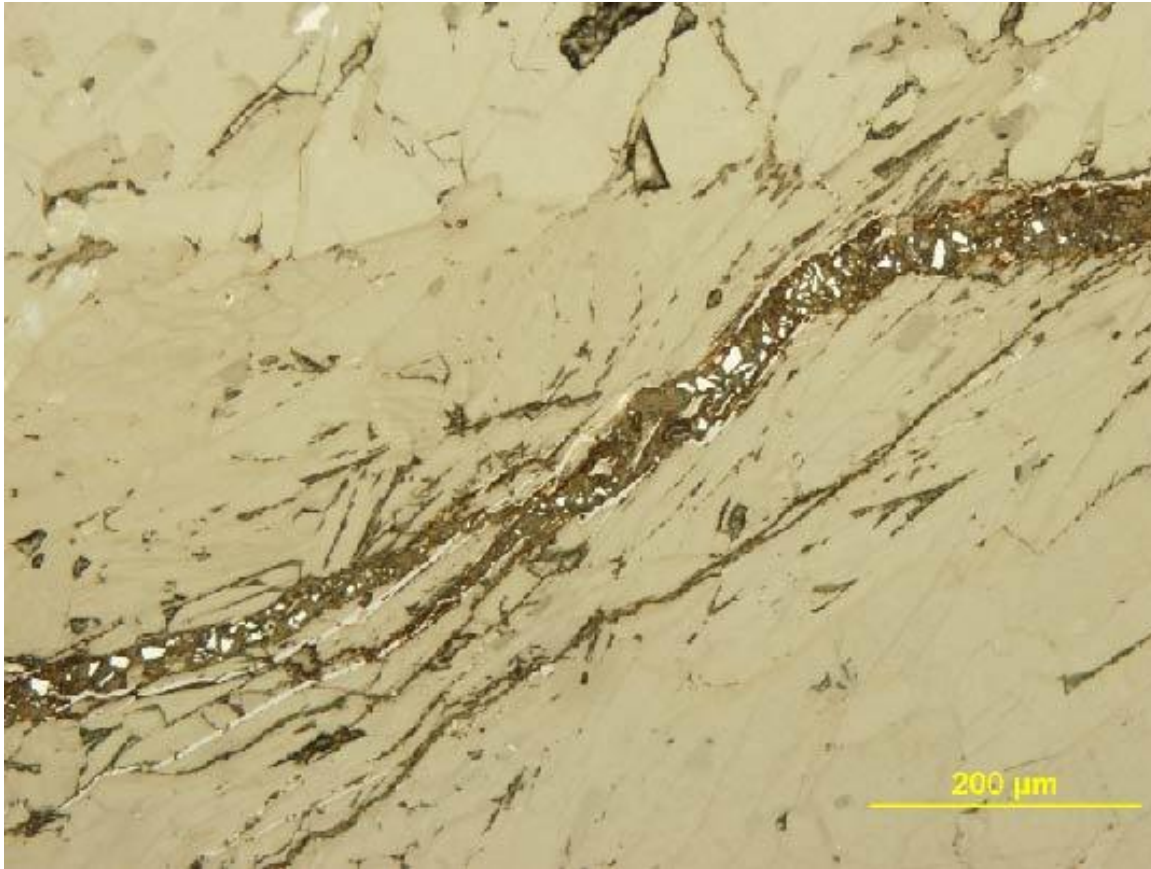


Fig. 3.29: Photomicrographs in reflected light from the McKay trench in the Pagwachuan property near Caramat (Sample MVS154). Angular clasts of pyrrhotite mineralization in folded fault breccia within garnet-hornblende-biotite schist.

3.2 Observations of historical outcrops in the Beardmore-Geraldton greenstone belt

Four classic outcrops were visited within the historical Beardmore-Geraldton greenstone belt, including the Leitch Mine, Missing Link outcrop, Highway 584 outcrop, and Highway 11 outcrop. The classic outcrops are commonly described in literature and used as stops for Beardmore-Geraldton greenstone belt field trips (Mason *et al.*, 1985; Mason and White, 1986; Smyk *et al.*, 2005).

The historical Leitch Mine is located north of Beardmore within the Beardmore-Geraldton greenstone belt. One oriented sample of chlorite-muscovite schist was collected from outcrop within the metapelitic unit in the Leitch Mine property. The chlorite-muscovite schist is composed of chlorite, albite feldspar, muscovite, and quartz. The albite feldspar is fractured while the quartz, chlorite, and muscovite deformed more ductilely, as displayed by evidence of undulatory extinction. Quartz veins cross-cut the foliation and exhibit open to isoclinal folds. The quartz in the quartz vein also displays undulatory extinction.

The Missing Link outcrop is located within the Paint Lake Shear Zone near Jellicoe. Three oriented samples were collected from outcrop. The samples of chlorite schist have an east-west strike and a 90° dip. No S-C fabric is noted in the outcrop. The entire outcrop of chlorite schist displays extreme grain size reduction with tightly spaced (less than 1 mm spacing between foliation bands), smooth, mylonitic, and schistose fabric. No evidence of recrystallization is noted in thin section. Ankerite alteration is extensive throughout the outcrop.

The outcrop at the fork in Highway 584 and Tower Road north of Geraldton is also located within the Beardmore-Geraldton greenstone belt. The outcrop is primarily a breccia overprinted with a schistose fabric (Fig. 3.30). Breccia clasts are angular and composed of chlorite schist, metasandstone, metasilstone, and metamorphosed feldspar porphyry to granite. The clasts show a preferred orientation along their long axis parallel to the east-west strike of the Barton Bay Deformation Zone. The flattened and elongated clasts also exhibit a vertical to near vertical dip. No petrographic samples were collected.

The former Mosher Mine is located only metres west of the outcrop and is along strike to the Barton Bay Deformation Zone that strikes throughout the area and outcrop.

The outcrop at the junction of Highway 584 and Highway 11 south of Geraldton is also within the Beardmore-Geraldton greenstone belt. The outcrop hosts primarily metamorphosed banded iron formation, chlorite schist, and metamorphosed feldspar porphyry. No samples were collected. All lithologies in outcrops in and around Geraldton display a foliation that follows the east-west striking Barton Bay Deformation Zone. The metamorphosed banded iron formation is folded both in cross section and plane view and exhibits a number of <10cm sheath folds elongated east-west with a gentle plunge towards the (Fig. 3.30). The metamorphosed feldspar porphyry appears to be porphyritic granite as it is composed mainly of medium- to coarse-grained feldspar and very fine-grained quartz. According to current workers the banded iron formation, metamorphosed feldspar porphyry, and metasedimentary lithologies host gold mineralization (Daniel Grabiec, personal communication, 2012).

3.9 Summary of the Wabigoon subprovince

The lithologies in the Wabigoon subprovince that host gold mineralization range from felsic meta-granodiorite and pegmatite plutons in the Elmhirst Lake pluton north of Jellicoe to amphibolite within the Paglamin Lake pluton east of Longlac. The alteration in the Wabigoon subprovince ranges from sericite in the Elmhirst Lake pluton to ankerite in the Missing Link outcrop within the Paint Lake shear zone. The metamorphic grade varies throughout the Wabigoon subprovince from greenschist facies north of Jellicoe to amphibolite in and around Longlac.

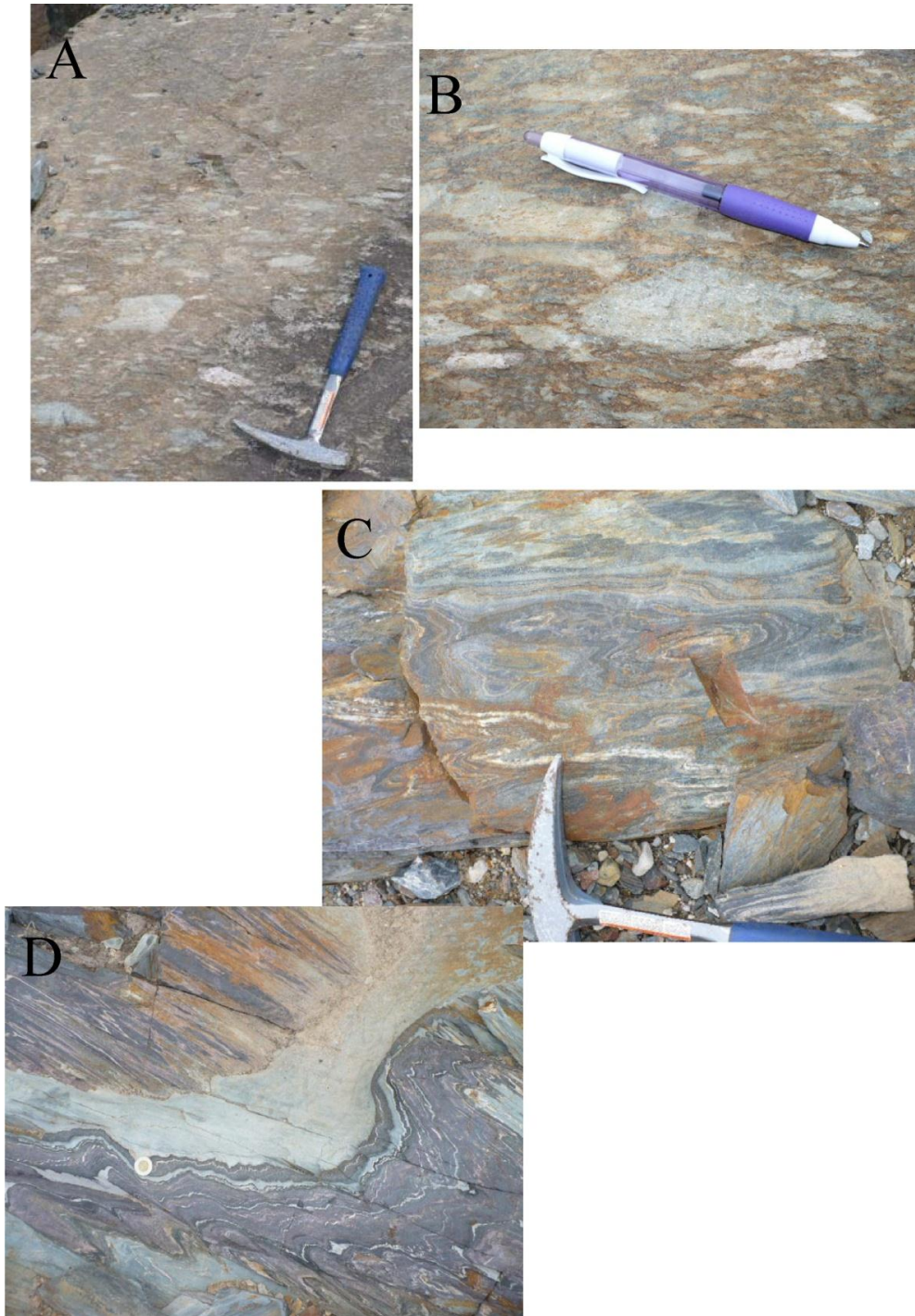


Fig. 3.30: Photos of outcrop from within the Beardmore-Geraldton greenstone belt. A and B) Folded fault breccia with angular clasts of chlorite schist and metagranitoid within a fine-grain muscovite-biotite schist at Highway 584 outcrop, C) Sheath folds in metamorphosed banded iron formation and chlorite schist at Highway 11 outcrop, D) Folded chlorite schist within metamorphosed banded iron formation at Highway 11 outcrop

The regional structures throughout the study areas in the Wabigoon subprovince are ductile to brittle-ductile shear zones. The HHSZ is a ductile to brittle-ductile shear zone that is present throughout the Castlewood property. The gold mineralization in the Castlewood property is located in schistose meta-granite and complexly folded, typically shear-related early and late folds, chlorite schist. The chlorite schist displays fractures in pyrite and dislocation creep with grain size reduction in quartz, undulatory extinction in chlorite, and biotite fringe around pyrite. The adjacent lithology of meta-granite displays evidence of dislocation creep in quartz, with undulatory extinction and irregular grain boundaries, while the albite plagioclase is competent and has inclusions of gold and sericite. No gold mineralization in the Castlewood property was found outside of the HHDZ.

The PLSZ is a ductile to brittle-ductile shear zone that is present throughout the Elmhirst property that includes the Golden Mile, Lucky Strike, Brenbar, Findian 3, and the Straights trenches. The PLSZ is present throughout the Elmhirst property and displays schistose to mylonitic fabric in all lithologies. The PLSZ displays evidence of ductile to brittle-ductile deformation in the Golden Mile and Lucky Strike trenches with fractures, micro-fractures, and quartz veins overprinted ductilely. Evidence of dislocation creep in quartz is present in the quartz veins with grain size reduction, irregular grain boundaries, and undulatory extinction common in areas of gold mineralization. Gold mineralization is present within subgrains of quartz, in pressure shadows around pyrite, and elongated parallel to foliation adjacent to pyrite. Complex

folds, typically as a shear-related late folds, in the Brenbar and Golden Mile trenches also host gold mineralization as does ductile overprinted fault breccia in the Brenbar trench.

3.8 Summary of the Beardmore-Geraldton greenstone belt

Gold mineralization is hosted in many different lithologies such as metamorphosed banded iron formation, metasandstone, and intermediate to mafic metavolcanics. Alteration in the Beardmore-Geraldton greenstone belt includes sericite in the metamorphosed feldspar porphyry in the Highway 11 outcrop to unaltered metavolcanics near the Leitch Mine property. The metamorphic grade increases from lower greenschist facies in the Leitch Mine property to amphibolite facies south of Seagram Lake in the Pagwachuan Lake property.

The regional to microstructures are consistent throughout the Beardmore-Geraldton greenstone belt. Gold mineralization is located in the belt within ductile to brittle-ductile shear zones with an east-west strike and near vertical dip, mylonitized quartz and quartz-carbonate veins striking parallel or at low angles to the regional shear zones, and microstructures providing evidence for both dislocation creep and brittle-ductile deformation (Fig. 3.31).

The PLSZ is located throughout the western portion of the Beardmore-Geraldton greenstone belt. The PLSZ crosscuts many lithologies, such as metamorphosed banded iron formation, meta-conglomerate, metavolcanics, and metamorphosed felsic plutonic rock. The schistose fabric of the chlorite schist and the long axis of the polymictic clasts in the meta-conglomerate within the historic Leitch Mine strike parallel to the PLSZ.

The quartz and quartz-carbonate veins strike also strike at low angles to near parallel to the PLSZ. Quartz veins in thin section display undulatory extinction and are folded.

Grain size reduction and schistose to mylonitic fabric can be identified throughout the western area of the Beardmore-Geraldton but it is most extreme in the Missing Link outcrop. The Missing Link outcrop showcases the PLSZ with schistose to mylonitic fabric striking east-west with a near vertical dip. The schistose to mylonitic fabric is <2 cm between bands within the PLSZ while the schist outside of the PLSZ is typically 5-10 cm between schistose bands and rarely displays mylonitic fabric. The Missing Link outcrop displays the greatest grain size reduction in the study area, from 100 μm to <10 μm in quartz grain size, which is consistent with previous work that has described the intense ductile deformation with evidence of dislocation creep and diffusion creep (Reilly, 1987).

The Barton Bay Deformation Zone is located throughout the eastern portion of the Beardmore-Geraldton greenstone belt in the Highway 11 and 584 outcrops and extends into the Pagwachuan property, south of Seagram Lake near Caramat. The metamorphosed banded iron formation and chlorite schist in the Highway 11 outcrop are complexly folded, typically as a shear-related early and late folds, with sheath folds while the metamorphosed feldspar porphyry is more competent with less grain size reduction and schistose texture. The Highway 584 outcrop also displays schistose texture that strikes east-west with a near vertical dip and it overprints angular, flattened, and elongated clasts of chlorite schist, metamorphosed banded iron formation, and

metamorphosed felsic plutonic lithologies with a very fine-grained matrix. The schistose fabric overprinting the angular clasts suggest brittle-ductile deformation within mainly ductile shear zones in the BBDZ.

The regional ductile to brittle-ductile shear zones within the Milestone property are located in and around the Paglamin Lake pluton and are collectively named the KKSZ, or the Klotz and Klob Lake Shear Zones. The amphibolite and meta-granodiorite are foliated with occasional mylonitic textures. Evidence of dislocation creep is present in the amphibolite with albite plagioclase displaying undulatory extinction, grain size reduction, and irregular grain boundaries. Fractures are common within pyrite and pyrrhotite. Gold mineralization is common within hornblende or along chlorite grain boundaries where chlorite has partially to completely replaced hornblende. Gold mineralization is also located within inclusions in pyrite, with and without other sulphide minerals present.

3.9 Summary of the Quetico subprovince

The lithologies in the Quetico subprovince near Caramat that host gold mineralization range from garnet-biotite schist to garnet-hornblende-biotite schist. No gold mineralization is present in any other lithologies, such as the meta-granodiorite or metamorphosed banded iron formation. The alteration in the Quetico subprovince ranges from hematite alteration in diorite and gabbro plutons to unaltered lithologies, like the garnet-hornblende-biotite schist. Alteration may or may not be present where gold mineralization occurs. The metamorphic grade is consistently amphibolite facies within the study area in the Quetico subprovince.

The BBDZ continues from the Beardmore-Geraldton greenstone belt into the Pagwachuan property in the Quetico subprovince. The ductile to brittle-ductile shear zones of the BBDZ strike east-west to northeast-southwest with near vertical dip to the south and north. Gold mineralization occurs within the McKay trench in the garnet-biotite schist and garnet-hornblende schist with and without pyrite and pyrrhotite mineralization in ductile to brittle-ductile shear zones. Quartz veins within the garnet-hornblende-biotite and garnet-hornblende schist along the northern shore of McKay Lake typically strike at low angles or parallel to the regional shear zones and may be shear-related late folds.

The gold mineralization in the Quetico subprovince is located within the BBDZ where both dislocation creep and fractures occur in the same lithology, like in the garnet-biotite schist and garnet-hornblende-biotite schist in the McKay trench and in the field north of McKay Lake. On the microscopic scale the gold mineralization within the McKay trench in the BBDZ is within fractures in garnet, along hornblende-quartz grain boundaries, along quartz subgrains, and along gently folded fluid inclusion trails in quartz veins (Fig. 3.31). Evidence of brittle deformation, in the form of fractures, occurred within competent minerals, like garnet, within a ductilely deformed quartz matrix.

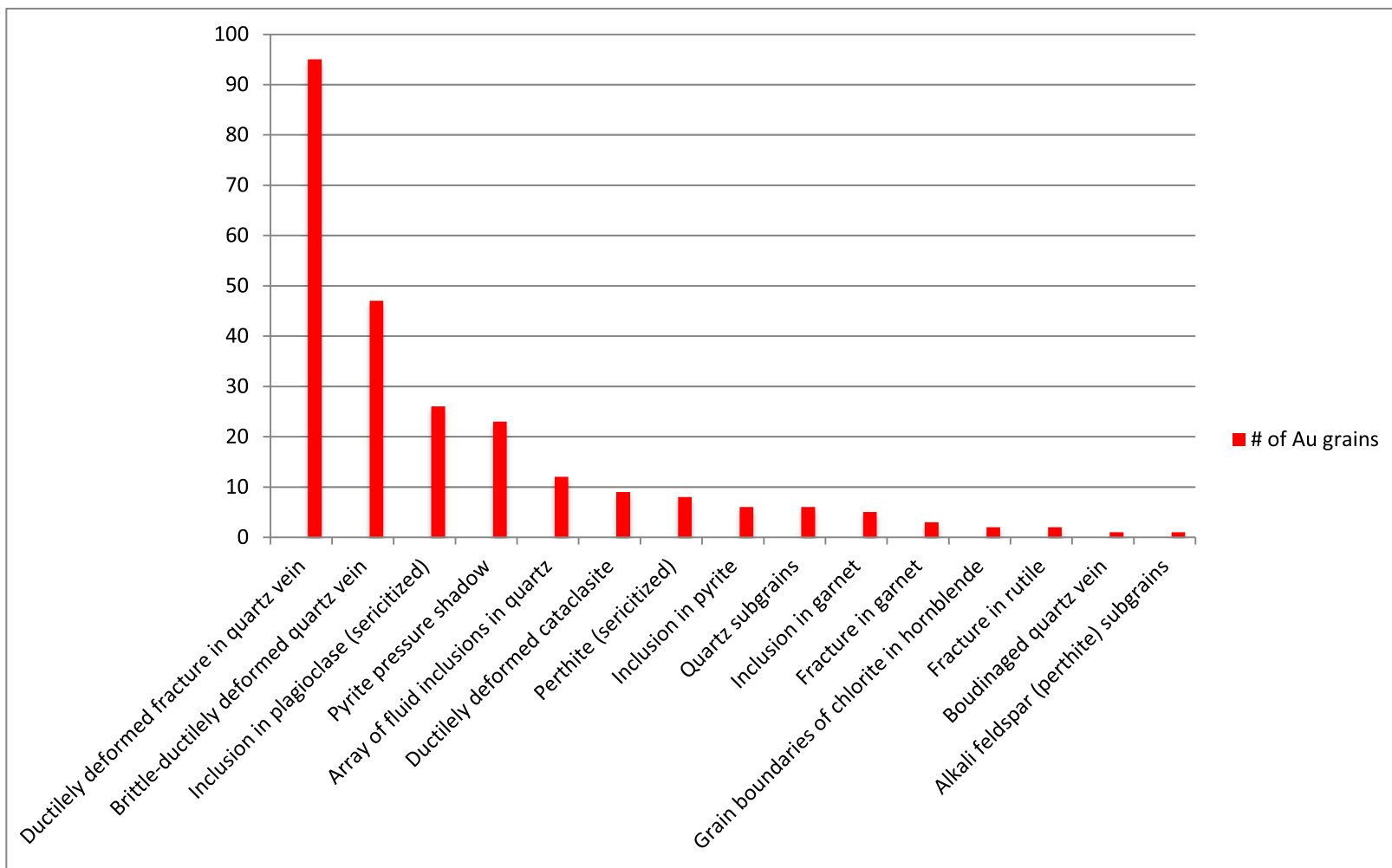


Figure 3.31: Occurrence and distribution of gold grains in thin section (n=237)

4-DISCUSSION AND INTERPRETATIONS

4.1 Overview

Mapping and petrographic studies completed within this study provide evidence for gold mineralization being present in association with many types of lithologies, styles of alteration, and grades of metamorphism throughout the study area in the Beardmore-Geraldton greenstone belt and Wabigoon and Quetico subprovinces. Although gold mineralization is located in varying lithologies, alterations, metamorphic grades, and subprovinces the structures and microstructures that hosts the gold mineralization are consistent.

Structure and microstructure are the controlling factors in gold mineralization within the Wabigoon and Quetico subprovinces and Beardmore-Geraldton greenstone belt in the study area. Gold mineralization is always present within east-west striking, steeply dipping, ductile to brittle-ductile regional shear zones where mylonitized or folded and boudinaged quartz veins, fault breccia, and fractured minerals in a matrix of ductilely-deformed minerals are present.

Lithologies that host gold mineralization within the study area include metamorphosed banded iron formation, meta-granodiorite, sericite schist, albite-muscovite schist, folded, boudinaged, and mylonitized quartz veins, chlorite-albite schist, meta-granite, metasandstone, meta-pegmatite, metamorphosed feldspar porphyry, amphibolite, garnet-hornblende-biotite schist, and syenite where they are present within ductile to brittle-ductile shear zones. The same lithology, even within the same outcrop,

will not host gold mineralization if it is not within a ductile to brittle-ductile shear zone. Gold mineralization is present within unaltered lithologies as well as lithologies with hematite, sericite, ankerite, calcite, or clay alteration. Gold mineralization is present within lithologies that have been metamorphosed to the lower greenschist, upper greenschist, and at least the amphibolite facies of metamorphism in the study area. No grade of regional metamorphism is more preferable for gold mineralization. Gold mineralization is not present in areas of contact metamorphism, such as at contacts with diabase dikes and sills.

Gold mineralization is only present within regional shear zones in the Beardmore-Geraldton greenstone, such as the Burrows River Deformation Zone north of Caramat. The gold mineralization continues to the north into the eastern Wabigoon subprovince within the Paint Lake Shear Zone near Jellicoe in the Missing Link property and the Humbolt High Strain Zone north of Jellicoe within the Castlewood property. The Barton Bay Deformation Zone is located within the Highway 11 and Highway 584 outcrops and Pagwachuan properties in the Beardmore-Geraldton greenstone belt and Wabigoon and Quetico subprovinces.

Gold mineralization is located within ductile to brittle-ductile shear zones, between massive, non-foliated or lineated competent lithologies and smooth, penetrative, very tightly spaced (<2 mm foliation spacing) mylonites. The areas of gold mineralization are located in lithologies that display penetrating, anastomosing, moderately rough foliations that are tightly spaced (2 cm foliation spacing) with a

moderately preferred orientation of porphyroclasts and porphyroblasts. The alteration, metamorphic grade, and subprovince may vary but the structure is always present.

Visible gold is located within hand samples of ductilely to brittle-ductilely deformed quartz veins in the Golden Mile and Brenbar properties in the Elmhirst Lake pluton. Within quartz veins the gold is present along quartz-quartz boundaries and pyrite-quartz grain boundaries. The gold is located in folded healed fractures in quartz and also in the pressure shadows of competent, euhedral, and coarse-grained pyrite. Gold mineralization is also located in the pressure shadows of garnet within pyrrhotite and grunerite, like in the McKay trench near Caramat.

Microstructures that host gold mineralization within regional shear zones always show evidence of dislocation creep, such as undulatory extinction, subgrain boundary formation, and irregular grain boundaries. Microstructures that provide evidence for dislocation creep are located within ductilely deformed minerals that compose the matrix, such as quartz, feldspars, micas, etc. Subgrains and irregular grain boundaries commonly host gold mineralization. Minerals that have been brittlely deformed, like pyrite, garnet, amphiboles, etc. are located adjacent to the less competent minerals and only display fractures, if deformed at all. The boundary between the competent and incompetent mineral may exhibit fractures, veins, or fringes. It is in this boundary that gold mineralization commonly occurs. Quartz, biotite, and calcite commonly form fringes around pyrite. Folded healed fractures in areas of fringe around pyrite host gold mineralization while the regular fringe does not. Folded and boudinaged quartz veins and

fluid inclusions are commonly associated with gold mineralization in addition to hosting it. Strain heterogeneities occur along the boundaries between competent and incompetent minerals during ductile deformation and veins, fringe, and fractures are formed around the competent mineral. Veins and fractures occur when the strain is too great for crystal-plastic flow in the competent mineral to keep up, and loss of cohesion and precipitation occurs (Hill *et al.*, 2011).

Gold mineralization is located along grain and subgrain boundaries in less competent minerals that deform by dislocation creep, such as along quartz-quartz and quartz-mica (chlorite, muscovite, biotite) boundaries. Gold mineralization is located along grain boundaries that are irregular and in smooth subgrain boundaries. Gold mineralization is also located along deformation twins in albite in the Brenbar property and along exsolution lamellae in perthite in the Pagwachuan trench #2. This suggests that gold may be swept through the crystal lattice during deformation and concentrating along planar defects.

Fluid inclusions in quartz veins are in close proximity to gold mineralization in the Elmhirst, Castlewood, Milestone, and Pagwachuan properties. In sample MVS091, collected from the quartz vein from the Golden Mile trench in the Elmhirst property, there is one instance of a fluid inclusion appearing to host the gold mineralization. Metamorphic fluids may transport or enhance the movement of gold mineralization.

Previous workers in the study area have noted the relationship between regional shear zones and gold mineralization (Tyson, 1945; Peach, 1951; Pye, 1951; Mackasey, 1975, 1976; Mackasey and Wallace, 1978; Macdonald, 1983; Lavigne, 1983; Buck and Williams, 1984; Mason *et al.*, 1985; Kehlenbeck, 1986; Kresz and Zayachivsky, 1993; Straub, 1998; Stott *et al.*, 2002; Smyk *et al.*, 2005; Culshaw *et al.*, 2006; DeWolfe *et al.*, 2007). The competency contrasts between different lithologies have been proposed by previous workers as potential conduits for gold-bearing fluids to propagate, such as within boundary between the albite porphyry adjacent to metasediments near Geraldton (Hornwood and Pye, 1955; Macdonald, 1983; Mason *et al.*, 1985).

Evidence from mapping and petrography in this study suggests that within ductile to brittle-ductile shear zones the differences in rheology between lithologies or competent minerals create opportunities for a loss of cohesion in normally competent, crystalline metamorphic lithologies. Gold mineralization occurs in areas of brittle-ductile deformation at rheological differences due to a loss of cohesion at the outcrop and microscopic scale in the form of breccias, veins, and fractures that were subsequently overprinted by ductile deformation.

On the microscopic scale gold mineralization is located within ductilely deformed veins, fractures, or breccias or within adjacent microstructures that exhibit evidence of dislocation creep. Gold mineralization in quartz and albite is located along irregular grain boundaries, subgrains, and deformation twins. Grain boundaries between

competent and less competent minerals also host gold mineralization (e.g., pyrite-quartz, plagioclase-hornblende).

The previous workers were therefore correct in the assumption that gold mineralization is located at competency contrasts as these areas commonly display evidence for brittle-ductile deformation. Arrays of fluid inclusions are also common within the ductilely deformed gold mineralized quartz veins and may be samples of fluid in the system.

4.2 Structure

Gold mineralization is located throughout the study area in lithologies that have remained relatively competent within regional ductile to brittle-ductile shear zones. The Castlewood property is located in the Humbolt High Strain Zone within the Wabigoon subprovince. The Elmhirst property, Leitch Mine, and Missing Link outcrop are located within the Paint Lake Shear Zone in the Beardmore-Geraldton greenstone belt and Wabigoon subprovince. The Milestone property is located in the Klob Lake Shear Zone and the Klotz Lake Shear Zone within the Wabigoon subprovince and Beardmore-Geraldton greenstone belt. The Highway 11 and Highway 584 outcrops are located in the Barton Bay Deformation Zone within the Beardmore-Geraldton greenstone belt. The Barton Bay Deformation Zone extends east into the Pagwachuan property within the Beardmore-Geraldton greenstone belt and Wabigoon and Quetico subprovinces. The regional shear zones typically strike east-west, mimicking the subprovince boundaries, with a near vertical dip except in areas of complex folds or anastomose around competent lithologies. Where shear zones anastomose around competent lithologies the strike and

dip of foliation may vary greatly, to as much as a strike of north-south or a dip of 45° in any direction.

The relatively competent lithologies observed within regional shear zones have a penetrative, rough to moderately rough foliation and host schistose fault breccia and folded and boudinaged quartz veins. Gold mineralization increases where the penetrative, anastomosing foliation within the regional ductile shear zone is disrupted due to strain heterogeneity. In areas of gold mineralization the foliation is tightly spaced (usually <3 cm foliation spacing), penetrative, anastomosing, and moderately rough with porphyroclasts and porphyroblasts moderately defining the foliation and lineation. Gold mineralization is commonly found in areas with strain incompatibilities, such as within complex folds or at lithological boundaries.

Strain incompatibilities control gold mineralization throughout the study area. Gold mineralization is hosted in ductilely deformed quartz veins between lithologies that deformed differently. Ductilely deformed quartz veins commonly host gold mineralization in these historical gold camps and mines as well as in current gold properties. The folded, boudinaged, and mylonitized quartz veins provide evidence for fracturing, and therefore open space, early in the deformational history. The ductilely deformed quartz veins host wall rock and crack and seal textures that provide evidence that the quartz veins have been repeatedly refractured throughout time. The ductilely deformed quartz veins are typically found along lithological contacts but can occur at lithofacies contacts, such as the Pagwachuan trench #1 in the Pagwachuan property. The

quartz veins rarely have cross-cutting veins of carbonate, such as calcite or ankerite, or hematite present throughout the vein. The calcite, ankerite, and hematite are not more or less favourable to gold mineralization. The lithologies that are relatively competent within shear zones in the study area are most likely to be fractured and host gold mineralization while the surrounding less competent lithologies deform ductilely and host little to no gold. Mylonites in the relatively more competent lithologies are common and are typically <10 cm wide.

In thin section the relatively competent lithologies have a rough, schistose fabric anastomosing around fractured porphyroblasts. The gold mineralization is located in fractured porphyroblasts and deformed fractures, veins, and breccia. Previous workers have noted gold mineralization within competent minerals, such as pyrite, arsenopyrite, and sphalerite (Laird, 1937; MacDonald; 1943; Pye, 1951).

The least competent lithologies have a penetrative, smooth, tightly spaced foliation and commonly a crenulation. In thin section the less competent lithologies exhibit smooth, tightly spaced foliation with extreme grain size reduction and subgrains. Mylonites are common in the less competent lithologies and are >10 cm wide. Gold mineralization in the less competent lithologies is rare and occurs in fractured porphyroblasts that have not undergone as extensive grain size reduction as the rest of the lithology.

Brittle-ductile deformation is present throughout the study area, typically as gold mineralized, ductilely deformed fault breccia, quartz veins, and quartz-carbonate veins. Fault breccia with an overprinted schistose fabric is present in the Brenbar, Golden Mile, and Lucky Strike trenches within the Elmhirst pluton. Ductilely deformed fault breccia is also located in Highway 584 outcrop north of Geraldton and in the Pagwachuan trench #2, near Caramat. The overprinted foliation in the fault breccia and quartz and quartz-carbonate veins typically strike parallel or at low angles to the regional shear zones. Quartz veins that strike at high angles to the regional shear zones, like the Straights trench, do not host gold mineralization.

The microstructures mimic the regional structures with the less competent minerals defining the foliation and anastomose around the more competent minerals. The less competent minerals display evidence of dislocation creep, such as undulatory extinction, grain size reduction, subgrains, irregular grain boundaries, grain boundary area reduction, and ribbon structure. The more competent minerals display evidence of brittle deformation, such as fracture and breccia.

Gold mineralization is present in thin section at the boundary between competent and less competent minerals (e.g., the hornblende-quartz grain boundary in garnet-hornblende schist within the McKay trench). Also within the McKay trench, gold mineralization is also located within fractures of garnet while the quartz and biotite display evidence of dislocation creep. Pressure shadows around competent minerals commonly host gold mineralization, like the pressure shadows around pyrite in the quartz

vein within the Golden Mile trench. Gold mineralization is also common as inclusions in the competent mineral, such as within albite in the meta-granite within the Castlewood property. Microscopic folded fractures, breccia, veins, and boudins are all common microstructures in thin section where gold mineralization is present. Folded fractures, breccia, veins, and boudins all host gold mineralization in metamorphosed pegmatite of the Brenbar trench in the Elmhirst property. Gold mineralization is also present within ductilely deformed minerals, like subgrains in quartz grains within the Golden Mile trench of the Elmhirst property and subgrains in plagioclase in the Milestone property. Deformation twins in albite and exsolution lamellae in perthite also host gold mineralization, such as within the Pagwachuan trench #2 in the Pagwachuan property.

4.3 Rheology

The competency of the lithologies or minerals within the lithologies can be related to the original protolith, later quartz and quartz-carbonate veins, and their competency throughout metamorphism. In the lithologies that have been affected by greenschist facies metamorphism the gold mineralization is located in fractured, competent minerals (e.g., albite and pyrite) and quartz veins in lithologies that have remained competent (e.g., meta-granodiorite and chlorite-albite schist). Gold mineralization also occurs in quartz veins along irregular grain boundaries and subgrains of quartz. The quartz in the quartz veins display evidence of dislocation creep with undulatory extinction, subgrains, and irregular grain boundaries present. Dislocation creep occurs in quartz during ductile deformation at temperatures in the greenschist facies of metamorphism or higher (Tullis, 2002).

In the lithologies that have been affected by amphibolite facies metamorphism the gold mineralization is located in fractured, competent minerals (e.g., garnet and hornblende) and in quartz veins within lithologies that have remained competent (e.g., amphibolite and meta-granodiorite). Gold mineralization also is located in subgrains and irregular grain boundaries of albite and quartz. Dislocation creep occurs in feldspar during ductile deformation at temperatures in the amphibolite facies of metamorphism or higher (Tullis, 2002).

Gold mineralization is also located at the boundary between competent minerals and less competent minerals where a loss of cohesion could have occurred, analogous to fault breccia on the outcrop scale, regardless of metamorphic grade. Gold mineralization is less likely to be present in areas that exhibit evidence of grain boundary area reduction and recrystallization. No gold mineralization was present within structures or microstructures with brittle deformation that has not been overprinted by ductile deformation (e.g., fault gouge and straight fractures).

Competent lithologies that host gold mineralization within ductile to brittle-ductile shear zones vary throughout the study areas. In the lithologies that have been affected by greenschist facies metamorphism the competent lithologies are commonly chlorite-albite schist, meta-gabbro, and metasedimentary lithologies with competent components with an arkose protolith. At the transition between greenschist and amphibolite facies metamorphism (e.g., near Geraldton), the gold mineralization is present within competent metamorphosed feldspar porphyry and to a lesser amount in

complexly folded, metamorphosed banded iron formation. In the lithologies that have been affected by at least amphibolite facies metamorphism the competent lithologies that host gold mineralization are amphibolite, meta-granodiorite, syenite, garnet-biotite schist, and garnet-hornblende-biotite schist. The presence of quartz and quartz-carbonate veins at low angles to the regional foliation may increase the competency of the original lithology. The metamorphosed banded iron formation and metasediments in the Leitch Mine near Beardmore host quartz veins at low angles to the regional foliation that have been complexly folded and display moderately rough foliation where gold mineralization is present. The eastern extent of the metamorphosed banded iron formation and metasedimentary lithologies near Jellicoe along Sturgeon River are parallel to the regional foliation, rarely exhibit any folds aside from gentle open folds, have a smooth foliation, have little to no quartz or quartz-carbonate veins, and subsequently have no gold mineralization.

The metamorphosed banded iron formation in the Highway 11 outcrop near Geraldton displays complex folding at variable angles to foliation, similar to the metamorphosed banded iron formation near Beardmore and both host gold mineralization. Metamorphosed banded iron formation in the Pagwachuan trench #1 near Caramat is parallel to foliation, exhibits gentle open folds, and hosts no gold mineralization.

Evidence of retrograde metamorphism and alteration is commonly present within areas of extensive quartz veins and fault breccia where fluid was able to enter the system.

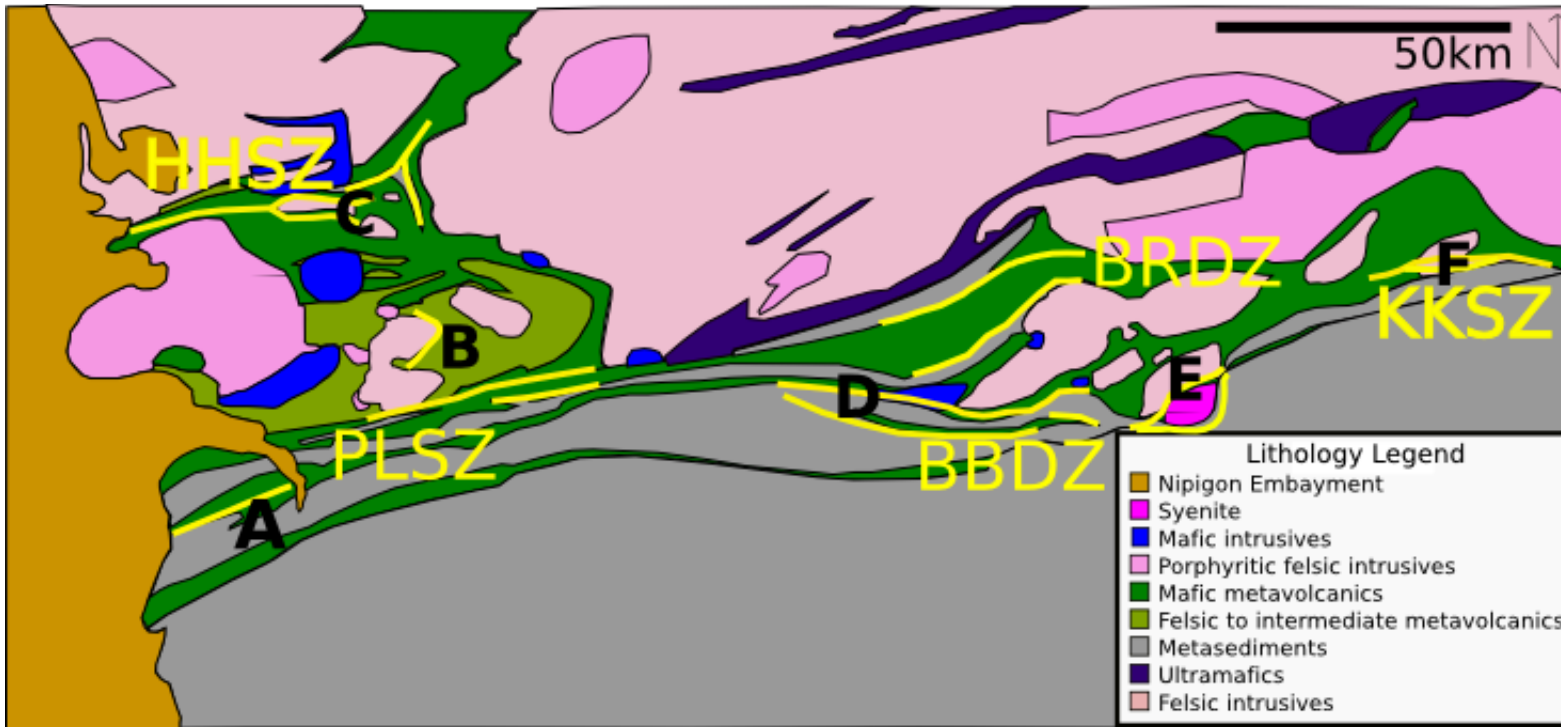


Fig. 4.1: Geological map of regional shear zones along the Wabigoon and Quetico subprovince boundary (solid yellow lines). The Humbolt Bay High Strain Zone (HHSZ) is located in the Castlewood trench within the Elmhirst property. The Paint Lake Shear Zone (PLSZ) is located within the Leitch Mine, Missing Link outcrop, and in the mapped study area of the Elmhirst property. The Barton Bay Deformation Zone and Burrows River Deformation Zone are located within the Highway 11 and Highway 584 outcrops and in the mapped study area of the Pagwachuan property. The Klotz Lake Shear Zone and Klob Lake Shear Zone (KKSZ) are located in the Milestone property (After Akuman, 1980; Buck, 1986; Reilly, 1987; Kresz and Zayachivsky, 1993; Johns *et al.*, 2003; LaFrance *et al.*, 2004).

Gold mineralization may be present within areas of alteration although not in all cases. Calcite is present within the mylonitized and boudinaged quartz vein in the Golden Mile trench in the Elmhirst property near Jellicoe although from microscopic cross-cutting relationships it is later than the quartz and is not in contact with gold. Ankerite alteration is present within the Brenbar trench and Missing Link outcrop in the Elmhirst property although the Brenbar trench hosts gold mineralization, while the Missing Link outcrop hosts sporadic gold mineralization. Sericite alteration is common in the metamorphosed feldspar porphyry in the Highway 11 outcrop near Geraldton although it is not always present within the metasedimentary lithologies in the same outcrop. Hematite is present within meta-granodiorite and syenite in and around Pagwachuan trench #2 in the Pagwachuan property near Caramat regardless of gold mineralization. Garnet-hornblende schist in the McKay trench of the Pagwachuan property near Caramat is unaltered and hosts gold mineralization. Pyrite and silica, in the form of quartz, display microstructures that suggest they have been part of the metamorphic mineral assemblage during peak prograde metamorphism and ductile deformation. As such, they are considered in this study to be part of the stable metamorphic mineral assemblage although they could have been introduced earlier into the system and thus considered alteration or a mass volume change.

Metamorphic grade increases from lower greenschist facies near Beardmore in the Leitch Mine property, to the transition between greenschist and amphibolite facies in the Highway 11 and 584 outcrops near Geraldton, and to at least amphibolite facies in the Milestone property near Jellicoe and the Pagwachuan property near Caramat. Gold

mineralization is present throughout the entire study area, regardless of metamorphic grade. Gold mineralization is present within the study area within ductile to brittle-ductile shear zones regardless of metamorphic grade.

In the Milestone property east of Longlac the gold mineralization is present in both the amphibolite and the meta-granodiorite but is higher in the amphibolite. Since both lithologies host gold mineralization it is not the lithology that is the controlling factor on gold and nor is it alteration, as the meta-granodiorite is the most altered. Their different metamorphic histories, and therefore differing rheologies, throughout deformation may be the limiting factor. The mafic protolith underwent greenschist facies metamorphism with albite and chlorite forming at the expense of plagioclase and pyroxenes and hornblende and plagioclase forming in amphibolite facies. During metamorphism the rheology of the amphibolite was considerably weaker than the granodiorite as primarily feldspar-quartz composition was unreactive and stable. The rheological contrast could provide minute pore space for gold to be transported throughout the two lithologies on a regional scale. A similar process could also have occurred throughout the entire study area.

In contrast, in the Elmhirst property north of Jellicoe it is the meta-granodiorite and not the mafic meta-volcanic lithologies that host the gold mineralization. If there was to be a lithological or chemical trap the same lithologies should consistently host the gold mineralization. The lithologies within the Elmhirst property reached upper greenschist facies metamorphism and as such the mafic meta-volcanic lithologies are

composed of fine- to medium-grained chlorite, albite, and minor epidote while the meta-granodiorite is composed of coarse-grained plagioclase and quartz. The meta-granodiorite is considerably more rheologically competent than the fine-grained, chlorite-rich meta-volcanic lithologies, and as such hosts the gold mineralization.

On the microscopic scale, less competent minerals deformed more ductilely through deformation mechanisms such as dislocation creep while more competent minerals deformed brittely through deformation mechanisms such as fracturing. In garnet-hornblende-biotite schist within the McKay trench of the Pagwachuan property the quartz shows evidence for dislocation creep while the adjacent garnet hosts gold mineralization within straight fractures.

In addition to rheological contrast the rate of strain is also important for gold mineralization. The quartz vein in the Brenbar trench within the Elmhirst property near Jellicoe has two types of pyrite-quartz grain boundaries. Within the same thin section, the pyrite that exhibits folded quartz fringe does not host gold mineralization while the pyrite that has folded, healed fractures where the fringe would be located does host gold mineralization. The quartz fringe around the pyrite appears to have deformed at a strain rate synchronous or similar to the pyrite while the fractured quartz around the other pyrite did not. The healed fracture in quartz adjacent to the pyrite may have occurred due to a loss of cohesion due to differing strain rates. A loss of cohesion and subsequent gold mineralization can occur within minerals that deform at different rates of strain (Hill *et al.*, 2011).

Gold mineralization occurs both within competent lithologies in ductilely and brittle-ductilely deformed quartz veins and within the host rock in ductile to brittle-ductile shear zones. Gold also occurs at the margins of competent lithons where ductile to brittle-ductile shear zones anastomose around them or form ductilely deformed fractures within them (Hill *et al.* 2011). Immediately outside of these competent lithon margins are pressure shadows that are typically complexly folded, typically as a shear-related early and late folds, and host gold mineralization, e.g., along the margin of the Elmhirst Lake Pluton (Carreras *et al.*, 2005).

Rheological contrasts occur at all scales throughout the study area where gold mineralization is present. The Wabigoon-Quetico subprovince boundary is a regional-scale rheological contrast with mainly metamorphosed greenstone belts and granitoid plutons to the north and metasedimentary lithologies to the south. Gold mineralization is located throughout this subprovince boundary both within historical mining camps and later gold exploration camps. The primarily east-west striking regional ductile shear zones are typically transcurrent and penetrate many types of lithologies and styles of alteration. It is only the lithologies that remained moderately competent during ductile and brittle-ductile deformation that host gold on a regional scale, such as ductilely deformed fault breccia in the Elmhirst pluton and not schistose metavolcanic lithologies in the Elmhirst property. On the trench scale gold mineralization occurs along contacts between two lithologies of varying rheology, such as chlorite schist in contact with ductilely deformed fault breccia in pegmatite within the Brenbar trench of the Elmhirst property. On the microscopic scale gold mineralization is commonly located in contact

or as pressure shadows around rheologically competent minerals next to less competent minerals, such as the hornblende-quartz grain boundary in the McKay trench in the Pagwachaun property.

4.4 Suprovinces and greenstone belt

4.4.1 Wabigoon subprovince

Gold mineralization within the study area is not restricted to one specific greenstone belt or subprovince but continues throughout the Wabigoon and Quetico subprovinces and Beardmore-Geraldton greenstone belt within relatively competent lithologies in ductile to brittle-ductile shear zones.

Gold mineralization in the Wabigoon subprovince occurs in lithologies and quartz veins within the Paint Lake Shear Zone and Humbolt High Strain Zone that exhibit brittle-ductile deformation on all scales. The Paint Lake Shear Zone typically strikes east-west with a vertical dip except around competent plutons, such as where it anastomoses around the Elmhirst pluton. Gold mineralization in the Elmhirst pluton within the Golden Mile, Lucky Strike, Findian 3, and Brenbar trenches is located within folded, boudinaged, and mylonitized quartz veins, and adjacent schistose meta-granodiorite within the Paint Lake Shear Zone.

Gold mineralization within the Castlewood property in the Elmhirst property is hosted along the margins of the rheologically more competent meta-granodiorite next to the less competent chlorite schist. In thin section gold mineralization is located in competent albite and within ductilely deformed fault breccia. The less competent chlorite schist exhibits grain size reduction and hosts no gold mineralization. Gold mineralization

is also located within ductilely deformed quartz veins, complexly folded areas (shear-related early and late folds), and lithological contacts within the meta-granodiorite pluton. Gold mineralization is not present within open anticlines or synclines within the area but in areas of more complex folds, such as shear-related early and late folds, and sheath folds in shear zones (Carreras *et al.*, 2005).

4.4.2 Beardmore-Geraldton greenstone belt

The Leitch Mine hosts gold mineralization within quartz and quartz-carbonate veins and chlorite-albite schist in the Paint Lake Shear Zone. The chlorite-albite schist behaves the more rheologically competently than the meta-conglomerate, meta-sandstone, and meta-banded iron formation. In thin section the chlorite defines the foliation and anastomoses around the fractured albite in the chlorite-albite schist. The metasedimentary lithologies deform more ductilely than the chlorite-albite schist with quartz, chlorite, and muscovite all defining the foliation. Folded quartz veins occur within the chlorite-albite schist and display undulatory extinction in quartz. The folded, boudinaged, and mylonitized quartz and quartz-carbonate veins that host gold mineralization are commonly located in the area of the boundary between two different lithologies that are significantly different rheologically, such as the metaconglomerate and meta-sandstone contact. Gold mineralization is also present within complex folds, i.e. shear-related early and late folds and sheath folds, in quartz veins and metamorphosed banded iron formation in the Beardmore area.

In the area of Geraldton the gold mineralization occurs in areas of rheological contrasts, such as lithological contacts of metamorphosed feldspar porphyry and meta-

banded iron formation within the Barton Bay Deformation Zone. Complexly folded meta-banded iron formation, typically shear-related early and late folds as well as sheath folds, also host gold mineralization (Carreras *et al.*, 2005). Gold mineralization within brittely-deformed structures is rarely noted except for Pye (1951) who mapped a later thrust fault that moved preexisting ore. On the smaller scale Pye (1951) also mapped irregular blebs of gold within fractured quartz veins and joints.

In the Milestone property the gold mineralization is located in the Klob Lake and Klotz Lake Shear Zones within rheological contrasts between more competent lithologies (e.g., amphibolite and meta-granodiorite), and less competent units (e.g., metasandstone). Gold mineralization is located within amphibolite and meta-granodiorite that displays foliation and lineation in hornblende and folded, boudinaged, and mylonitized quartz veins. Microboudins, microfolds, and veins are common within the quartz veins in thin section. Gold mineralization is located within the ductilely deformed quartz veins as well as within chlorite after hornblende and in euhedral pyrite as inclusions.

In the Pagwachuan property within the Wabigoon subprovince near Caramat the gold mineralization is located in the eastern continuation of the Barton Bay Deformation Zone. The rheological contrasts between a relatively more competent meta-granodiorite and syenite adjacent to less competent lamprophyre in the Pagwachuan trench #2 hosts gold mineralization in ductilely deformed fault breccia and quartz vein. Both the ductilely deformed quartz vein and fault breccia provide evidence for brittle-ductile deformation that hosts gold mineralization at a rheological contrast. In thin section gold

mineralization is located within subgrains in quartz within quartz veins, deformation twins in albite, fractures in rutile, and along perthite and albite boundaries.

4.4.3 *Quetico subprovince*

The gold mineralization in the Quetico subprovince is located within ductile to brittle-ductile shear zones in the southeastern continuation of the Barton Bay Deformation Zone. The McKay trench hosts gold mineralization in garnet-hornblende-biotite schist within fractured garnet, along the grain boundary of hornblende and quartz, and in folded quartz veins. Pyrrhotite is commonly located around garnet and along garnet and hornblende grain boundaries and also hosts gold mineralization.

4.5 Gold mineralization models

Many styles of gold mineralization have been proposed to explain the mineralization present within the Beardmore-Geraldton greenstone belt and surrounding area. Deposit models are used to explain where gold mineralization is presently located and are used to better model exploration, drilling, and mining. Commonly proposed models include porphyry, banded iron formation, placer, orogenic, and shear-zone-hosted gold deposits (Hattori, 1987; LaFrance *et al.*, 2004; Smyk *et al.*, 2005; L'Herueux and Therriault, 2009).

Porphyry deposits are commonly located along currently active oceanic-continental convergent boundaries in the upper kilometers to meters of crust. Current porphyry deposits are well-described worldwide including in Chile, Peru, and Philippines (Robb, 2005). Characteristic alteration styles, like phyllic and argillic alteration, are present outwards from the rising pluton due to convecting igneous and meteoric fluids.

Gold is present in solution in these fluids as gold complexes, such as Au-S and Au-Cl complexes, and precipitates as native gold and within sulphides. Stockwork quartz veins and normal faults are the common structures found within these deposits. Other metals are found in these deposits and are commonly Cu, Mo, Ag, etc. Porphyry deposits occur within felsic intrusive rocks within the upper kilometer in the crust (Robb, 2005).

Hattori (1987) proposed that magnetite and Fe³⁺ cations in biotite could reduce sulphide-gold complexes in the upwelling, magnetic Elmhirst Lake pluton as geophysical anomalies suggest. During regional mapping in this area and using more detailed geophysical maps it was found that the Elmhirst Lake pluton itself is not magnetic but the smaller feldspar porphyry stocks within it are. However, the feldspar porphyry stocks cross-cut the gold mineralization and do not host any gold mineralization. No undeformed stockwork quartz veins or characteristic alteration are present within the study area. The study area has also undergone at least lower greenschist facies metamorphism and as such is too deep in the crust to host porphyry deposits.

Epigenetic gold deposits in banded iron formation have been described in Archean banded iron formation and have been used to describe the gold mineralization in and around Geraldton (Fyon *et al.*, 1983; Barrett, and Fralick, 1986; LaFrance *et al.*, 2004; Smyk *et al.*, 2005; Robb, 2005). A limited amount of potentially epigenetic, banded iron formation gold mineralization was documented within thin bands of magnetite although no such mineralization has been found since in the area (Barrett, and Fralick, 1986; Pye, 1951). The majority of the gold mineralization within

metamorphosed banded iron formation occurs in banded iron formation that has been complexly folded. The gold mineralization within the banded iron formation near Geraldton is commonly found associated with sulphides, magnetite, hematite, and varying gangue minerals (Pye, 1951). Previous work in the Geraldton gold camps suggest gold was mobile as a thio-complex within quartz veins and reacted with magnetite in the banded iron formation (Barrett and Fralick, 1986). Alteration in banded iron formation deposits is highly variable from deposit to deposit but also within the same deposit (Fyon *et al.*, 1983; LaFrance *et al.*, 2004; Smyk *et al.*, 2005; Robb, 2005). Common structures within banded iron formation deposits are quartz veins, faults, and shear zones.

Mackasey (1975, 1976) proposed that placer deposits in meta-conglomerates within the study area could have been the source for gold mineralization since the adjacent metamorphosed arkose beds host gold mineralization. Mackasey proposed that metaconglomerates should be assayed to test if they are the host for a placer gold deposit. Metaconglomerates have been assayed for gold in this study by Kodiak Exploration Ltd. near Jellicoe at Sturgeon Bridge and by Prodigy Gold Inc. north and south of Seagram Lake near Caramat with no success. Strain partitioning within metaconglomerates could result in the mica-rich matrix taking up the majority of the strain, resulting in little opportunity for brittle-ductile deformation and gold mineralization. The metamorphosed arkose lithologies do host gold mineralization in the area of Geraldton, although stratigraphically adjacent to metaconglomerate, and may deform more brittely than the metaconglomerates and therefore host more gold mineralization.

Orogenic gold deposits, also commonly referred to as mesothermal gold or shear-zone-hosted gold deposits, are hosted in all types of lithologies, alteration styles, and metamorphic grades throughout the world (Groves *et al.*, 1998; Robb, 2005). Gold mineralization is typically associated with sulphides within major structures such as shear zones and faults. Quartz and quartz-carbonate veins are common hosts to the gold. Gold transport may be as gold complexes and moves along dilatational areas in large-scale structures like faults and shear zones (Groves *et al.*, 1998; Robb, 2005).

Shear zones in the study area were present during regional prograde greenschist and amphibolite facies metamorphism and orogenesis and continued as the area was unroofed and cooled to retrograde greenschist facies metamorphism. The gold mineralization within the shear zones was present during at least the amphibolite facies, as suggested by gold mineralization hosted within garnet in garnet-hornblende-biotite schist and hornblende in amphibolite in the McKay trench. The gold mineralization continued after prograde amphibolite metamorphism into retrograde greenschist facies metamorphism, as indicated by gold mineralization within retrograde metamorphic minerals (e.g., chlorite after hornblende in amphibolite in the Milestone property).

The gold mineralization within the study area should be considered shear-zone-hosted gold deposits as it most clearly states the variable lithologies, alteration structure, metamorphic grade, and most importantly where the gold is located. The orogenic gold deposit classification does not factor in the gold mineralization continuing after orogenesis

and into the unroofing stage. Shear-zone-hosted gold deposits typically occur within ductile to brittle-ductile shear zones along or near terrane boundaries (Hill *et al.*, 2011).

Similar deposits in the Superior province to the gold mineralization in the study area are the Red Lake, Hammond Reef, Hemlo, and Musselwhite Mines or gold camps. The controlling factors on gold mineralization within each of the mines and camps are structure and microstructure (Stinson and Hill, 2010; Hill *et al.*, 2011; Kolb, 2011; Gaspar, 2012). The structures are commonly ductile and brittle-ductile shear zones that anastomose around competent lithons (Stinson and Hill, 2010; Hill *et al.*, 2011). The microstructures that host gold mineralization within shear-zone-hosted gold deposits exhibit evidence of dislocation creep (Hill *et al.*, 2011; Kolb, 2010; Gaspar, 2012; Stinson and Hill, 2012). Gold mineralization is located within matrix minerals that exhibit undulatory extinction, grain size reduction, and subgrain boundary formation while the more competent minerals deform more brittlely (Kolb, 2010; Hill *et al.*, 2011; Stinson and Hill, 2012). Deposits outside of the Superior province with similar, and documented, structures and microstructures in Archean-aged lithologies include the Kalgoorlie region in western Australia (Bierlein *et al.*, 2006; Blewett *et al.*, 2010; Miller *et al.*, 2010; Morey *et al.*, 2007), Brazil (Coelho, *et al.*, 1990; Reinhardt and Davion, 2008), and southern Africa (Kisters *et al.*, 1998).

5-SUMMARY AND CONCLUSIONS

Gold mineralization is located in regional ductile to brittle-ductile shear zones from Beardmore in the western extent of the study area to Longlac in the east. Gold mineralization is only present within the regional shear zones in the study areas. No gold mineralization, even trace amounts, is identified in this study outside of the regional shear zones.

The gold mineralization occurs within different types of lithologies, styles of alteration, metamorphic grades, and in different subprovinces. The Leitch Mine in the Beardmore-Geraldton greenstone belt typically hosts gold in quartz veins, complexly folded metamorphosed banded iron formation, and folds and quartz veins in chlorite-albite schist. The Elmhirst property in the Wabigoon subprovince hosts gold within folded fractures in the Elmhirst meta-granodiorite pluton and the Castlewood property hosts gold mineralization in folded and boudinaged quartz veins and in meta-granite dykes adjacent to chlorite schist and metaconglomerate. The Highway 11 and 584 outcrops are located in the Beardmore-Geraldton greenstone belt and gold mineralization is located in metamorphosed and sheath folded arkose sandstones, banded iron formations, and quartz-feldspar porphyry. The Milestone and northern Pagwachuan properties are located within the Wabigoon subprovince with gold mineralization located within folded, boudinaged, and mylonitized quartz veins, amphibolite, metagranodiorite, and syenite. The southern Pagwachuan property is located in the Quetico subprovince where gold mineralization is located in folded, boudinaged, and mylonitized quartz veins and garnet-hornblende-biotite schist.

The lithologies that host gold mineralization have all been ductilely deformed within ductile to brittle-ductile shear zones. The shear zones typically strike east-west along the Wabigoon-Quetico subprovince boundary, although one instance of a shear zone in the Pagwachuan trench #2 near Caramat strikes northwest-southeast. Gold mineralization is located between competent lithologies and intensely, ductilely deformed mylonitic lithologies. The massive lithologies are usually mapped as igneous due to their equigranular textures, although they do rarely exhibit subtle deformational foliations, lineations, and grain size reduction. The mylonitic lithologies are usually less competent lithologies, such as chlorite schist, but can be rare within normally competent lithologies, like meta-granodiorite. The mylonitic lithologies have extremely tightly spaced, straight, penetrative nearly vertical-to-vertical foliation. Between the competent and massive lithologies and the mylonitic lithologies a lithology with tightly spaced, anastomosing, moderately rough foliation is located and hosts gold. The lithology between the intensely mylonitic and equigranular lithologies has a rough, anastomosing foliation due to competent porphyroblasts and porphyroclasts within a strongly deformed area.

Gold mineralization is located within regional to microscopic strain heterogeneities on all scales. Gold is located at meta-granodiorite-gabbro contacts that have been intensely ductilely deformed, sheath folds of banded iron formation in contact with metasandstone adjacent to feldspar porphyry, and at lithofacies contacts like from pebbly coarse-grained metasandstone to silty fine-grained metasandstone.

Strain heterogeneities also occur along the boundaries between competent and less competent minerals during ductile deformation and veins, fringe, and fractures are formed around the competent mineral. Veins and fractures occur when the strain rate is too great for crystal-plastic flow in the competent mineral to keep up, and loss of cohesion and precipitation occurs (Hill *et al.*, 2011).

Gold mineralization occurs in the study areas in ductile to brittle-ductile shear zones within normally competent lithologies, like amphibolite and meta-granodiorite in the Milestone property near Longlac in the Wabigoon subprovince. The amphibolite has retrograded to greenschist facies metamorphism within the area of highest strain. Gold mineralization is present at the amphibolite-meta-granodiorite contact but is concentrated more in the amphibolite. Since both lithologies host gold it is not the lithology that is the controlling factor on gold and nor is it alteration as the meta-granodiorite is the most altered. Their different metamorphic histories, and therefore differing rheologies, throughout deformation may be the limiting factor. The gabbro underwent greenschist facies metamorphism with albite and chlorite forming at the expense of high-An plagioclase and pyroxenes, and hornblende and high-An plagioclase forming in amphibolite facies. During metamorphism the rheology of the amphibolite was considerably weaker than the granodiorite as its primarily feldspar-quartz composition was stable. The rheological contrast could provide minute pore space for gold to be transported throughout the two lithologies on a regional scale.

Complex, shear-related early and late folds, and sheath folds could also create rheological contrasts, such as in the metamorphosed banded iron formation adjacent to metasandstone to metasilstone in Geraldton within the Beardmore-Geraldton greenstone belt (Carreras *et al.*, 2005). As banded iron formation and clastic metasedimentary rock, both primarily composed of quartz, deforms readily at greenschist facies temperatures the sheath folds are easily formed within high strain areas. The sheath folds, once formed, may create strain heterogeneities on a regional to outcrop scale. Where these folds are located adjacent to lithologies that do not deform as easily, such as feldspar porphyry, pore space is again created and gold is concentrated.

The gold mineralization located between the equigranular and mylonitic lithologies is highest when located at a rheological contrast. During metamorphism and deformation the rheology of the rock and minerals changes considerably. If the two lithologies participate in metamorphic reactions at different pressures and temperatures, like gabbro and granodiorite, gold mineralization may be further increased. On the microscopic scale it is the competent minerals, such as pyrite, garnet, amphibole, and plagioclase that must be present adjacent to rheologically weak minerals, such as quartz, muscovite, chlorite in order for gold mineralization to occur. During deformation minute pore space is created when the rheologically weak minerals or lithologies deform more easily than the rigid minerals lithologies and temporary porosity is formed. Gold and other minerals, such as quartz, precipitate when temporary porosity is created.

While the structure and microstructure are always present where gold mineralization occurs the lithology, alteration, metamorphic grade, and subprovince vary. The types of alteration present in the study areas range from unaltered to sericite, calcite, ankerite, and hematite. Gold mineralization is present with or without alteration and no type or types of alteration is more likely to host gold.

On the microscopic scale it is the competent minerals, such as pyrite, garnet, amphibole, and plagioclase that must be present adjacent to rheologically weak minerals, such as quartz, muscovite, and chlorite in order for gold mineralization to occur. During deformation minute pore space is created when the rheologically weak minerals deform more easily than the rigid mineral lithologies and temporary porosity is formed. Gold and other minerals, such as quartz, precipitate when temporary porosity is created.

The gold mineralization in the study area within the Wabigoon and Quetico subprovinces and Beardmore-Geraldton greenstone belt is located in ductile to brittle-ductile shear zones in microstructures that exhibit evidence of brittle-ductile deformation, such as fracture and dislocation creep. Evidence of multiple generations of folded and boudinaged quartz veins, and fractures are overprinted by ductile deformation where gold mineralization is present within the entire study area. Gold mineralization is present along grain and subgrain boundaries within quartz veins, with and without fluid inclusions. Gold mineralization is located along the boundary between competent minerals and less competent minerals and the gold may define a foliation or located within mineral fringe. Fractures within competent minerals also host gold mineralization,

like within garnet and pyrite, while the surrounding matrix displays evidence of dislocation creep.

The types of alteration present in the study area range from unaltered to sericite, calcite, ankerite, and hematite. Gold mineralization is present with or without alteration and no style of alteration is more likely to host gold. Sulphide and oxide mineralization also vary and are a poor indicator of gold mineralization.

Gold mineralization is present within lithologies that are of igneous origin, like the ductilely deformed syenite that has been unreactive to metamorphism to lithologies of sedimentary origin that have undergone amphibolite facies metamorphism, such as the garnet-hornblende-biotite schist. Some lithologies, like the kyanite schist in the McKay trench near Caramat in the Quetico subprovince, may have undergone multiple metamorphic events.

Metamorphism changes the rheological contrasts between rigid and weak minerals by either prograde metamorphism, such as the growth of garnet, or retrograde metamorphism, via the growth of chlorite at the expense of amphibole. Therefore to a small degree lithology, alteration, and metamorphism affect gold mineralization, although only in so far as it affects rheology and therefore structure.

4.5.1 Recommendations

Gold mineralization in the study area can therefore be predicted from knowledge of regional structure and microstructures. Future workers in the study area should first

map the regional ductile and brittle-ductile shear zones, carry out traverses perpendicular to the regional trend, and assay all relatively competent lithologies in the area until the massive lithologies are encountered outside of the shear zone. Focus should be on relatively competent lithologies that have tight, anastomosing, moderately rough foliation with rotated and foliated porphyroblasts and porphyroclasts. Future workers should not be concerned about lithological type, alteration style, metamorphic grade, or what subprovince or terrane they are sampling from, only the regional structure and microstructure.

7-REFERENCES

- Amukun, S.E., 1980. Geology of the Conglomerate Lake Area, District of Thunder Bay; Ontario Geological Survey Report 197, 101p. Accompanied by Map 2429, scale 1:31 680 (1 inch to ½ mile).
- Amukun, S.E., 1983. Klob Lake; Ontario Geological Survey Map 2469, Precambrian Geology Series, scale 1 inch to ½ mile, Geology 1979.
- Barrett, T.J., and Fralick, P.W. 1986, Resedimentation associated with the gold bearing banded iron-formation in the Geraldton-Beardmore Greenstone Belt, Ontario; Ontario Geological Survey, Open File Report 5577, 27p.
- Bierlein, F.P, Groves, D.I., Goldfarb, R.J., and Dube, B., 2006. Lithospheric controls on the formation of provinces hosting giant orogenic gold deposits. *Mineralium Deposita*, 40, 874-886.
- Blackburn, C.E., and Johns, G.W., 1988. A stratigraphic reconnaissance of the Eastern Wabigoon Subprovince; in Summary of Field Work and Other Activities 1988, Ontario Geological Survey, Miscellaneous Paper 141, p.163-168.
- Blewett, R.S., Henson, P.A., Roy, I.G., Champion, D.C., and Cassidy, K.F., 2010. Scale-integrated architecture of a world-class gold mineral system: The Archaean eastern Yilgarn Craton, Western Australia, *Precambrian Research*, 183, 230-250.
- Brodie, K., Fettes, D., Harte, B., and Schmid, R. 2007. A systematic nomenclature for metamorphic rocks: 3. Structural terms including fault rock terms, Recommendations by the IUGS Subcommittee on the Systematics of Metamorphic Rocks, Recommendations, web version 01.02.2007.
- Bruce, E.L. 1937a. The Eastern Part of the Sturgeon River Area (Jellicoe-Sturgeon River Section); Ontario Department of Mines, Volume 45, 1936, Part 2, p.1-59. Accompanied by Map 45a, scale 1:63 360 or 1 inch to 1 mile.
- Bruce, E.L., 1937b. New Developments in the Little Long Lac Area; Ontario Department of Mines, Annual Report, 1936, Volume 45, Part 2, p. 1-59. Accompanied by Map 45a, scale 1 inch to 1 mile.
- Buck, S., 1986. Structural studies and gabbro mylonitization within the Barton Bay deformation zone, Geraldton, Ontario; unpublished M.Sc. thesis, Brock University, p.172.
- Buck, S. and Williams, H.R. 1984. Structural studies in the Geraldton area; in Summary of Field Work 1984, Ontario Geological Survey, Miscellaneous Paper 119, p. 208-211.
- Carreras, J., Druguet, E., and Grier, A., 2005. Shear zone-related folds, *Journal of Structural Geology*, 27, p. 1229-1251.
- Coelho C.E.S., Touray J.C., Beny C., Giuliani Gaston, 1990. Quartz fabrics and fluid inclusions volatiles at Fazenda Brasileiro gold mine: a preliminary petrographical and Raman microprobe

study in *Bulletin de Liaison de la Société Française de Minéralogie et de Cristallographie*, v. 2, 1, p. 23.

Culshaw, N., Purves, M., Reynolds, P., and Stott, G., 2006. Post-collisional upper crust faulting and deep crustal flow in the eastern Wabigoon subprovince of the Superior Province, Ontario: Evidence from structural and $^{40}\text{Ar}/^{39}\text{Ar}$ data from the Humboldt Bay High Strain Zone, *Precambrian Research*, v.145, p.272-288.

Czeck, D. M. and Poulsen, K. H., 2010. Field trip guide: Deformation in the Rainy Lake Region: A Fabulous Display of Structures Controlled by Rheological Contrasts. Institute on Lake Superior Geology 56th Annual Meeting, International Falls, MN, 2010; 56 Part 2, 47-75.

Czeck, D. M., Fissler, D. A., Horsman, E., and Tikoff, B., 2009. Strain analysis and rheology contrasts in polymictic conglomerates: an example from the Seine metaconglomerates, Superior Province, Canada. *Journal of Structural Geology* 31, 1365-1376.

Davis, D.W., Pezzutto, F., and Ojakangas, R.W., 1990. The age and provenance of metasedimentary rocks in the Quetico Subprovince, Ontario, from single zircon analyses: implications for Archean sedimentation and tectonics in the Superior Province; *Earth and Planetary Science Letters*, 99, 3, p. 195-205.

Davis, D.W. and Smith, P.M., 1991. Archean gold mineralization in the Wabigoon subprovince, a product of crustal accretion: evidence from U-Pb geochronology in the Lake of the Woods area, Superior province, Canada, *Journal of Geology*, v. 99, 3, p. 337-353.

Devaney, J.R. and Fralick, P.W. 1985. Regional sedimentology of the Namewaminikan Group, northern Ontario: Archean fluvial fans, braided rivers, deltas and an aquabasin; in *Current Research, Part B*, Geological Survey of Canada, Paper 85-1B, p.125-132.

Devaney, J.R., and Williams, H.R., 1989. Evolution of an Archean subprovince boundary: a sedimentological and structural study of part of the Wabigoon-Quetico boundary in Northern Ontario; *Canadian Journal of Earth Sciences*, v. 26, p.1013-1026.

DeWolfe, J.C., Lafrance, B., and Stott, G. M., 2007. Geology of the shear-hosted Brookbank gold prospect in the Beardmore-Geraldton belt, Wabigoon subprovince, Ontario; *Canadian Journal of Earth Sciences*, v.44, p.925-946.

Fairbairn, H.W. 1938. Geology of the Northern Long Lake Area; Ontario Department of Mines, Annual Report, 1937, Volume 46, Part 3, p. 1-22. Accompanied by Map 46b, scale 1 inch to 1 mile.

Ferguson, S. A., Groen, H. A. and Haynes, Z. 1971: Gold Deposits of Ontario; Part 1 - Districts of Algoma, Cochrane, Kenora, Rainy River and Thunder Bay, Ontario Division of Mines, Mineral Resources Circular Number 13, 315 p.

Fyon, J., Crocket, J., and Schwarcz, H., 1983. The Carshaw and Malga iron-formation-hosted deposits of the Timmins area: Ontario Geological Survey, Miscellaneous Paper, 110, p. 98-110.

Gaspar, B., 2012. The Black Line Faults of the Red Lake Gold Mine, [Honours thesis], Lakehead University, Thunder Bay, Ontario.

Groves, D.I., Goldfarb, R.J., Gebre-Mariam, M., Hagemann, S.G., and Robert, F., 1998. Orogenic gold deposits: A proposed classification in the context of their crustal distribution and relationship to other gold types, *Ore Geology Reviews*, v. 13, p. 7-27.

Ghosh, S.K., Hazra, S., and Sengupta, S., 1999. Planar, non-planar and refolded sheath folds in the Phulad Shear Zone, Rajasthan, India, *Journal of Structural Geology*, v. 21, 12, p. 1715-1729.

Hart, T.R., terMeer, M. and Jolette, C. 2002. Precambrian geology of Kitto, Eva, Summers, Dorothea and Sandra townships, northwestern Ontario: Phoenix bedrock mapping project; Ontario Geological Survey, Open File Report 6095, 206p.

Hattori, K. 1987. Magnetic felsic intrusions associated with Canadian Archean gold deposits, *Geology*, v. 15, p. 1107-1111.

Hill, M.L., Kolb, M.J., Stinson, V.R., and Scott, R. 2011. Structural control of mineralization in shear-zone-hosted gold deposits: *Geological Society of America Abstracts with Programs*, v. 43, No. 5, p. 513.

Horwood, H.C. and Pye, E.G., 1955: *Geology of Ashmore Township*; Ontario Department of Mines, Volume 60,1951, Part5,105p. Accompanied by Map 1951-2, scale 1:12 000 or 1 inch to 1000 feet.

Hunt, R.G., and Salisbury, J.W., 1970. Visible and near-infrared spectra of minerals and rocks: 1 Silicate minerals. *Modern geology*, Vol. 1, pp. 283-300.

Johns, G.W., McIlraith, S., and Stott, G.M., 2003. Precambrian geology compilation map-Longlac sheet; Ontario Geological Survey, Map 2667, scale 1:250 000.

Kehlenbeck, M.M., 1986. Folds and folding in the Beardmore-Geraldton Belt; *Canadian Journal of Earth Sciences*, v.23, p.158-171.

Kisters, A.F.M., Kolb, J., Meyer, M.F., 1998. Gold mineralization in high-grade metamorphic shear zones of the REnco Mine, southern Zimbabwe, *Journal of Economic Geology*, v. 93, 5, p. 587-601.

Kolb, M.J. 2010. A microstructural study of Musselwhite Mine and Hammond Reef shear-zone-hosted gold deposits [Masters thesis], Lakehead University, Thunder Bay, Ontario.

Kresz, D. 1991. *Geology of the Lapierre Lake area, district of Thunder Bay*; Ontario Geological Survey, Open File Report 5779, 148p.

Kresz, D.V., and Zayachivsky, B., 1993. *Geology of the Seagram Lake Area*; Ontario Geological Survey, Open File Report 5802, p. 214.

Lafrance, B., DeWolfe, J., and Stott, G.M., 2004, A structural reappraisal of the Beardmore-Geraldton Belt at the southern boundary of the Wabigoon subprovince, Ontario, and implications for gold mineralization, *Canadian Journal of Earth Sciences*, v. 41, p. 217-235.

Laird, H.C. 1937: *The Western Part of the Sturgeon River Area (Sturgeon River-Beardmore Section)*; Ontario Department of Mines, Volume 45,1936, Part 2, p.61-117. Accompanied by Map 45a, scale 1:63 360 or 1 inch to 1 mile.

Langford, G.B. 1929: Geology of the Beardmore-Nezah Gold Area, Thunder Bay District; Ontario Department of Mines, Volume 37, 1928, Part 4, p.83-108. Accompanied by Map 37k, scale 1:63 360 or 1 inch to 1 mile.

Lavigne, M.J. Jr. 1983. Gold deposits of the Geraldton Area; in Summary of Field Work, Ontario Geological Survey, Miscellaneous Paper 116, p. 198-200.

Le Maitre, R.W., Bateman, P., Dudek, A., Keller, J., Lameyre, J., Le Bas, M.J., Sabine, P.A., Schmid, R., Sorensen, H., Streckeisen, A., Woolley, A.R. & Zanettin, B., 1989. A Classification of Igneous Rocks and Glossary of terms: Recommendations of the International Union of Geological Sciences Subcommission on the Systematics of Igneous Rocks. Blackwell Scientific Publications, Oxford, U.K.

L'Heureux, R. and Therriault, R. (2009). Technical Report on the Jacobus East Gold Property Thunder Bay Mining Division, Ontario, Canada, p. 33.

Macdonald, A.J. 1983. Iron formation-gold association: Evidence from Geraldton Area; p. 75-83 in the Geology of Gold in Ontario, edited by A.C. Colvine, Ontario Geological Survey, Miscellaneous Paper 110, p. 278.

MacDonald, R.D. 1943. Geology of the Hutchinson Lake Area; Ontario Department of Mines, Annual Report, 1941, Volume 50, Part 3. Accompanied by Map 50f, scale 1 inch to 1 mile.

Mackasey, W.O., 1975. Geology of Dorothea, Sandra, and Irwin Townships, District of Thunder Bay, Ontario Division of Mines, GR122, p. 83. Accompanied by Map 2294, scale 1 inch to ½ mile.

Mackasey, W.O., 1976. Geology of Walters and Leduc Townships, District of Thunder Bay, Ontario Division of Mines, GR149, 58p. Accompanied by Map 2356, scale 1 inch to ½ mile (1:31,680).

Mackasey, W.O. and Wallace, H. 1978. Geology of Elmhirst and Rickaby townships, District of Thunder Bay; Ontario Geological Survey, Report 168, 101p. Accompanied by Map 2373, scale 1:31 680.

Magi, D. 2010. Geology and gold mineralization of the Paint Lake Property, Beardmore-Geraldton Greenstone Belt, Ontario [Honours thesis], Lakehead University, Ontario, Canada.

Mason, J. and White, G. 1986. Gold Occurrences, Prospects, and Deposits of the Beardmore-Geraldton Area, Districts of Thunder Bay and Cochrane; Ontario Geological Survey, Open File Report 5630, 680p.

Mason, J., White, G., and McConnel, C., 1985. Field Guide to the Beardmore-Geraldton Metasedimentary-Metavolcanic Belt; Ontario Geological Survey, Open File Report 5538, p. 73.

Matheson, A.F. 1948. The Jellicoe Mine; p. 399-401 *in* Structural Geology of Canadian Ore Deposits, Canadian Institute of Mining and Metallurgy.

Miller, J., Blewett, R., Tunjic, J., and Connors, K., 2010. The role of early formed structures on the development of the world class St Ives Goldfield, Yilgarn, WA, Precambrian Research, 183, 292-315.

Mitchell, R.H., 1994, Suggestions for revisions to the terminology of kimberlites and lamprophyres from a genetic viewpoint. In Proc. Fifth Int. Kimberlite Conf. 1. Kimberlites and Related Rocks and Mantle Xenoliths (H.O.A. Meyer & O.H. Leonardos, eds.). Companhia de Pesquisa de Recursos Minerais (Brasilia), Spec. Publ. 1/A, 15-26.

Morey, A.A., Weinberg, R.F., and Bierlein, F.P., 2007. The structural controls of gold mineralization within the Bardoc Tectonic Zone, Eastern Goldfields Province, Western Australia: implications for gold endowment in shear systems. *Mineralium Deposita*, 42, 583-600.

Pan, Y. and Fleet, M.E., 1994, Granulite-facies metamorphism in the Quetico Subprovince, north of Manitouwadge, Ontario. *Canadian Journal of Earth Sciences*, 31, v. 9, p. 1427-1439.

Passchier, C.W., Trouw, R.A.J. 2005. *Micostructures* (2nd edition), Springer, 366 p.

Patterson, G.C., Mason, J.K, and Schnieders, B.R., 1985. Thunder Bay Resident Geologist Area, North Central Region; p 56-133 *in* Report of Activities 1984, Regional and Resident Geologists, edited by C.R. Kustra, Ontario Geological Survey, Miscellaneous Paper 122, 297p.

Peach, P.A., 1951, Preliminary Report on the Geology of the Blackwater-Beardmore Area, Ontario Department of Mines, Preliminary Report, 1951-7, p. 6.

Poulsen, K.H., 1983, Structural setting of vein-type gold mineralization in the Mine Centre-Fort Frances area: Implications for the Wabigoon subprovince, in Colvine, A.C., ed., *The geology of gold in Ontario: Ontario Geological Survey Miscellaneous Paper 110*, p. 174-180.

Poulsen, K.H. 2000, Geological setting of mineralization in the Mine Centre-Fort Frances area; Ontario Geological Survey, Mineral Deposits Circular 29, p. 78.

Pye, E.G., 1951, Geology of Errington Township, Little Long Lac Area, Ontario Department of Mines, v. 60, 6, p. 140. Accompanied by map 1951-7, scale 1 inch to 1000 feet.

Pye, E.G., Harris, F.R., Fenwick, K.G, and Baillie, J. 1966. Tashota-Geraldton sheet, Thunder Bay and Cochrane districts; Ontario Department of Mines, Map 2102, scale 1:253 440.

Ramsay, J. G., 1980. Shear zone geometry: A review, *Journal of Structural Geology*, v. 2, p. 83-99.

Reilly, B.A., 1987. Structural analysis of the Paint Lake Deformation Zone, northern Ontario; unpublished M.Sc. thesis, Brock University, p.189.

Reinhardt, M.C., and Davison, I., 1990. Structural and lithologic controls on gold deposition in the shear zone-hosted Fazenda Brasileiro Mine, Bahia State, Northeast Brazil, *Journal of Economic Geology*, v. 85, 5, p. 952-967.

Robb, L. 2005. *An introduction to ore forming processes*, Malden, Maryland, Blackwell Publishing.

- Rosas, F., Marques, F.O, Luz, A., and Coelho, S., 2002. Sheathfolds formed by drag induced by rotation of rigid inclusions in viscous simple shear flow: nature and experiment, *Journal of Structural Geology*, v. 24, 1, p. 45-55.
- Smyk, M., Fralick, P., Hart, T.R., 2005. Geology and gold mineralization of the Beardmore-Geraldton greenstone belt, In; Hollings, P. (Ed.), *Institute on Lake Superior Geology Proceedings, 51st Annual Meeting, Nipigon, Ontario, Part 2 - Field trip guidebook*, v.51, part 2, 3-39.
- Speed, A.A. and Craig, S. 1992. Beardmore-Geraldton historical research project; Ontario Geological Survey, Open File Report 5823, 283p.
- Spear, F., 1993. *Metamorphic phase equilibria and pressure-temperature-time paths*, Mineralogical Society of America, 799p. Volume, etc.
- Stinson, V.R. and Hill, M.L., 2010. Structure at Hammond Reef gold deposit [abstract]: in *Institute on Lake Superior Geology Proceedings, 56th Annual Meeting, International Falls, MN*, v.56, part 1, p. 64.
- Stinson, V.R. and Hill, M.L., 2012. Regional to microstructural control of gold mineralization along the Quetico-Wabigoon subprovince boundary [abstract]: in *Institute on Lake Superior Geology Proceedings, 58th Annual Meeting, Thunder Bay, ON*, v.58, part 1, p. 83.
- Straub, K.H., 1998. Mineralization and alteration of a Neoproterozoic auriferous deformation zone: Onaman-Toshota greenstone belt, Northwestern Ontario, [Honours thesis], Laurentian University, Sudbury, Ontario.
- Stott, G.M., 1984a. Geraldton sheet, Thunder Bay and Cochrane districts; Ontario Geological Survey, Preliminary Map P.241 (Revised), scale 1:126 720.
- Stott, G.M., 1984b. Lake Nipigon, Thunder Bay District; Ontario Geological Survey, Preliminary Map P.257 (Revised), scale 1:126 720.
- Stott, G.M., Corkery, T., Leclair, A., Boily, M., and Percival, J.A., 2007. A revised terrane map for the Superior Province as interpreted from aeromagnetic data: In *Institute on Lake Superior Geology Proceedings, 53rd Annual Meeting, Lutsen, Minnesota, Abstract*, v.53, part 1, p. 74-75.
- Stott, G.M., Davis, D.W., Parker, J.R., Straub, K.J. and Tomlinson, K.Y. 2002. Geology and tectonostratigraphic assemblages, eastern Wabigoon Subprovince, Ontario; Ontario Geological Survey, Preliminary Map P.3449, Scale 1:250 000.
- Stott, G.M., Morrison, D., Gale, V., and Wachowiak, N. 1996. Precambrian Geology of South-Central Onaman-Tashota Greenstone Belt; Ontario Geological Survey, Preliminary Map P.3352, scale 1:50 000.
- Tomlinson, K.Y., Stott, G.M., Percival, J.A., and Stone, D. 2004. Basement terrane correlations and crustal recycling in the western Superior Province: Nd isotopic character of granitoid and felsic volcanic rocks in the Wabigoon subprovince, N. Ontario, Canada. *Precambrian Research*, v.132, p. 245-274.
- Trouw, R.A.J., Passchier, C.W., Wiersma, D. J. 2009. *Atlas of Mylonites and related structures* (1st edition), Springer, 322 p.

- Tullis, J. 2002. Deformation of Granitic Rocks: Experimental Studies and Natural Examples, *Reviews in mineralogy and geochemistry*, v. 51, part 1, p. 51-95.
- Twiss, R.J. and Moores, E.M., 2007. *Structural Geology*, 2nd ed.: New York, W.H. Freeman, p. 736.
- Tyson, A.E., 1945. Report on gold belts in the Little Long Lac-Sturgeon River District, *Canadian Mining Journal*, v. 66, n. 12, p. 839-850.
- White, S.H., Burrows, S.E., Carreras, J., Shaw, N.D., and Humphreys, F.J., 1980. On mylonites in ductile shear zones, *Journal of Structural Geology*, v. 2, 1-2, p. 175-187.

Appendix A: Table of sample locations and descriptions

Sample #	Location and description
MVS001	Milestone Property, Longlac; Drill hole: MS10-17, 400.9 metres. Quartz vein (irregular grain boundaries, subgrains) and minor plagioclase (sericitization), biotite, & calcite.
MVS002	Golden Mile, Hercules Property, Jellicoe; Hand sample, NAD 83, UTM Zone 16N: 5518458N/0452221E. Mylonitized and micro-boudinaged, 2m wide quartz vein, strikes 118°/72°. Quartz vein (irregular grain boundaries, subgrains), minor muscovite, & euhedral pyrite.
MVS003	Golden Mile, Hercules Property, Jellicoe; Hand sample, NAD 83, UTM Zone 16N: 5518463N/0452224E. Foliated chlorite schist 96°/82°. Foliated chlorite schist with chlorite, plagioclase, and euhedral pyrite.
MVS004	Golden Mile, Hercules Property, Jellicoe; Hand sample, NAD 83, UTM Zone 16N: 5518467N/0452224E. Massive granodiorite. Metagranodiorite; porphyroclasts of plagioclase (sericitized), chlorite, muscovite, pyrite.
MVS005	Golden Mile, Hercules Property, Jellicoe; Hand sample, NAD 83, UTM Zone 16N: 5518458N/0452221E. Ductilely deformed quartz vein, 2m wide, strikes 118°/72°. Quartz vein (fluid inclusion-rich quartz, irregular grain boundaries, subgrains)
MVS006	Elmhirst, Hercules Property, Jellicoe; Hand sample, NAD 83, UTM Zone 16N: 5516262N/0452774E. Massive crystal tuff and euhedral pyrite. Meta-tuff, coarse grained euhedral pyrite & anhedral very-fine grained pyrite; completely sericitized plagioclase, chlorite, epidote, carbonate, completely chlorite altered porphyroblasts of pyroxene.
MVS007	Lucky Strike, Hercules Property, Jellicoe; Hand sample, NAD 83, UTM Zone 16N: 5518110N/0452474E. Ductilely deformed metre-wide quartz-carbonate vein with chlorite and pyrite, strikes 135°/21°. Quartz vein, trace pyrite and pyrite with magnetite rims, calcite, chlorite.
MVS008	Golden Mile, Hercules Property, Jellicoe; Hand sample, NAD 83, UTM Zone 16N: 5518463N/0452224E. Chlorite schist within granodiorite adjacent to quartz vein. Chlorite anastomoses around plagioclase, strongly foliated. Meta-tuff, v.f.g. pyrite elongated parallel to foliation; chlorite anastomoses around plagioclase, strongly foliated.
MVS009	Elmhirst, Hercules Property, Jellicoe; Hand sample, NAD 83, UTM Zone 16N: 5516338N/0452960E. Crystal tuff with up to 4mm plagioclase crystals with 40cm wide. Crystal tuff with up to 4mm plagioclase crystals; Anhedral pyrite, carbonate, epidote, chlorite, very altered.
MVS010	Golden Mile, Hercules Property, Jellicoe; Hand sample, NAD 83, UTM Zone 16N: 5518459N/0452218E. Granodiorite 80cm from quartz vein, hematite veinlets, and foliation strikes 125°/75°. Metagranodiorite; Quartz (recrystallized grains), plagioclase (sericitization), chlorite, muscovite, carbonate, pyrite.
MVS011	Elmhirst, Hercules Property, Jellicoe; Hand sample, NAD 83, UTM Zone 16N: 5518459N/0452218E. Diabase dyke and apophysis (aphanitic to fine-grained) striking at 28 degrees with varying dip due to non-linear contact, 82°NE dip in one location. No chill margins or baked margins, trace euhedral pyrite. Diabase; subophitic, pyroxene 50%, plagioclase 45%, and chlorite 5%.

MVS012A	Lucky Strike, Hercules Property, Jellicoe; Hand sample, NAD 83, UTM Zone 16N: 5518097N/0452476E. Ductilely deformed quartz vein, xenoliths of chlorite schist, foliation strikes 134°/59°. Angular fault breccia and quartz vein sampled. Quartz vein (irregular grain boundaries), epidote, angular breccia.
MVS012B	Lucky Strike, Hercules Property, Jellicoe; Hand sample, NAD 83, UTM Zone 16N: 5518097N/0452476E. Ductilely deformed quartz vein, xenoliths of chlorite schist, foliation strikes 134°/59°. Fault gouge, angular clasts of quartz, feldspar, and pyrite.
MVS013	Lucky Strike, Hercules Property, Jellicoe; Hand sample, NAD 83, UTM Zone 16N: 5518118N/0452449E. Quartz vein adjacent to chlorite schist, foliation strikes 142°/57°. Quartz vein (irregular grain boundaries and subgrains), calcite, trace pyrite.
MVS014	Golden Mile, Hercules Property, Jellicoe; Hand sample, NAD 83, UTM Zone 16N: 5518458N/0452217E. Granodiorite 2m north of ductilely deformed quartz vein, 125°/75°SW. Metagranodiorite; plagioclase (sericitization), quartz, chlorite (rutile needles), calcite.
MVS015	Elmhirst, Hercules Property, Jellicoe; Hand sample, NAD 83, UTM Zone 16N: 5516377N/0452948 ^E . Massive, crystalline, fine-grained to medium grained diabase with subophitic texture, trace pyrite and moderate chlorite. Ophitic texture, 45% pyroxene, 45% plagioclase, 5% chlorite, and 5% biotite, trace anhedral magnetite and chalcopyrite.
MVS016	Elmhirst, Hercules Property, Jellicoe; Hand sample, NAD 83, UTM Zone 16N: 5516360N/0452750E. Crystal lapilli tuff with plagioclase crystals, euhedral 3mm long, pyrite is euhedral, 1%, some stringers. Meta-lapilli tuff; very fine grained, plagioclase, epidote, chlorite, biotite, carbonate, opaques.
MVS017	Golden Mile, Hercules Property, Jellicoe; Hand sample, NAD 83, UTM Zone 16N: 5518460N/0452221E. Ductilely deformed quartz vein adjacent to chlorite schist. Quartz vein (subgrains, irregular grain boundaries, undulatory extinction), muscovite, chlorite.
MVS018	Golden Mile, Hercules Property, Jellicoe; Hand sample, NAD 83, UTM Zone 16N: 5518460N/0452211E. NE-trending foliation in granodiorite adjacent to quartz vein and chlorite schist. Meta-granodiorite; Plagioclase (sericite altered), quartz, calcite, chlorite, anhedral magnetite.
MVS019	Lucky Strike, Hercules Property, Jellicoe. Hand sample, NAD 83, UTM Zone 16N: 5518116N/0452449E. Strongly foliated schist adjacent to Lucky Strike quartz vein, strikes 136°/58°. Meta-granodiorite; Plagioclase, quartz, chlorite, calcite, pyrite and magnetite elongated parallel to foliation in chlorite.
MVS020	Castlewood Property, Jellicoe; Hand sample, NAD 83, UTM Zone 16N: 5538010N/0448011E. Chlorite schist, foliated 292°/85°. Chlorite schist; Quartz veins, extreme grain size reduction.
MVS021	Castlewood Property, Jellicoe; Hand sample, NAD 83, UTM Zone 16N: 5538021N/0448015E. Meta-granite and quartz vein, strikes 298°/90°. Meta-granodiorite; ductilely deformed quartz veins, chlorite; 25 Au inclusions in albite feldspar and sericite.
MVS022	Brenbar Property, Jellicoe; Hand sample, NAD 83, UTM Zone 16N: 5510544N/0442457E, Ductilely deformed fault breccia (pegmatite host rock), with tourmaline matrix. Various types of xenoliths (chlorite rich, plagioclase rich, angular, etc.), schorl tourmaline, trace pyrite, arsenopyrite, 5 specks of Au.

MVS023	Castlewood Property, Jellicoe; Hand sample, NAD 83, UTM Zone 16N: 5538032N/0448022E. Chlorite schist and quartz vein, foliated 261°/89°. Chlorite, quartz, biotite, pyrite (biotite fringe), chalcopyrite, magnetite, pyrrhotite inclusions parallel to foliation within pyrite.
MVS024	Brenbar Property, Jellicoe; Hand sample, NAD 83, UTM Zone 16N: 5510551N/0442460E. Chlorite schist foliated 062°/84°. Chlorite, quartz, pyrite (magnetite rims, pyrrhotite inclusions) in fractured albite & quartz vein.
MVS025	Brenbar Property, Jellicoe; Hand sample, NAD 83, UTM Zone 16N: 5510550N/0442463E. Quartz vein strikes 050°/83°. Quartz vein (irregular grain boundaries, subgrains); chlorite, muscovite, pyrite (quartz fringe); 1 speck of Au in ductilely deformed fractured quartz vein, 1 speck in fracture oblique to euhedral pyrite
MVS026	Brenbar Property, Jellicoe; Hand sample, NAD 83, UTM Zone 16N: 5510789N/0442543E. Quartz vein adjacent to chlorite schist and sericite schist foliated 093°/89.5°. Quartz vein (irregular grain boundaries, subgrains); albite feldspar, muscovite, chlorite; 8 specks of Au in ductilely deformed fractures in quartz vein; chalcopyrite and azurite in fractures.
MVS027	Brenbar Property, Jellicoe; Hand sample, NAD 83, UTM Zone 16N: 5510789N/0442552E. Quartz-carbonate vein, pyrite-rich, 062°/82°. MVS027A: Quartz vein (recrystallized grain boundaries), calcite; boudinaged fault breccia; 4 specks of Au along breccia along biotite-chlorite grain boundaries; MVS027B: Quartz vein (recrystallized grain boundaries), calcite; magnetite in folded fractures in pyrite; MVS027C: Pegmatite; albite plagioclase, muscovite, quartz; ductilely deformed fractures in pyrite that are filled with magnetite.
MVS028	Brenbar Property, Jellicoe; Hand sample, NAD 83, UTM Zone 16N: 5510789N/0442543E. Chlorite schist adjacent to quartz vein strikes 063°/82°. Chlorite, albite plagioclase, quartz ; Bifurcating, schistose fault gouge with fractured pyrite, pyrrhotite, and magnetite.
MVS029	Brenbar Property, Jellicoe; Hand sample, NAD 83, UTM Zone 16N: 5510789N/0442543E . Sericite schist adjacent to quartz vein, strikes 086°/85°. Quartz, muscovite; 7 specks of Au in brittle-ductilely deformed quartz vein.
MVS030	Castlewood Property, Jellicoe; Hand sample, NAD 83, UTM Zone 16N: 5538036N/0448030E. Pyrite-rich quartz vein and chlorite schist, strikes 288°/89°. Chlorite, muscovite, biotite, quartz with fractured pyrite with pyrrhotite, sphalerite, and magnetite inclusions.
MVS031	Brenbar Property, Jellicoe; Drill hole BB10-14, 368 metres. Mylonite in muscovite schist. Muscovite schist; Mylonite; Muscovite, quartz (grain size reduction), calcite; Euhedral pyrite defines foliation.
MVS032	Brenbar Property, Jellicoe; Drill hole BB10-14, 406 metres. Mylonite in muscovite schist. Muscovite, quartz (extreme grain size), calcite ; Euhedral pyrite defines foliation
MVS033	Brenbar Property, Jellicoe; Drill hole BB10-14, 401.4 metres. Mylonite in muscovite schist. Muscovite, quartz (boudinaged qtz vein, rotated dextrally, extreme grain size reduction), calcite.
MVS034	Brenbar Property, Jellicoe; Drill hole BB10-14, 373 metres. Mylonite; Muscovite schist. quartz, (brittle-ductilely deformed quartz vein, grain size reduction), calcite.

MVS035	Brenbar Property, Jellicoe; Drill hole BB10-14, 188 metres. Muscovite schist. Mylonite; Muscovite, quartz vein (folded, grain size reduced), pyrite (quartz fringe), calcite.
MVS036	Brenbar Property, Jellicoe; Drill hole BB10-14, 163.8 metres. Muscovite schist. Mylonite; Muscovite, quartz, albite plagioclase (rare undulatory extinction in plagioclase), calcite.
MVS037	Hercules Property, Jellicoe; Drill hole HR06-02, 19.5 metres. Meta-granodiorite.
MVS038	Hercules Property, Jellicoe; Drill hole HR06-02, 30.3 metres. Meta-granodiorite.
MVS039	Hercules Property, Jellicoe; Drill hole HR06-02, 27 metres. Meta-granodiorite.
MVS040	Hercules Property, Jellicoe; Drill hole HR06-02, 11 metres. Meta-granodiorite.
MVS041	Hercules Property, Jellicoe; Drill hole HR06-02, 14 metres. Meta-granodiorite.
MVS042	Hercules Property, Jellicoe; Drill hole HR06-02, 15 metres. Meta-granodiorite.
MVS043	Hercules Property, Jellicoe; Drill hole HR06-02, 23 metres. Meta-granodiorite.
MVS044	Hercules Property, Jellicoe; Drill hole HR06-02, 7.2 metres. Meta-granodiorite.
MVS045	Hercules Property, Jellicoe; Drill hole HR06-02, 19 metres. Meta-granodiorite.
MVS046	Hercules Property, Jellicoe; Drill hole HR06-02, 20.3 metres. Meta-granodiorite.
MVS047	Hercules Property, Jellicoe; Drill hole HR06-02, 22 metres. Meta-granodiorite.
MVS048	Hercules Property, Jellicoe; Drill hole HR08-84, 44.25 metres. Meta-granodiorite.
MVS049	Hercules Property, Jellicoe; Drill hole HR08-84, 77 metres. Meta-granodiorite.
MVS050	Hercules Property, Jellicoe; Drill hole HR08-84, 73 metres. Meta-granodiorite.
MVS051	Hercules Property, Jellicoe; Drill hole HR08-84, 52 metres. Meta-granodiorite.
MVS052	Hercules Property, Jellicoe; Drill hole HR08-84, 125.35 metres. Meta-granodiorite.
MVS053	Hercules Property, Jellicoe; Drill hole HR08-84, 125 metres. Meta-granodiorite.
MVS054	Hercules Property, Jellicoe; Drill hole HR08-212, 54.3 metres. Meta-granodiorite.
MVS055	Hercules Property, Jellicoe; Drill hole HR08-212, 61.6 metres. Meta-granodiorite.
MVS056	Hercules Property, Jellicoe; Drill hole HR08-212, 280 metres. Meta-granodiorite.
MVS057	Hercules Property, Jellicoe; Drill hole HR08-212, 294 metres. Meta-granodiorite.
MVS058	Hercules Property, Jellicoe; Drill hole HR08-84, 58.3 metres. Meta-granodiorite.
MVS059	Hercules Property, Jellicoe; Drill hole HR08-274, 15.7 metres. Meta-granodiorite.
MVS060	Hercules Property, Jellicoe; Drill hole HR08-274, 29 metres. Meta-granodiorite.
MVS061	Hercules Property, Jellicoe; Drill hole HR08-274, 29.15 metres. Meta-granodiorite.
MVS062	Hercules Property, Jellicoe; Drill hole HR08-273, 100 metres. Meta-granodiorite.
MVS063	Hercules Property, Jellicoe; Drill hole HR08-273, 133 metres. Meta-granodiorite.

MVS064	Hercules Property, Jellicoe; Drill hole HR08-273, 133.9 metres. Meta-granodiorite.
MVS065	Hercules Property, Jellicoe; Drill hole HR08-273, 183.3 metres. Meta-granodiorite.
MVS066	Hercules Property, Jellicoe; Drill hole HR08-273, 186.1 metres. Meta-granodiorite.
MVS067	Hercules Property, Jellicoe; Drill hole HR08-273, 204 metres. Meta-granodiorite.
MVS068	Hercules Property, Jellicoe; Drill hole HR08-273, 226 metres. Meta-granodiorite.
MVS069	Hercules Property, Jellicoe; Drill hole HR08-273, 291 metres. Meta-granodiorite.
MVS070	Hercules Property, Jellicoe; Drill hole HR09-333, 4.5 metres. Meta-granodiorite.
MVS071	Hercules Property, Jellicoe; Drill hole HR09-333, 74.5 metres. Meta-granodiorite.
MVS072	Hercules Property, Jellicoe; Drill hole HR09-333, 75 metres. Meta-granodiorite.
MVS073	Hercules Property, Jellicoe; Drill hole HR09-333, 130 metres. Meta-granodiorite.
MVS074	Hercules Property, Jellicoe; Drill hole HR09-333, 165.5 metres. Meta-granodiorite.
MVS075	Hercules Property, Jellicoe; Drill hole HR09-333, 165.7 metres. Meta-granodiorite.
MVS076	Hercules Property, Jellicoe; Drill hole HR09-333, 173 metres. Meta-granodiorite.
MVS077	Hercules Property, Jellicoe; Drill hole HR09-333, 175 metres. Meta-granodiorite.
MVS078	Hercules Property, Jellicoe; Drill hole HR09-333, 196.9 metres. Meta-granodiorite.
MVS079	Hercules Property, Jellicoe; Drill hole HR09-333, 223 metres. Meta-granodiorite.
MVS080	Hercules Property, Jellicoe; Drill hole HR09-333, 347 metres. Meta-granodiorite.
MVS081	Hercules Property, Jellicoe; Drill hole HR09-333, 360 metres. Meta-granodiorite.
MVS082	Hercules Property, Jellicoe; Drill hole HR09-333, 374 metres. Meta-granodiorite.
MVS083	Hercules Property, Jellicoe; Drill hole HR09-333, 376 metres. Meta-granodiorite.
MVS084	Hercules Property, Jellicoe; Drill hole HR10-419, 112 metres. Ductilely deformed meta-granodiorite, subtle foliation. Albite plagioclase (gently folded plagioclase with crosscutting fractures), muscovite, quartz (subgrains and undulatory extinction), chlorite, calcite.
MVS085	Hercules Property, Jellicoe; Drill hole HR08-253, 44.3 metres. Ductilely deformed meta-granodiorite, subtle foliation. Albite plagioclase (gently folded plagioclase), muscovite, quartz (subgrains and undulatory extinction), chlorite, calcite.

MVS086	Hercules Property, Jellicoe; Drill hole HR08-188, 235 metres. Ductilely deformed meta-granodiorite, subtle foliation. Albite plagioclase (gently folded), quartz (undulatory extinction, subgrains), muscovite, chlorite.
MVS087	Hercules Property, Jellicoe; Drill hole HR08-297, 790.4 metres. Ductilely deformed meta-granodiorite, subtle foliation. Albite plagioclase, quartz, chlorite ; folded fractures; 1 speck of gold in inclusion in pyrite
MVS088	Hercules Property, Jellicoe; Drill hole HR07-51, 20 metres. Ductilely deformed meta-granodiorite, foliated and sericitized. Albite plagioclase (completely sericitized), quartz (“quartz eyes”, undulatory extinction); trace pyrite magnetite.
MVS089	Hercules Property, Jellicoe; Drill hole HR07-51, 6 metres. Meta-granodiorite, sericitized. Albite plagioclase (completely sericitized), quartz (grain boundary area reduction, nearly subgrain-free quartz), chlorite;
MVS090	Hercules Property, Jellicoe; Drill hole HR07-51, 26 metres. Meta-granodiorite, completely sericitized, mylonite. Albite plagioclase, quartz (boudinaged and rotated quartz vein, extreme grain size reduction, calcite (ribbons); Pyrite (quartz fringe).
MVS091	Hercules Property, Jellicoe; Drill hole HR07-51, 31 metres (sample 1). Ductilely deformed quartz vein, visible gold. Quartz (ductilely deformed, irregular grain boundaries, subgrains), calcite, muscovite, pyrite; 3 Au specks along subgrain boundaries in quartz; 17 Au specks along grain boundaries in quartz; 10 Au specks along grain boundaries of quartz related to fluid inclusions; 28 Au specks and blebs in ductilely deformed fractures in quartz veins; 4 Au specks in pressure shadows around euhedral pyrite; 2 Au specks along the pyrite-quartz grain boundary; 3 Au specks along the pyrite-quartz grain boundary and foliated; 14 Au specks in ductilely deformed fractures in quartz veins along quartz-muscovite boundaries; 38 Au specks along muscovite-muscovite grain boundaries; 25 Au specks along the quartz-muscovite grain boundary; 1 Au speck as an inclusion in euhedral pyrite
MVS092	Hercules Property, Jellicoe; Drill hole HR07-51, 31 metres (sample 2). Ductilely deformed quartz vein. Quartz (irregular grain boundaries, subgrains), calcite, muscovite, pyrite; Fractures in c.g. pyrite and not f.g. pyrite.
MVS093	Hercules Property, Jellicoe; Drill hole HR07-51, 31 metres (sample 3). Ductilely deformed quartz vein. Quartz (irregular grain boundaries, subgrains), calcite, muscovite, pyrite; Pyrite is located in muscovite along quartz vein.
MVS094	Hercules Property, Jellicoe; Drill hole HR07-51, 31 metres (sample 4). Ductilely deformed quartz vein. Quartz (irregular grain boundaries, subgrains), calcite, muscovite, pyrite; Fractured pyrite along ductilely deformed quartz veins.
MVS095	Hercules Property, Jellicoe; Drill hole HR07-51, 31 metres (sample 5). Ductilely deformed quartz vein and meta-granodiorite. Quartz (some veins, subgrains), albite plagioclase, muscovite, chlorite, fracture pyrite with magnetite in the linear fractures.
MVS096	Hercules Property, Jellicoe; Drill hole HR07-51, 37.3 metres. Ductilely deformed meta-granodiorite. Albite plagioclase (completely sericitized), quartz (grain boundary area recovery), muscovite, chlorite; Trace py.
MVS097	Hercules Property, Jellicoe; Drill hole HR07-51, 40 metres. Mylonite, chlorite schist. Chlorite, albite plagioclase (fractured); Euhedral arsenopyrite, anhedral magnetite and trace chalcopyrite.

MVS098	Hercules Property, Jellicoe; Drill hole HR07-51, 74.5 metres. Meta-granodiorite. Plagioclase (completely sericitized), quartz (undulatory extinction, equigranular), muscovite, chlorite; Trace pyrite.
MVS099	Hercules Property, Jellicoe; Drill hole HR07-51, 133 metres. Amphibole-rich meta-granodiorite. C.g. hornblende, plagioclase (undulatory extinction), chlorite, epidote; Trace pyrite.
MVS100	Hercules Property, Jellicoe; Drill hole HR07-51, 150 metres. Biotite-rich meta-granodiorite, sericitized. Albite plagioclase (completely sericitized), quartz (nearly equigranular, undulose extinction), muscovite, chlorite; Trace chalcopyrite and pyrite.
MVS101	Hercules Property, Jellicoe; Drill hole HR10-388, 31metres. Meta-granodiorite. Albite plagioclase (deformation twins), quartz (grain size reduction), muscovite, chlorite; Trace pyrite.
MVS102	Hercules Property, Jellicoe; Drill hole HR08-155, 68.4 metres. Meta-granodiorite. Albite plagioclase (gently folded and deformation twins), quartz (grain size reduction), muscovite, chlorite; Trace pyrite.
MVS103	Hercules Property, Jellicoe; Drill hole HR10-424, 215 metres. Meta-granodiorite. Albite plagioclase, quartz (boudinaged veins, sheath folds, grain size reduction); Trace pyrite
MVS104	Hercules Property, Jellicoe; Drill hole HR10-424, 181.4 metres. Meta-granodiorite with “quartz eyes” and quartz vein. Albite plagioclase, quartz (grain size reduction, grain boundary recovery, boudinaged), muscovite, calcite; Trace pyrite and magnetite.
MVS105	Hercules Property, Jellicoe; Drill hole HR10-424, 181.6 metres. Foliated meta-granodiorite and quartz vein. Albite plagioclase, quartz (folded and boudinaged veins, undulatory extinction, grain size reduction), muscovite; Subhedral pyrite.
MVS106	Hercules Property, Jellicoe; Drill hole HR10-424, 126.8 metres. Meta-granodiorite. Albite plagioclase, quartz (undulatory extinction and grain size reduction), chlorite, epidote; Anhedral pyrite, chalcopyrite, and magnetite.
MVS107	Hercules Property, Jellicoe; Drill hole HR10-424, 56 metres. Meta-granodiorite and quartz vein. Albite plagioclase (completely replaced by sericite), quartz (equigranular, grain boundary recovery), hornblende (completely replaced by chlorite and epidote); Trace pyrite.
MVS108	Milestone Property, Longlac; Dril hole MS10-67, 13.3 metres. Amphibolite with sericitized plagioclase. Albite plagioclase (irregular grain boundaries, undulatory exctinction, partially replaced by sericite), hornblende (folded, replaced by chlorite and actinolite), quartz (smooth grain boundaries), calcite; Trace pyrite and chalcopyrite.
MVS109	Hercules Property, Jellicoe; Drill hole HR09-333, 128 metres. Meta-granodiorite. Albite plagioclase (completely sericitized and sausseritized), quartz (undulatory exctinction), Euhedral pyrite and anhedral chalcopyrite.
MVS110	Hercules Property, Jellicoe; Drill hole HR10-468, 78.63-78.7 metres. Meta-granodiorite. Albite plagioclase, quartz (coarse-grained vein, grain size reduction), muscovite, calcite; Euh pyrite.
MVS111	Milestone Property, Longlac; Dril hole MS10-39, 154 metres. Foliated amphibolite. Albite plagioclase (undulatory extinction), quartz (coarse-grained vein, grain size reduction, multiple generations of veins), hornblende (epidote and chlorite replaced), calcite; Euhedral pyrite, anhedral chalcopyrite and magnetite, 2 specks of Au along chlorite grain boundaries.

MVS112	Milestone Property, Longlac; Dril hole MS10-39, 161.5 metres. Foliated amphibolite with ductilely deformed quartz veins. Plagioclase (undulatory extinction), hornblende (chlorite and epidote replaced), quartz (veins, grain size reduction), calcite (veins); Euhedral to subhedral pyrite with chalcopyrite inclusions.
MVS113	Milestone Property, Longlac; Dril hole MS10-39, 184 metres. Strongly foliated amphibolite with ductilely deformed quartz veins. Plagioclase (undulatory extinction), hornblende (epidote and chlorite replaced), quartz (folded, grain size reduction, lattice preferred orientation), calcite (veins); Euhedral pyrite, inclusions of pyrrhotite, magnetite; 1 Au anhedral inclusion with, pyrrhotite, magnetite, arsenopyrite, chalcopyrite, cobaltite in pyrite; 1 Au anhedral inclusion in pyrite; 1 instance of Au in contact with aforementioned minerals as one anhedral inclusion in pyrite, 2 specks of Au along chlorite boundaries, 1 speck of gold in pyrite pressure shadow.
MVS114	Milestone Property, Longlac; Dril hole MS10-39, 184.5 metres. Strongly foliated amphibolite with ductilely deformed quartz veins. Plagioclase (undulatory extinction), hornblende (epidote and chlorite replaced), quartz (vein, lattice preferred orientation, irregular grain boundaries); Anhedral chalcopyrite and magnetite inclusions in euhedral pyrite; 1 anhedral Au inclusion in pyrite.
MVS115	Milestone Property, Longlac; Drill hole MS10-39, 197 metres. Foliated amphibolite. Plagioclase (undulatory extinction), hornblende (chlorite, anastomosing around plagioclase, and epidote replaced hornblende), quartz (vein), calcite (vein); Trace magnetite and chalcopyrite.
MVS116	Milestone Property, Longlac; Drill hole MS10-39, 201.5 metres. Bleached-looking amphibolite. Plagioclase (equigranular, partially sericitized), hornblende (chlorite and epidote replaced), quartz (undulatory).
MVS117	Milestone Property, Longlac; Drill hole MS10-18B, 329.1 metres. Amphibolite and ductilely deformed quartz veins. Plagioclase (deformation twins, partially sericitized), hornblende (epidote and chlorite replaced), quartz (undulatory extinction, subgrains, boudinaged quartz veins, irregular grain boundaries), biotite, muscovite, calcite; Anhedral pyrrhotite and cobaltite as inclusions in euhedral pyrite; 3 anhedral Au inclusions in pyrite, 1 anhedral Au inclusion with chalcopyrite inclusion in pyrite.
MVS118	Milestone Property, Longlac; Drill hole MS10-18B, 447.2 metres. Amphibolite and ductilely deformed quartz veins. Plagioclase (deformation twins), hornblende (chlorite and epidote replaced), quartz (grain size reduction, undulatory extinction), biotite; Euh coarse-grained pyrite, anhedral chalcopyrite.
MVS119	Leitch Mine, Beardmore; Hand sample. Metasiltstone, chlorite schist. Very fine-grained chlorite, muscovite, quartz (undulatory extinction, folded qtz-calcite veins), calcite.
MVS130	Pagwachuan area, Caramat; NAD 83, UTM 16N: 5499155N/0535983E. Chloritized diorite. No gold mineralization.
MVS131	Pagwachuan area, Caramat; NAD 83, UTM 16N: 5507291N/0546366E. Metaconglomerate, slump features, near granite ridge. No gold mineralization.
MVS132	Pagwachuan area, Caramat; NAD 83, UTM 16N: 5501498N/0539547E. Matrix-supported conglomerate, magnetic, foliated 136°/70°NW. BIF, meta-granodiorite, quartz, rounded to sub-rounded clasts up to 20cm long. No gold mineralization.

MVS133	Pagwachuan area, Caramat; NAD 83, UTM 16N: 5502276N/0538985E. Mylonite in meta-granodiorite with quartz ribbons. Quartz ribbons are all approximately E-W (266°/90°). No gold mineralization.
MVS134	Missing Link, Paint Lake shear zone, Jellicoe; NAD 83, UTM 16N: 5511220N/0466744E. Quartz vein within mylonite. Ankerite (deformation twins), quartz (boudinaged veins, ribbons, irregular grain boundaries, 3 rd greatest grain size reduction in study)
MVS135	Missing Link, Paint Lake shear zone, Jellicoe; NAD 83, UTM 16N: 5511220N/0466744E. Quartz vein and chlorite schist within mylonite. Chlorite, ankerite (anastomosing foliation around boudins of ankerite and quartz vein), quartz (vein, 2 nd greatest grain size reduction in study), muscovite.
MVS136	Missing Link, Paint Lake shear zone, Jellicoe; NAD 83, UTM 16N: 5511220N/0466744E. Chlorite schist within mylonite. Chlorite (defines the smooth, parallel foliation), ankerite, quartz (grain size reduction)
MVS137	Pagwachuan trench #2, Caramat; NAD 83, UTM 16N: 5503726N/0542583E. Syenite; Alkali feldspar (fractures cross cut undulatory extinction, subgrains), quartz (fractured, irregular grain boundaries, undulatory extinction, vein), muscovite.
MVS138	McKay trench, Caramat; NAD 83, UTM 16N: 5497547N/0540460E. Kyanite-biotite schist. Quartz (undulatory extinction, vein), biotite, muscovite, kyanite (partially replaced by muscovite).
MVS139	McKay trench, Caramat; NAD 83, UTM 16N: 5497547N/0540460E. Kyanite-biotite schist. Quartz (undulatory extinction, vein), biotite, muscovite, kyanite (partially replaced by muscovite).
MVS140	McKay trench, Caramat; NAD 83, UTM 16N: 5497547N/0540460E. Kyanite-biotite schist. Quartz (undulatory extinction, vein), biotite, muscovite, kyanite (partially replaced by muscovite).
MVS141	McKay trench, Caramat; NAD 83, UTM 16N: 5497541N/0540460E. Garnet-hornblende-biotite schist. Garnet (fractured), biotite (anastomoses around quartz and plagioclase), biotite, albite plagioclase, chlorite (replaces biotite).
MVS142	McKay trench, Caramat; NAD 83, UTM 16N: 5497541N/0540459E.. Boudinaged quartz vein, parallel to crenulation (220°/45°). Quartz vein (boudins, subgrains, undulatory extinction).
MVS143	McKay trench, Caramat; NAD 83, UTM 16N: 5497501N/054363E. Garnet-hornblende schist, within quartz boudin. Garnet (fractured), hornblende (hornblende anastomoses around garnet), quartz (undulatory extinction), albite plagioclase, muscovite.
MVS144	McKay trench, Caramat; NAD 83, UTM 16N: 5497442N/0540333E. Fine-grained meta-sandstone. Quartz (undulatory extinction, veins), albite plagioclase (no evidence of dislocation creep).
MVS145	McKay trench, Caramat; NAD 83, UTM 16N: 5497522N/0540388E. Garnet-biotite schist. Garnet (fractures), hornblende, quartz (undulatory extinction); Minor pyrite.
MVS146	McKay trench, Caramat; NAD 83, UTM 16N: 5497523N/0540389E. Garnet-hornblende-biotite schist. Garnet (fractures), quartz (undulatory extinction), hornblende, glaucophane (minor); 1 Au speck in fracture in garnet, 2 Au specks along quartz-amphibole grain boundary as an inclusion in garnet.

MVS147	Pagwachuan trench #1; NAD 83, UTM 16N: 5497525N/0540401E. Garnet-hornblende-biotite schist. Garnet (brittle-ductilely deformed fractures, brittle fractures), quartz (ribbons, quartz fringe around pyrite), biotite, hornblende, muscovite; Minor magnetite and arsenopyrite.
MVS148	Pagwachuan trench #2 (syenite trench), Caramat; NAD 83, UTM 16N: 5503726N/0542583E. Unaltered syenite and <1cm straight quartz vein. Syenite; Alkali feldspar (fractures cross cutting perthitic twins, irregular grain boundaries, and subgrains), quartz (fractures cross cutting undulatory extinction, subgrains), muscovite, rutile (fractured); 3Au specks in subgrains in quartz, 1 Au speck in fractured rutile, 7 specks in muscovite, 1 speck in perthitic twins in alkali feldspar.
MVS149	Pagwachuan trench #2 (syenite trench), Caramat; NAD 83, UTM 16N: 55503727N/0542574E. Altered, yellow clay, granodiorite adjacent to syenite with <1cm wide ductilely deformed quartz veins. Meta-granodiorite; Albite plagioclase (undulose extinction, subgrains), quartz (undulose extinction, subgrains), muscovite; Disseminated pyrite with minor magnetite rims.
MVS150	Pagwachuan trench #2 (syenite trench), Caramat; NAD 83, UTM 16N: 5503735N/0542576E. Phlogopite and euhedral pyrite-rich lamprophyre Lamprophyre; Phlogopite, amphibole (phlogopite reaction rims), massive; Euhedral pyrite.
MVS151	Pagwachuan trench #2 (syenite trench), Caramat; NAD 83, UTM 16N: 5503740N/0542580E. Least deformed meta-granodiorite in trench. Meta-granodiorite; Albite plagioclase, quartz, muscovite, chlorite; Pyrite and magnetite along sericite and chlorite grain boundaries.
MVS152	Pagwachuan trench #2 (syenite trench), Caramat; NAD 83, UTM 16N: 5503735N/0542576E. Most deformed meta-granodiorite and quartz vein in trench. Meta-granodiorite; Albite plagioclase, quartz, muscovite, chlorite; Pyrite and magnetite along sericite and chlorite grain boundaries.
MVS153	McKay trench area, Caramat; UTM 16N:5497673N/0540308E. Isoclinally folded banded iron formation, oxide facies. MVS153A: Garnet schist; Garnet (fractures), quartz (veins, subgrains), muscovite, hornblende; 2 Au specks in fractured garnet, 2 specks of Au along gently folded fluid inclusion trail, 1 Au speck along hornblende grain boundaries, 2 Au specks along quartz-amphibole grain boundaries; 2 Au specks along quartz subgrains; MVS0153B: Metamorphosed banded iron formation; Quartz (undulatory extinction), grunerite; Medium to coarse-grained magnetite.
MVS154	McKay trench area, Caramat; UTM 16N: 5497674N/0540315E Ductilely deformed garnet schist within folded banded iron formation. Strong vertical lineation in garnet. Garnet is sub- to euhedral and defines a strong vertical mineral lineation. Metamorphosed banded iron formation transition into garnet schist; Quartz (undulatory extinction); Trace pyrite and magnetite, minor magnetite.